Investigating the source and fate of organic nitrogen in Arctic marine sediments using a novel multi-proxy approach

A thesis submitted to the University of Manchester for the degree of

Doctor of Philosophy

2022

Emma C. Burns

School of Natural Sciences

Department of Earth and Environmental Sciences

Taken by author on board the RRS James Clark Ross during ARISE sampling campaign May 2018

Table of Contents

List of Figures

List of Tables

List of Abbreviations

Abbreviation	Meaning
AA	Amino acid
Ala	Alanine
ANOVA	Analysis of variance
ARISE	Arctic Isotopes and Seals
ArW	Arctic Water
Asp	Aspartic acid
AW	Atlantic Water
BG	Beaufort Gyre
BHP	Bacteriohopanepolyols
BMBF	German Federal Ministry of Education and Research
BSO	Barents Sea Opening
CAO	Changing Arctic Ocean
CSIA-AA	Compound specific isotope analysis of amino acids
DI	Degradation Index
DLS	Dmitry Laptev Strait
EAA	Essential amino acids
EGC	East Greenland Current
EI	Electron ionisation
ERF	Effective radiative forcing
ESAS	East Siberian Arctic Shelf
GC-FID	Gas Chromatography-Flame Ionisation Detection
GC-IRMS	Gas Chromatography-Isotope Ratio Mass Spectrometry
GDGT	glycerol dialkyl glycerol tetraethers
Glu	Glutamic acid
Gly	Glycine
GRAR	Great Russian Arctic Rivers
HPLC	High performance liquid chromatography
ICD	Ice Complex Deposit
Ileu	Isoleucine
IPCC	Intergovernmental Panel on Climate Change
ISSS-08	International Siberian Shelf Study 2008
Leu	Leucine
MIZ	Marginal ice zone
NCC	Norwegian Coastal Current
NCC_AW	Norwegian Coastal Current and Atlantic Water
NEAA	Non-essential amino acids
NERC	Natural Environment Research Council
NESS	Nearshore East Siberian Sea
Nle	Norleucine
NLS	Nearshore Laptev Sea
OC	Organic carbon
OESS	Offshore East Siberian Sea
OLS	Offshore Laptev Sea
OM	Organic matter
ON	Organic nitrogen
PAA	Particulate amino acids

PCA	Principle component analysis
PF	Polar Front
Phe	Phenylalanine
PN	Particulate nitrogen
POM	Particulate organic matter
PPRI	Phenol to pyridine ratio
Pro	Proline
PSW	Polar surface water
PW	Pacific Water
Py-GCMS	Pyrolysis-Gas Chromatography Mass Spectrometry
RCP	Representative concentration pathway
RF	Radiative forcing
SCC	Siberian Coastal Current
SIF	Single ion filtering
SPLITT	Split flow thin-cell fractionation
Src-Aas	Source amino acids
SST	Sea surface temperature
SWERUS-C3	Swedish-Russian-United States research cruise
SWI	Sediment-water interface
TC	Total carbon
TDAA	Total dissolved amino acids
TEF	Trophic enrichment factor
TerrOM	Terrestrial organic matter
THAA	Total hydrolysable amino acids
TN	Total nitrogen
TOC	Total organic carbon
TP	Trophic position
TPD	Transpolar drift
Tr-Aas	Trophic amino acids
Val	Valine

Thesis Abstract

Nitrogen plays a critical role in controlling marine primary productivity and what is subsequently buried in the sediments, and is becoming increasingly important across the Arctic Ocean as sea ice melts and light availability is no longer the dominant control. Changes in the nitrogen source to primary producers alter the isoscape of a region and subsequently what is buried in marine sediments. It is crucial we understand these alterations of the isoscape and how these might change in the future as the Arctic continues to change in response to climate warming. Here, as part of the ARISE project we focus on two unique areas of the Arctic, the East Siberian Arctic Shelf (ESAS) and the Barents Sea and Fram Strait region. Marine surface sediments of both regions were analysed using a multi-proxy approach involving elemental composition (carbon and nitrogen), bulk stable isotopes ($\delta^{13}C$ and $\delta^{15}N$), macromolecular analyses (Py-GCMS; pyrolysis gas chromatography mass spectrometry), amino acid composition (using GC-FID; gas chromatography flame ionisation detection) and compound specific isotope ($\delta^{15}N$) analysis (GC-IRMS; gas chromatography isotope ratio mass spectrometry).

Analysis of the ESAS sediments indicate a dominance of terrestrially derived OM in the nearshore areas and distinct terrestrial to marine transects in an offshore direction across all proxies used. The ^{15}N at both a bulk and compound specific (amino acid) level differed between the different nearshore regions of the ESAS indicating a qualitative difference in the terrestrial nitrogen delivered to these areas. This correlation persisted offshore suggesting the nearshore patterns impact offshore sediments. In addition, the link between bulk and amino acid analyses confirms that inorganic nitrogen is not the primary cause of the near shore differences observed at bulk level. In the Barents Sea and Fram Strait regions the major

controls on sedimentary organic matter composition were the relative position of the sample to the polar front, marginal ice zone and/or terrestrial inputs. Unlike the ESAS region, inorganic nitrogen produced a de-coupling between bulk and amino acid ^{15}N, highlighting the limitations of using bulk analyses in this region. The baseline ^{15}N varied across the region depending on the major controls above and in some areas whether nitrate was limited in the water column.

Collectively, this study shows that baseline values in the isoscape differ across the Arctic as well as within regions, highlighting the need for each region to be studied as individual areas. In addition, as these regions change in response to climate change it will be vital to have a well constrained baseline for accurate assessments of sedimentary organic matter compositions and the quality of organic matter delivered from various sources. This project forms a vital contribution to the ARISE projects first effort in producing these baseline values and trying to understand what underpins these changes.

Declaration

No portion of the work referred to in the thesis has been submitted in support of an application for another degree or qualification of this or any other university or other institute of learning

Copyright Statement

i. The author of this thesis (including any appendices and/or schedules to this thesis) owns certain copyright or related rights in it (the “Copyright”) and s/he has given the University of Manchester certain rights to use such Copyright, including for administrative purposes.

ii. Copies of this thesis, either in full or in extracts and whether in hard or electronic copy, may be made only in accordance with the Copyright, Designs and Patents Act 1988 (as amended) and regulations issued under it or, where appropriate, in accordance with licensing agreements which the University has from time to time. This page must form part of any such copies made.

iii. The ownership of certain Copyright, patents, designs, trademarks and other intellectual property (the “Intellectual Property”) and any reproductions of copyright works in the thesis, for example graphs and tables (“Reproductions”), which may be described in this thesis, may not be owned by the author and may be owned by third parties. Such Intellectual Property and Reproductions cannot and must not be made available for use without the prior written permission of the owner(s) of the relevant Intellectual Property and/or Reproductions.

iv. Further information on the conditions under which disclosure, publication and commercialisation of this thesis, the Copyright and any Intellectual Property and/or Reproductions described in it may take place is available in the University IP Policy (see http://documents.manchester.ac.uk/DocuInfo.aspx?DocID=2442 0), in any relevant Thesis restriction declarations deposited in the University Library, the University Library’s regulations (see http://www.library.manchester.ac.uk/about/regulations/) and in the University’s policy on Presentation of Theses.

Acknowledgements

Firstly, I would like to thank my main supervisor, Professor Bart van Dongen, for his support and guidance throughout the project. I thoroughly enjoyed being your student and GTA over the last 5 years and will look back fondly on memories made during the Tenerife fieldtrip. Your very 'Dutch' approach to things ultimately kept the project on track when things started to get difficult. I would also like to thank my second supervisor, Professor George Wolff, your expertise was crucial to the project and your feedback always constructive and helpful, thank you for everything. Finally, my last supervisor, Dr Rachel Jeffreys, your amino acid knowledge greatly improved my understanding of the project and your unwavering support, even when times were tough, was vital in me persisting with what sometimes felt like a tunnel with no light. I would also like to thank the Changing Arctic Ocean programme funded through the UKRI Natural Environment Research Council for funding this project.

It is well known in research that the glue that really sticks it all together are the laboratory technicians, in my case Dr Louisa Norman and Dr Sharon Fraser. Louisa, you ran samples for me when I could not, answered all of my random questions and put up with me being seasick while being your roommate on a ship for a month, you are an awesome human being and the ARISE project was really lucky to have you on-board (figuratively and literally!). Sharon, you became much more than just a lab technician but also a friend, you helped me when I had to set up my experiments at Manchester and did not know what I was doing! You also provided support and friendship when things got tough, thank you for listening to me moaning about amino acids!

To everyone on the ARISE team, particularly Professor Claire Mahaffey, Dr Elliot Price and Dr Camille de la Vega, it has been a pleasure to work with you over these last 4 years and your support has been invaluable to this project. I would also like to thank my research group based the University of Manchester, Organic Geochemistry Group, our weekly meetings have been the one constant through my project and I will miss our catch ups over coffee and a figure! A massive thanks is in order to my uni gals (Alana, Emily, Katrina and Natalie), I truly don't know what I would have done without you, our breakdowns in the office to our trips away, it is all memories that I will cherish forever and I can't wait to see where life takes you all, you deserve the best it has to give. Rhys, our coffee catch ups were something I looked forward to weekly

and really bolstered me when things got hard, thank you for always listening! Abbi, I am so thankful for your friendship throughout this PhD, you and your family have always been there for me whether that be for a laugh or a cry or the occasional brunch, keep being you because that's what I love so much. Laura, I think it is fair to say I would have gone mad without you around, your words of encouragement, love and support have kept me going throughout this PhD and I am so lucky to have you.

To the Walker family, Peter, Sophie and Sam, your support and guidance over the last 4 years has been a great reassurance to me and I am so grateful to have been welcomed into such a lovely family. Last but certainly not least, Henry, I think you will be just as relieved as I am for me to finish this PhD! It has been a rollercoaster 4 years but you have stuck by my side through all of it and I could not ask for a better partner in crime to take on the world with. Thank you for all of your support and love, I know it has not been an easy ride.

And finally, to my family, dad, mum and Rebecca, one thing I can say for certain is that none of this would have been possible without you. You have supported me in every imaginable way and I am forever indebted to you for this. You were there for me through the highs and the lows, to celebrate the wins and to be a shoulder to cry on and to pick me up when I was down. I am so lucky to have such an amazing support system at home and I hope I have made you proud.

Without the support of the people and organisations above, I would not have been able to complete this project, each and every one of you has helped me to get to this point and I am so thankful to all of you.

Taken by author on a hike up to Trollsteinen, Svalbard September 2019

Chapter 1 Project Relevance and Thesis Structure

1.1 Project relevance

This PhD studentship is part of the ARISE project (ARctic Isotopes and SEals) funded by the Natural Environment Research Council (NERC) as part of the Changing Arctic Ocean (CAO) programme. The CAO was conceived following the UK Foreign and Commonwealth Office report '*Adapting to change-UK policy towards the Arctic*' in 2013 and the House of Lords Select Committee report '*Responding to a Changing Arctic'* in 2015 and aims to provide an understanding of how the changing ice and ocean characteristics of the Arctic region will impact the biogeochemical and ecological regimes of the Arctic Ocean, focussing on what we know from past and current observations and predictions for future change. To achieve these outcomes two wide-ranging research challenges were identified:

1. To develop a quantified understanding of the structure and functioning of Arctic ecosystems.

2. To understand the sensitivity of Arctic ecosystem structure, functioning and services to multiple stressors and the development of projections of the impacts of change.

Initially four large projects were funded (Arctic PRIZE, ARISE, ChAOS and DIAPOD) to address these research challenges, followed by a further twelve jointly funded by NERC and the German Federal Ministry of Education and Research (BMBF). The ARISE project specifically aimed to provide a 'pan-Arctic' approach to assess ecosystems changes using historical and recent observations. By not focussing solely on single site studies the project aims to provide the 'large scale vision' required to accurately evaluate effects of environmental change across the Arctic. The ARISE project consists of four modules:

- Module 1. Detecting variability in the isoscape
- Module 2. Arctic predators as indicators of change
- Module 3. Past decadal change in the Arctic
- Module 4. Quantifying effects of environmental change on seals

This project contributes primarily to module 1, although there are inter-connections between each module. Module 1 aims to constrain the spatial and temporal variability of the isoscape and to understand what causes these variations. The '*isoscape*' for most of project ARISE is the isotope composition at the base of the food web, variability at the base can translate to large scale shifts higher up the food web. Understanding the isoscape enables us to more accurately determine whether changes in higher levels originate from genuine shifts in an organism trophic level or are due to deviations from differing inputs at the base. The isoscape can also refer to the spatial distribution of the isotopes geographically, for instance in sediments or suspended particles. It is predicated that as the Arctic has undergone and undergoes rapid change, the variations of organic matter input at the base of the food web and across the sedimentary isoscape will become harder to constrain. This project focussed on two regions undergoing rapid change in the Arctic Ocean: the East Siberian Arctic Shelf (ESAS) and the Barents Sea and Fram Strait.

1.2 Thesis Structure

The thesis is presented in the alternative format of submission by journal article. It comprises of this project relevance chapter (Chapter 1), an evaluation of the current appropriate literature (Chapter 2) and two data chapters that have been prepared with the intention for journal submission (Chapter 3 and 4). The organisation of the data chapters is based around two study regions encompassing all of the analytical techniques used rather than splitting the studies by technique, this was acknowledged to be the most appropriate way of giving the full picture for each region. A final conclusions chapter draws together the outcomes and future work arising from this project.

Chapter 2 considers literature relevant to the project alongside two Arctic region case studies of the East Siberian Arctic Shelf (ESAS) and the Barents Sea and Fram Strait region.

Chapter 3 is the first of two data chapters and focusses on the ESAS, the largest continental shelf on Earth extending hundreds of kilometres offshore. This region presents a unique setting where multiple terrestrial inputs of organic matter (permafrost, riverine and coastal erosion) are washed on to the shelf and mix with marine organic matter input. As the temperatures in this region continue to rise the amount of previously frozen terrestrial organic matter making its way to the shelf will increase, some parts of the coastline have already been subject to cliff failures leading to losses of up to 10 m yr^{-1}. However, we currently have very limited understanding as to what impact this is currently having on the nitrogen and organic matter pool, which is essential to understand as nitrogen containing compounds are known to limit primary productivity and sediments are known to sequester carbon in the ocean.

Chapter 4 is the second of the two data chapters focussing on the Barents Sea and Fram Strait region, as the largest opening to the Arctic Ocean it is exposed to the increased heat transfer from the Atlantic Ocean, in addition to atmospheric temperatures rising. This has led to the thickness and extent of the sea-ice decreasing and open-ocean conditions persisting for more of the year. These changes alter the water column through modifying the nitrate source to primary producers as Atlantic water encroaches further, this imparts a distinct signature and has consequences for the isotopic composition of particulates and sedimentary organic matter. Moreover, the timing of and duration of the bloom period is altered which further modifies the amount of particulate organic matter and subsequently the under lying sediments. Understanding how these changes are modifying the isoscape will be critical for understanding future change in the region.

Chapter 5 summarises the conclusions of the project and recommendations for future work in this field and around the Arctic regions.

Photo taken by author of male polar bear on ice floe in the Fram Strait, May 2018

Chapter 2 Literature Review

2.1 Climate Change

Climate change has been a focal point of environmental news for the last decade (Svoboda, 2017) and its importance has only increased following summits leading to the Kyoto protocol (IPCC, 2014), Paris agreements (European Commission, 2016) and COP26 in Glasgow that have attempted to mitigate its effects. Climate change is defined as the warming of the planet due to trapped anthropogenic gases (mainly CO_2, CH_4, N_2O) some of which are the result of the industrial revolution; concentrations of these gases are currently at the highest they have ever been documented (average annual concentration of gases: 419ppm CO_2 , 1896ppb CH_4 and 332ppb N_2O; IPCC, 2021). It is recognised that this warming is caused by a variety of processes (Fig. 2.1) and is already causing multiple physical changes including ocean warming, sea level rise and a decrease in snow and ice cover (IPCC, 2014). Radiative forcing (RF) measures the change in the energy balance of the atmosphere as a result of changes in forcing agents, such as greenhouse gases, which contribute to climate change. Effective radiative forcing (ERF) includes forcings measured in the RF but also natural variations such as cloud cover (IPCC, 2014). As progressive Intergovernmental Panel on Climate Change reports are published it has become “unequivocally” clear that human activity has warmed the climate (IPCC, 2021).

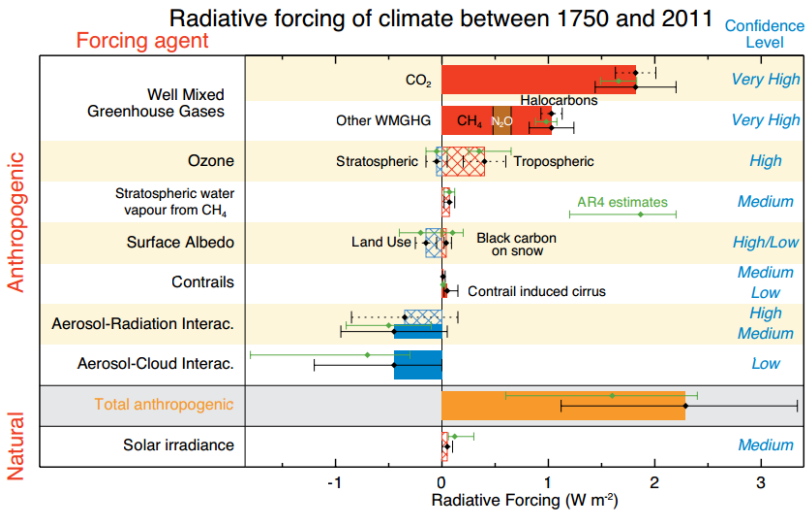

Figure 2.1 Forcing by concentration change between 1750 and 2011 with associated uncertainty range (solid bars are ERF, hatched bars are RF, green diamonds and associated uncertainties are for RF assessed in AR4). (IPCC, 2014).

Greenhouse gases absorb infra-red radiation reflected from the Earth's surface and re-radiate heat energy that causes net warming of the atmosphere (Walsh, 2014). It is widely recognised that greenhouse gases (e.g. CO_2, H_2O) keep the planet 'warm enough' to preserve life; in their absence, the surface temperatures on Earth would be around -18°C and life would not exist as we know it today. However, their excessive production by human activity has led to the concentrations of these gases surpassing natural fluctuations (Harris, 2010). As a consequence, the excess trapped gases cause an imbalance in Earth's energy budget, as the greenhouse gases re-radiate energy back to Earth rather than it leaving the atmosphere (RF). This leads to an excess of heat, the majority of which is stored in oceans and to a lesser extent the atmosphere. It is unlikely that changes in solar irradiance caused the observed increases in recent average surface temperatures indicating that these can be discounted when considering warming (IPCC, 2021).

These changes affect all aspects of the Earth's systems including the environment and therefore the human population. The expected consequences have so far included increased oceanic, atmospheric and land temperatures, increased occurrence of exceptional weather

events such as droughts and flooding episodes and the increasing levels of atmospheric CO_2 have led to ocean acidification (IPCC, 2014). The most recent IPCC report illustrates the importance of adapting to and mitigating climate change impacts now, to not only reduce further warming but to better prepare future generations for the changing environment (IPCC, 2022).

2.2 Arctic and Warming

It is widely recognised that the effects of climate change are greatest at the poles, mainly due to a phenomenon known as polar amplification, or Arctic amplification when it occurs 60-90°N (Brock and Xepapadeas, 2017). Although the exact processes that drive this amplification are still debated, many form positive feedbacks which in turn lead to further increases in polar amplification (IPCC, 2021). When compared to elsewhere, such as the equatorial regions, the Arctic is experiencing, on average, up to two times the rate of temperature increase compared to global averages over the last few decades and further predictions by the (IPCC, 2019) show this trend is set to continue (Fig. 2.2). Considering that the Polar Regions form part of the Earths oceanic and atmospheric systems, climate changes in these regions will lead to impacts that can be felt across the globe. Impacts such as rising sea levels as sea ice and glaciers melt, further highlighting the importance of understanding Arctic change (IPCC, 2021).

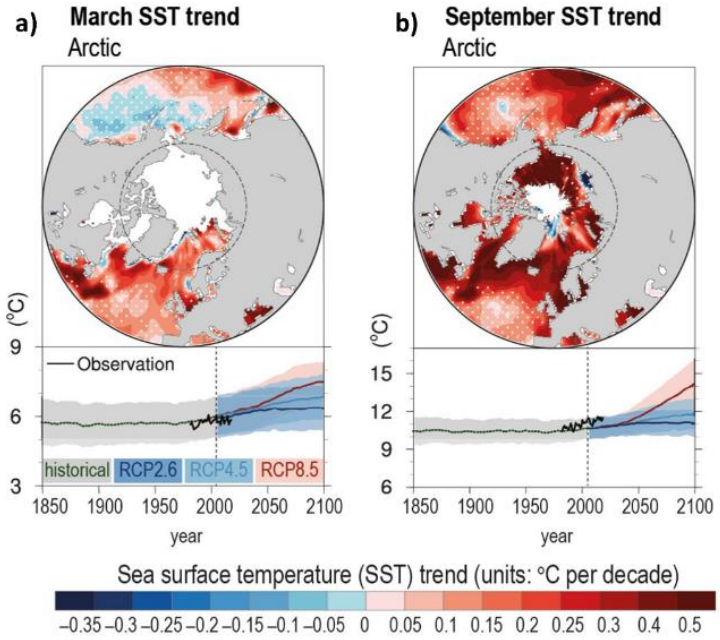

Figure 2.1 Maps of linear trends of Arctic sea surface temperature (SST) for 1982-2017 in March (a) and September (b). Stippled areas show the trends that are insignificant statistically. Dashed circle indicates the Arctic Circle. Under each map are the time series of SST. Black, green, blue and red curves show observations and shaded areas show standard deviations of models against the representative concentration pathway (RCP) projections for greenhouse gas concentrations in the atmosphere. Adapted from IPCC, 2019.

Growing concern regarding climate change in Polar Regions has stimulated research into Arctic change. This has been reflected in special reports including the House of Lords 'Responding to a changing Arctic' (House of Lords, 2014) and the IPCC's 'Climate change and the oceans and the cryosphere' (IPCC, 2019), alongside an increase in large research programmes with significant amounts of funding (e.g. NERC, Changing Arctic Ocean, £16m). There are many factors that influence the strength of warming felt in the Arctic but Walsh (2014) identifies three to be key. The first is the reduction in albedo due to loss of sea ice and snow cover, therefore increasing the amount of solar radiation absorbed and reducing the amount reflected back into the atmosphere. The second is the increased humidity as a function of the enhanced temperatures occurring in the Arctic, which leads to more atmospheric water vapour, one of the most potent greenhouse gases. This leads to a positive feedback to warming and also corresponds to increased descending infrared radiation further

increasing surface temperature. Finally heat energy is driven up towards the Arctic via atmospheric and oceanic circulation creating a ”Northern Hemisphere heat sink” (Lemke and Jacobi, 2012).

The increase in energy transfer to the Arctic region affects the oceans, coastal areas and surrounding continental shelves in different ways. The most apparent of these is the decreasing summer and winter sea ice cover and thickness. Sea ice has a high albedo meaning it can better reflect solar radiation entering the atmosphere back to space and provides a barrier between the air and ocean (Fig. 2.3; IPCC, 2014). A particular problem for the Arctic regions is their strong seasonality associated with a summer melt period. The end of summer - early autumn period sees a decrease in sea ice due to increased solar radiation being absorbed by the oceans during the summer sea ice melt, which is released back into the atmosphere later on in the season (Perovich and Richter-Menge, 2009). The increasing Arctic surface air temperatures, which are rising by double the amount compared to global averages, are supporting this melt and have led to a *ca.* 13% decline in summer sea ice per decade (IPCC, 2019). This has a direct consequence on the ecology of the Arctic from the base of the food web to top predators. The loss of sea ice, for instance, increases the amount of light available to primary producers to use for growth, which has led to a 57% increase in marine primary productivity in the Arctic since 1998 (Lewis, Dijken and Arrigo, 2020). It has been suggested for apex predators such as polar bears, which use sea ice to hunt and feed on, the reduction in sea ice extent and thickness will lead to a population decrease of the species by up to a third in the next half century (Tartu *et al.*, 2017; Guglielmi, 2018).

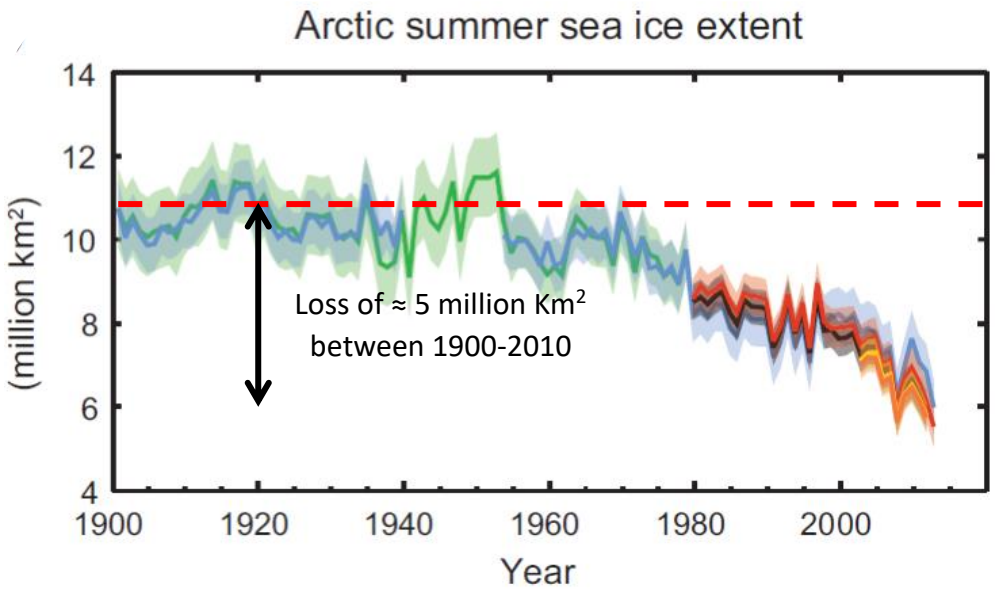

Figure 2.3. The extent of Arctic July-August-September average sea ice; coloured lines represent different data sets. Adapted from IPCC, 2014.

The recent sea ice retreats have produced a stronger wave strength, as the increasing extent of open ocean leads to a longer wave fetch. This has led to undercutting of coastal cliffs, block failure and amplified thermo-erosional processes (Hoque and Pollard, 2016).

Arctic warming is also observed in the terrestrial environment; the land surrounding the Arctic Ocean is dominated by continuous permafrost, which is defined as frozen ground that is consistently below zero degrees for over two years (Oliva and Fritz, 2018). It is made predominantly of two layers (Fig. 2.5); an active layer that thaws annually and a layer beneath which remains frozen year round (Zimov, Schuur and Chapin, 2006; Feng *et al.*, 2015).

Warming is causing increased river discharge from the drainage basins in these regions (Savelieva *et al.*, 2000; Peterson *et al.*, 2002; Yang *et al.*, 2002; Dittmar and Kattner, 2003). The Arctic Ocean, relative to its volume, has the largest input of fresh water compared to all other oceans, mostly due to the large rivers that drain into it, such as the Lena, Ob, Yenisey and Mackenzie. Combined these rivers account for approximately 10% of total river discharge on Earth (Dittmar and Kattner, 2003 and references therein) and have recorded increased

discharge since monitoring began in the 1930s (Semiletov *et al.*, 1998), with a stronger flow seen during the typical low flow months of November to April, likely due to the increased thawing of catchment areas dominated by permafrost (Peterson *et al.*, 2002). In all scenarios of climate change set out by the IPCC fourth assessment report, river runoff will further increase by up to 28% by the end of the century (Kattsov *et al.*, 2007). Permafrost can also be found along the Siberian coastline forming 'ice complex deposits' which are subject to enhanced coastal erosion due to their high ice content making them more susceptible to thawing and undercutting, up to 10m yr^{-1} in some parts of the East Siberian Arctic Shelf (ESAS; Hoque and Pollard et al., 2016 ; Fig. 2.4b).

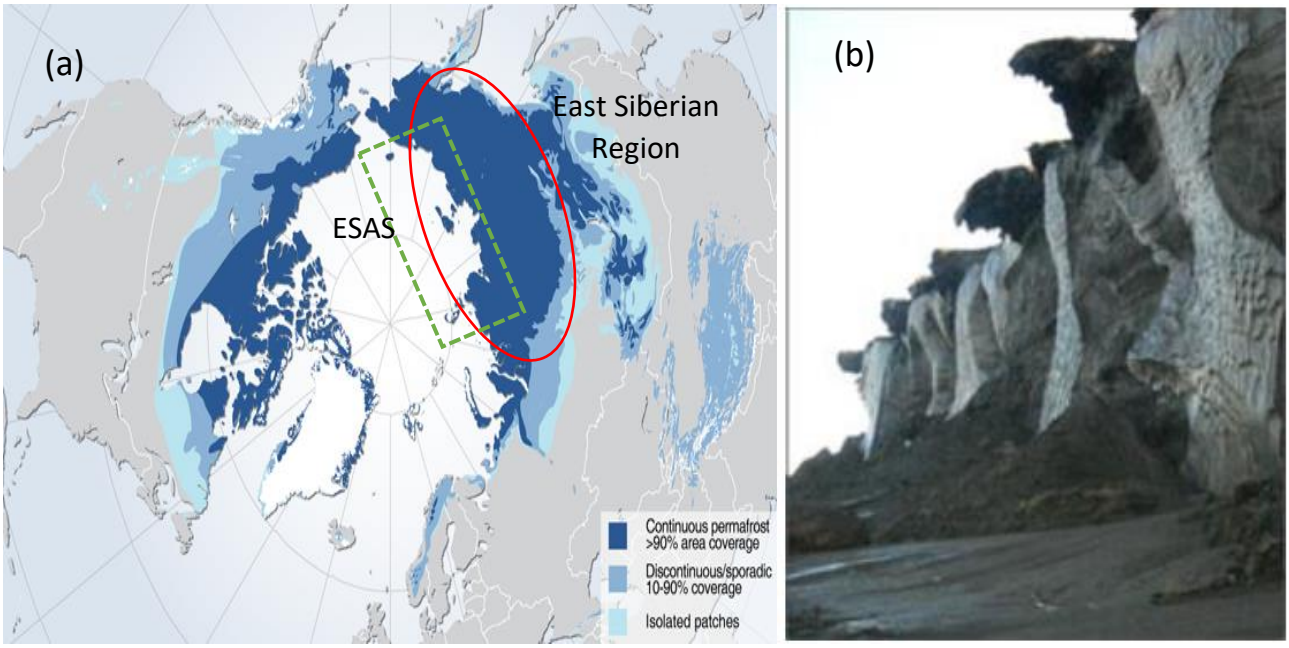

Figure 2.4 (a) Permafrost extent in the northern hemisphere adapted from Buis, (2013), red oval indicating the Siberian region and dashed green rectangle the East Siberian Arctic Shelf (ESAS). (b) Picture showing coastal erosion of ice complex deposits in the East Siberian Arctic area. Taken by Igor Semiletov.

The Arctic region as a whole is undoubtedly sensitive to the observed increases in oceanic and atmospheric temperatures brought on by climate change, as a result of enhanced greenhouse gas production over the last century. The region is particularly interesting due to

the large amount of organic matter stored in both terrestrial and marine permafrost which when subject to thawing and degradation is known to release carbon dioxide and other potent greenhouse gases. As a consequence, research has focussed on understanding the fate of the organic matter and how it feeds back to the global carbon cycle.

2.3 Carbon cycling in the Arctic

Diagenesis of organic matter through the water column and sedimentation can alter the compositional and isotopic state of particulates meaning the resulting OM has a different composition to that of the original OM (Brahney *et al.*, 2014). A large proportion (30-99%; Henrichs, 1992) of OM is thought to be remineralised during early diagenesis. Generally carbon compounds are considered more refractory than nitrogen compounds meaning there is a preferential accumulation leading to increases in the C/N ratio with increased diagenesis (Lehmann *et al.*, 2002). There is also an assumption that higher C/N ratios are also associated with the input of terrestrial material but the above demonstrates that in regions lacking a significant terrestrial input this is not the case and the increase in C/N might be more likely due to increases in decomposition through diagenesis.

According to Tarnocai *et al.*, (2009), roughly half of all organic carbon stored in soils worldwide, equivalent to about 1672 Pg, is found in the Arctic regions. By comparison, this organic carbon pool larger than the total amount of carbon dioxide in the atmosphere at approximately 730 Pg (Zimov, Schuur and Chapin, 2006). Bischoff *et al.* (2016), indicated that 60% of the organic carbon is in permafrost and the remaining is either in taliks (annually unfrozen ground surrounded by permafrost) or in the active layer, which thaws seasonally and is increasing in depth as atmospheric temperatures rise. Enhanced warming has a large impact on these frozen carbon stocks, which have the potential to create positive feedbacks

to the global climate change cycle (Stendel and Christensen, 2002). The changing hydrology of the permafrost is leading to a landscape dominated by thermokarstic features, which promotes degradation of organic matter by bacteria, archaea and methanogens releasing carbon dioxide and methane, depending on availability of oxygen (Bruhwiler, 2021). The increases in thermokarstic processes promotes organic matter degradation on land and also leads to increased drainage of the active layer, which leads to an increase in the amount of organic matter making its way to the river and eventually to the shelf seas (Fig. 2.5; Feng, *et al.*, 2015). Slopes, river banks and coastlines with permafrost are subject to slumping and enhanced erosion as a results of thawing, encouraging further transport of material (Rudy *et al.*, 2017). The terrestrial organic matter (TerrOM) is mainly plant-derived and can contain material from both the active layers and 'old' permafrost deposits as warming continues (van

Dongen *et al.*, 2008; Karlsson *et al.*, 2011; Semiletov *et al.*, 2011; Vonk *et al.*, 2012a; Feng *et al.*, 2015).

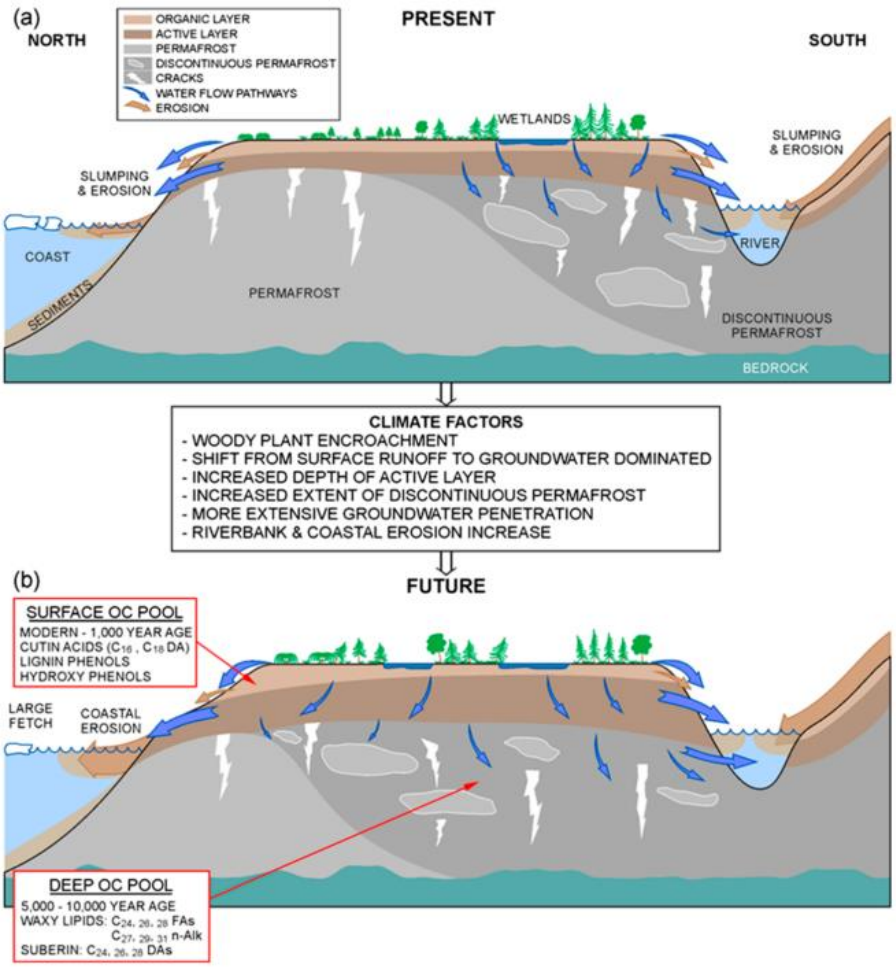

Figure 2.5 Showing current (a) and future projections (b) of terrestrial organic matter distribution and transport in the Arctic region from Feng et al., (2015).

Some permafrost in the Arctic is also found in sub-sea deposits, such as on the continental shelf in Siberia, which became inundated during the Holocene transgression (Bauch *et al.*, 2001). These deposits contain similar amounts of carbon to terrestrial permafrost, together with methane hydrates that are a frozen deposits highly concentrated in methane (Ruppel and Kessler, 2017). Both sub-sea permafrost and hydrate deposits are also susceptible to thawing (Shakhova *et al.*, 2010), however there are still uncertainties as to

the extent of feedbacks to global climate change, should we see continuing increases in Arctic Ocean sea temperatures (Ruppel and Kessler, 2017).

Across the Arctic, sediment grain size decreases with increasing distance from the coast, which is mainly caused by the high energy in shallow water resulting in the winnowing of fine material and deposition in deeper and less energetic shelf regions (Dudarev *et al.*, 2006). This could have a major impact on the transport of terrestrial OM across the shelf system as certain types of organic matter have been associated with distinct grain sizes. Indeed, analyses of different fractions obtained using the split flow thin-cell fractionation (SPLITT; Gustafsson *et al.*, 2000) method indicate that hydrodynamic sorting exerts first-order control on the redistribution of terrestrial OC by selectively mobilising the fraction of OC sorbed onto fine-grained particles while matrix free plant debris preferentially accumulates near the coast with coarse-grained sediments (Tesi *et al.*, 2016).

2.4 Regional considerations

It is clear from the many scientific studies focusing on the Arctic region that the interactions between ocean, ice, atmosphere and land mean it cannot be considered as one large region in the context of climate change. In fact, the Arctic contains many distinct areas that interact with each other in different ways depending on the region's location. Hence, two key contrasting regions of scientific interest were identified and are discussed in the next sections. The first is the East Siberian Arctic Shelf (ESAS) area, a key region for studying significant terrestrial inputs of TerrOM (Martens *et al.*, 2021; Fig. 2.6). In contrast, the second region, the Barents Sea and Fram Strait is a region of high marine productivity and nutrient input and outflow from the Arctic.

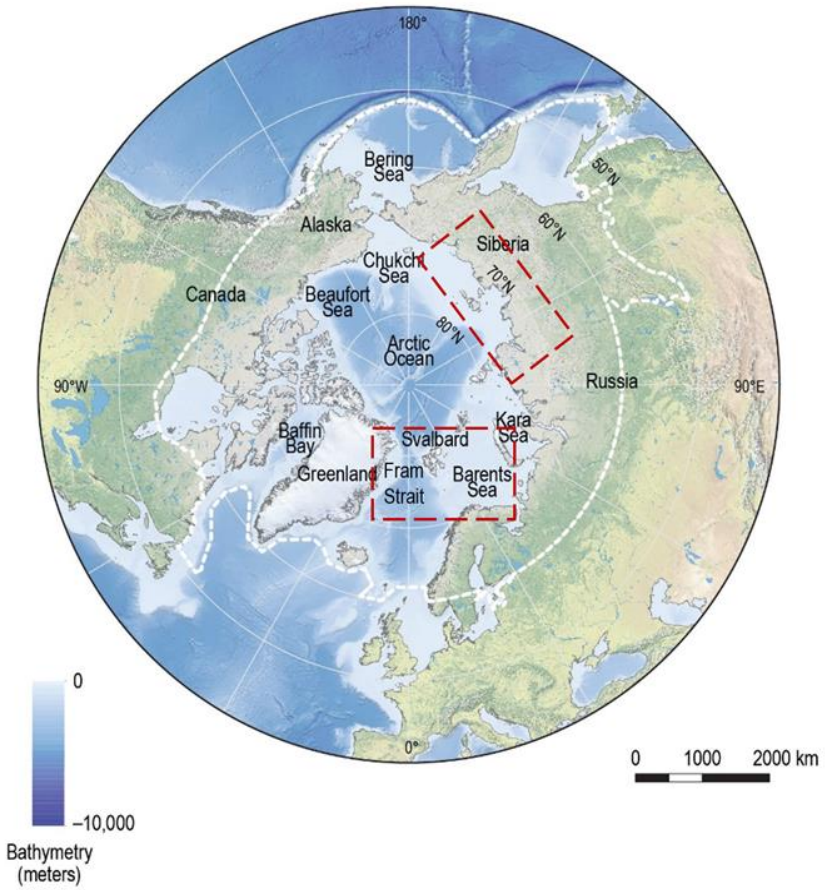

Figure 2.6 The Arctic region with white dashed line representing approximate boundary for arctic region in relation to particular cryosphere or oceanic components. Dashed red lines indicate case study regions for this project. Adapted from IPCC, 2019.

2.4.1 The East Siberian Arctic Shelf

The ESAS is situated along the most northern coastline of Siberia, Russia, and presents a complex regime (geochemically, hydrologically and biologically) where a shallow continental shelf (half of which is less than 30m deep; Jakobsson *et al.*, 2008) meets the Arctic Ocean. The ESAS forms part of the Eurasian Arctic Shelf, which is the biggest continental shelf on Earth and covers approximately a third of the Arctic Ocean (Sánchez-García *et al.*, 2011a; Fig. 2.7).

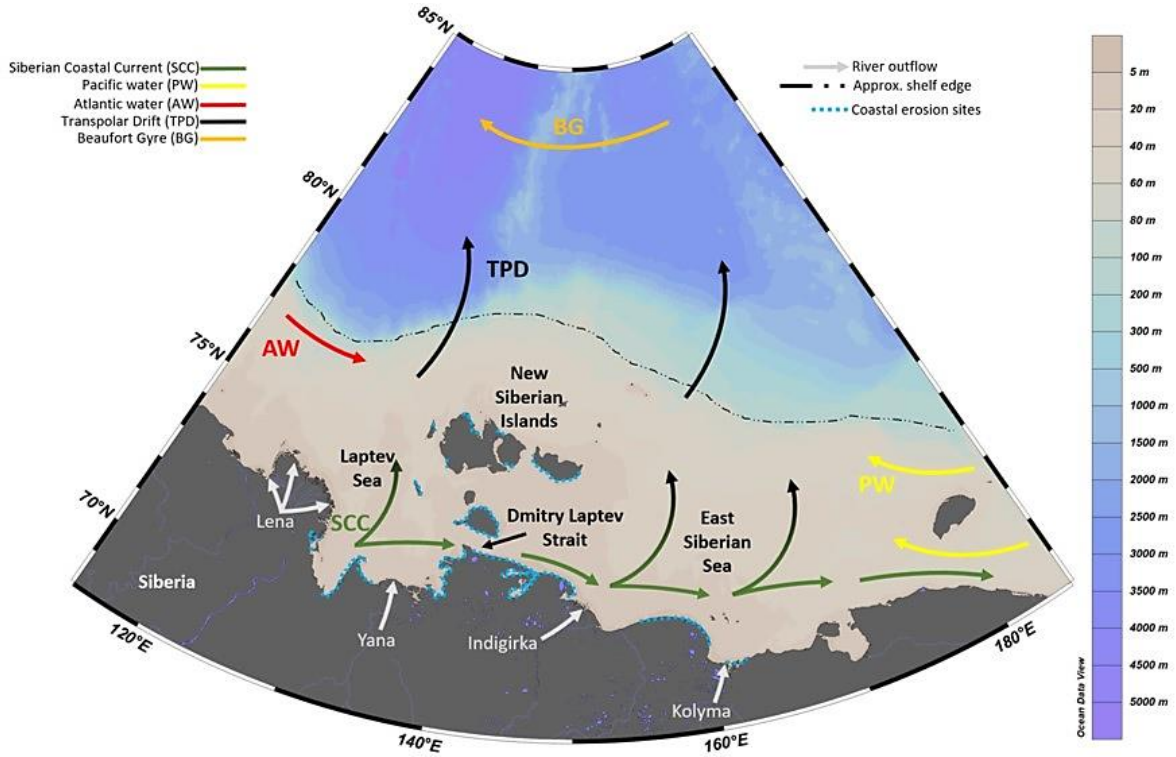

Figure 2.7 Schematic of the East Siberian Arctic Shelf (ESAS) indicating general circulation of water masses and river inputs with coloured arrows; Siberian Coastal Current (SCC), Pacific water (PW), Atlantic water (AW), Transpolar Drift (TPD), Beaufort Gyre (BG) and grey arrows labelled with river outflows. Dashed black lines indicates the approximate position of the shelf edge where there the deep basin starts. Dashed blue lines along the coastline indicate areas undergoing enhanced rates of coastal erosion (>1 m yr^{-1}, Lantuit et al., 2011). Colour bar on left represents water depth across the shelf, slope and deeper basin. Base map created in Ocean Data View.

The interplay of the terrestrial and marine domains within the shelf region are the main drivers in creating this unique environment. There are four rivers delivering freshwater and sediment to the shelf which transport the majority of their discharge during the 'spring freshet' as temperatures increase from the winter (Holmes *et al.*, 2012; see Table 2.1). The

Lena, Indigirka and Kolyma form three of the five Great Russian Arctic Rivers, GRARs, and drain from an area of 3680 × 10^3km^2 which is almost entirely underlain by continuous permafrost, particularly in the Eastern regions (Sparkes *et al.*, 2018). As temperatures increase across these watersheds, the amount and depth of thawing permafrost is increasing, leading to longer and stronger freshets and further fluvial erosion as the rivers have extra energy (Feng *et al.*, 2015).

Table 2.1 Average discharge and sediment delivery annually (1970-1995) for the four major rivers along the East Siberian Arctic Shelf (Gordeev, 2006).

River	Discharge Km^3yr^{-1}	Sediment $Mt\ yr^{-1}$
Lena	523	21
Yana	32	4
Indigirka	54	11
Kolyma	122	10

A distinctive feature of the ESAS coastline are the Pleistocene Yedoma ice complex deposits (ICDs; Fig. 2.4b); these are formed of frozen water and sediment and are particularly susceptible to warming due to their high water content (Section 1.2). The ICDs also form a large part of the sediment load delivered to the shelf as they are subject to thawing in a similar way to terrestrial permafrost (Vonk *et al.*, 2012a). Elevated mean air/water temperatures have led to these deposits being undercut and eroded, as ice cover decreases and wave action increases and sea level rises at an alarming rate (blue dashed line Fig. 2.7; Hoque and Pollard, 2016). Collectively, the increase in river discharge and erosion of coastal ICDs and subsequent degradation of the organic matter released through these pathways has led to observed increases in acidification of the shelf seas. Projections for the future show further increases in acidification, especially with increasing temperatures reducing the capacity of the oceans

as a CO_2 sink, which will likely be translocated across the Arctic Ocean and not just a feature of the ESAS alone (Semiletov *et al.*, 2016).

The ESAS is subject to diverse coastal and oceanic currents, which further complicate hydrographic systems (Fig. 2.7). The Siberian Coastal Current (SCC) flows along the Siberian coastline from West to East through the Dmitry Laptev Strait and as it does so incorporates, at least in part, outflows of the major rivers alongside ICD sediment input. The addition of fresher river water to the SCC likely gives it its buoyancy and is a major factor in the strength of the current, giving it a similar seasonality to that of the rivers in the region (Weingartner et al., 1999). Branches of the SCC are driven northwards from the pull of the Transpolar Drift (TPD) and Beaufort Gyre (BG), where mixing of a number of different water masses occurs and SCC water is either transported across the central Arctic Ocean towards to the Fram Strait via TPD or enters the BG oscillation (Weingartner and Danielson, 1999). The TPD system is also responsible for the transport of sea ice from the Laptev and East Siberian Seas to the Fram Strait and beyond (Charette *et al.*, 2020). The degree to which TPD incorporates Siberian-origin water and ice is heavily dependent upon the strength of Arctic Oscillation. During negative phases, the TPD originates primarily from the ESAS region whereas during positive phases the TPD moves eastward to incorporate Pacific origin water also (Charette *et al.*, 2020). A biogeochemical difference between the western and eastern regions of the ESAS has been noted previously (e.g. Semiletov, 2005; Karlsson *et al.*, 2015) and has been partly attributed to the influx of Pacific-origin waters in East Siberian Sea. These enter the Arctic basin through the Bering Strait and branch off towards the ESAS, Chukchi Sea and Beaufort Sea. Pacific waters originate from a distinct biogeochemical system that is typically associated with higher concentrations of macronutrients and therefore imparts a very different signature to that of Atlantic or central Arctic Ocean origin waters (Granger *et al.*, 2013, 2018; Buchanan

et al., 2022). The isotopic signature of Pacific origin nitrate is usually more enriched in ^{15}N (~8‰) relative to Atlantic and Arctic waters (Atlantic Halocline ~5.6‰), although this can fluctuate during the seasons and occurs due to differences in nitrogen cycling between these basins (Granger *et al.*, 2018). The input of Pacific-origin water to the East Siberian Sea supports higher rates of primary production in the region (5-10 times higher than that of the western region; Carmack and Wassmann, 2006) and leads to notable increases in marine particulate organic matter compared to the western regions (Brüchert *et al.*, 2018). A modified branch of Atlantic origin water, sometimes referred to as Atlantic Arctic Water, enters the Laptev Sea from the west (Fig. 2.7) which is characterised by high salinity and lower nutrient load than Pacific origin water (Bauch *et al.*, 2011).

As with water mass provenance in the region, shelf sediments form a complex picture with organic matter originating from rivers and terrestrial permafrost, coastal erosion and marine productivity. Due to the thawing of the permafrost river basins in Eastern Siberia and undercutting of ICDs there has already been an increase in the export of TerrOM to the shelf and projections show this to only increase further as temperatures continue to rise (IPCC, 2014).

The fate of this TerrOM is a topic of interesting debate and was the major draw for multiple cruises in the last decade, particularly the ISSS-08 and SWERUS-C3 cruises (Semiletov and Gustafsson, 2009). This is why, primarily due to the large volume of research and its unique characteristics with ICDs, permafrost and river all interacting in one region, the focus of this review is on the ESAS. Prior to the extensive research completed from the two fieldwork campaigns mentioned above, it was thought that TerrOM in the Arctic behaved conservatively and was comparable with global mechanisms (Stein and MacDonald, 2004).

TerrOM was thought to be more refractory than marine organic matter and mechanisms for its removal were thought to be limited (Canuel and Martens, 1996; Hedges and Oades, 1997; van Dongen *et al.*, 2000). However, analysis of the ESAS sediments shows a different narrative, a large fraction of the material transported by the rivers is being degraded close to the point of origin, which indicates the feedback for the global carbon cycle has been severely underestimated as has its impact on greenhouse gas emissions (e.g. van Dongen *et al.*, 2008; Karlsson *et al.*, 2011; Sánchez-García *et al.*, 2011b; Tesi *et al.*, 2014; Doğrul Selver *et al.*, 2015; Bröder *et al.*, 2016).

Further studies over the last decade have shown that there is a substantial amount of organic matter being delivered to the ocean via coastal erosion (rather than purely riverine material) acting as another integrator for land ocean exchanges (Vonk *et al.*, 2012a; Feng *et al.*, 2013; Doğrul Selver *et al.*, 2015). In fact, most of the TerrOM that is delivered to the shelf derives from erosion at the coastline typically from ICD's (Vonk *et al.*, 2012a; Tesi *et al.*, 2014). Material derived from ICD's typically goes through less alteration and degradation than riverine material (Feng *et al.*, 2015), although still does not act uniformly and is more labile than thought (Sparkes *et al.*, 2016). This trend is reflected in the increasing resistance to degradation along a west to east transect where age increases and degradation decreases, thought to be caused by the colder and drier climate but also by the greater abundance of coastal ice complex deposits (Feng *et al.*, 2015). As is the case for fluvial-derived material, erosion of ICDs also leads to degradation close to the coast within the water column which is an additional positive feedback as degradation usually leads to the outgassing of carbon dioxide (Vonk *et al.*, 2012).

2.4.2 The Barents Sea and Fram Strait

Another key region of interest is the area in which Atlantic water flows into and Polar water flows out of the Arctic basin; this comprises of the Barents Sea opening and the Fram Strait (Fig. 2.8). The Barents Sea opening starts at the most northern point of mainland Norway and stretches to the most southerly reaches of Svalbard, a Norwegian archipelago in the Arctic. The Fram Strait stretches from the North-East coastline of Greenland to the West coast of Svalbard (Fig. 2.8).

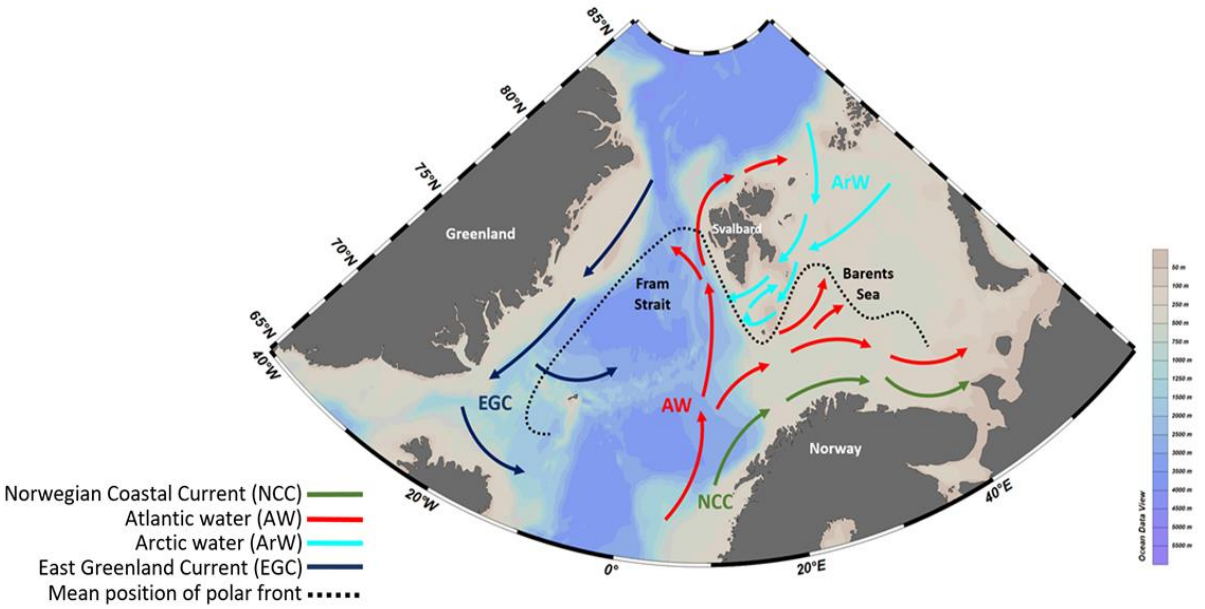

Figure 2.8 Schematic of Fram Strait and Barents Sea case study site indicating general circulation of water masses with coloured arrows; Atlantic Water (AW), Artic Water (ArW), East Greenland Current (EGC) and the Norwegian Coastal Current (NCC). Dashed black line indicates mean position of polar front, Barents Sea front from Stevenson *et al.,* 2020 and Fram Strait front from Perner *et al.,* 2019. Base map created in Ocean Data View.

Warm and saline Atlantic water flows in through these two openings, as it does, it branches off to the east into the Barents Sea, mixing with the Norwegian Coastal Current and to the north where it forms the West Spitsbergen Current; eventually both branches make it into the deep Arctic basins. The trajectory of these water masses entering the Arctic basin is largely controlled by bathymetry of the shelf and trough systems found throughout these

regions (Knies, 2005). Colder and less dense polar water enters the Barents Sea from the North and where it meets the Atlantic waters, a polar front is expressed through changes in sea surface temperature, salinity and nutrient concentrations (Barton *et al*., 2018). In the Fram Strait, the polar waters exit the Arctic basin *via* the East Greenland Current system (Våge *et al.*, 2018). This also transports sea ice southward and produces an east-west divide across the Strait which is marked by a front where the two main water masses meet (East Greenland Polar Front System: Paquette *et al.*, 1985).

Across these regions, the increase in both Atlantic water heat transfer and atmospheric temperatures are driving a reduction in multiyear sea ice cover and earlier ice breakup periods (Onarheim *et al.*, 2014). These change the structure of the region's seas to a more Atlantic regime ('Atlantification'; Lind *et al.* 2018), and cause the polar front to move further north as temperatures increase (Oziel *et al.*, 2020). Light availability was thought to be the main limiting factor in Arctic primary productivity, as the summer bloom was typically triggered by the spring/summer sea ice thawing. However, the reduction in sea ice means nutrient availability will likely surpass this in importance now and into the future, as multiyear ice decreases in extent and nutrient import from the Atlantic and Pacific increases (Tuerena *et al.*, 2021). The inputs of nutrient rich waters to these regions hold particular importance for the plankton community composition and dynamics, adding to the increased productivity measured as Atlantic waters encroach into Arctic basins further (Knies, 2005; Arrigo and van Dijken, 2015). In the Barents Sea and Fram Strait these changes in the physical environment have impacts on all parts of the ecosystem and consequently nutrient cycles and organic matter sedimentation (Faust *et al.*, 2020).

Marine surface sediments found across the Barents Sea and Fram Strait can have many organic matter inputs from differing sources depending on the sampling location (Freitas *et al.*, 2020). For example, the association to terrestrial inputs from coastal erosion, glacial melt and terrestrial matter entrained in sea-ice, which can be more resistant to degradation and be less reactive than fresher sources (Freitas *et al.*, 2020). Marine primary productivity can also contribute significant amounts of organic matter to the seafloor, particularly around areas of increased nutrient input and higher productivity such as marginal ice zones and during bloom periods (Knies and Martinez, 2009).

$\delta^{13}C_{TOC}$ and ratios of total organic carbon to total nitrogen (C/N ratio) are commonly used tools in the region to determine the source and fate of sedimentary organic matter (e.g. Schubert and Calvert, 2001; Knies and Martinez, 2009; Sanchez-Vidal *et al.*, 2015; Koziorowska, Kuliński and Pempkowiak, 2016; Kumar *et al.*, 2016). These indices indicate that there are clear sub-regions within the area that are impacted by the influx of TerrOM more than others. The areas close to the coast of Svalbard and inner fjords exhibit what would be expected for typical terrestrially-influenced sediments with lighter $\delta^{13}C_{TOC}$ values and higher C/N ratios (-25.2‰ and 20-50, respectively; Knies and Martinez, 2009). In contrast, a higher amount of marine organic matter is found in the South Western Barents Sea and along the marginal ice zone where primary productivity is higher, marked by heavier $\delta^{13}C_{TOC}$ and lower C/N ratios (-21.2‰ and 7-15, respectively; Knies and Martinez, 2009). The Fram Strait region is characterised by a more marine-dominated system as expected in a somewhat open ocean environment influenced by influxes of major water masses and seasonality in primary productivity (Hebbeln, Wefer and Geowissenschaften, 1991)

2.4.3 Key outcomes of regional reviews

1. The ESAS and Barents Sea/ Fram Strait regions do indeed have very different and complex systems. Whereby, the organic matter export in the ESAS is largely controlled by riverine and coastal erosion input which is in contrast to the Barents Sea and Fram Strait where marginal ice zones and mixing of water masses dominate organic matter composition. Highlighting the need for more regionally-focussed research with good spatial resolution to fully understand processes and implications for the wider Arctic region.
2. Justifiably the majority of research focus, particularly in the ESAS, has been around the carbon cycle and its feedback to global climate change. This is still a very prominent area of research with much still up for debate, evident in the scientific literature.
3. Less is known about the nitrogen cycle, its speciation and mechanisms of change in comparison to the carbon cycle. If research thus far suggests an increase in organic matter and carbon entering the Arctic basins as a whole then it would be reasonable to assume this equally leads to an increase in nitrogen, highlighting the need for further investigation.

The sections below illustrate why it is becoming increasingly important to understand nitrogen cycling in the Arctic Ocean regions and how terrestrial inputs have a significant role to play as they do in the carbon cycle.

2.5 Nitrogen in the Arctic

The nitrogen cycle within the worlds' oceans is a complex system and because of its strong links to other elemental cycles, like carbon, it can have impacts of the global climate. There are transactions within the cycle that add to the fixed or retained nitrogen pool, such as deposition of N_2 from the atmosphere and biological N_2 fixation. When diazotrophs directly fix N_2 in the ocean they convert it to ammonium (NH_4^+) which is much more biologically available than the original gaseous form (Pajares and Ramos, 2019). Ammonium is assimilated into particulate organic matter (phytoplankton) and through progressive oxidation is converted to nitrite (NO_2^-) and nitrate (NO_3^-) in a process known as nitrification, this is a pathway for the release of nitrate into the oceans (Hutchins and Capone, 2022). Nitrite can also be converted back to nitrogen gas through a process known as denitrification, this is a sink of fixed nitrogen in oceans, which can also occur in sediments (Robinson *et al.*, 2012). The consumption of particulate organic matter leads to remineralization and the subsequent release of ammonium (Hutchins and Capone, 2022).

Inorganic nitrogen compounds in the surface waters of the oceans tend to be the limiting macronutrient (relative to phosphate and silicate) in the growth of phytoplankton meaning that changes in the availability of nitrogen will affect the food chain from the bottom up (Dauwe and Middelburg, 1998; Dittmar, Fitznar and Kattner, 2001). Phosphate concentrations in the oceans also influence phytoplankton abundance and growth and are intrinsically linked to the amount of nitrogen available to organisms, in some settings organisms fixing nitrogen may be limited by the availability of phosphorus (Paytan and McLaughlin, 2007). Silicate is an important nutrient primarily for diatoms, which use it to make biogenic silica forming the external layers of cell walls (Rey, 2012; Ward *et al.,* 2022).

Organic nitrogen may also be important with it being are one of the dominant sources of bioavailable nitrogen to the Arctic Ocean (Dittmar, 2004). It is therefore important to understand the fate of organic nitrogen compounds, particularly the fate of terrestrial inputs. A recent study by Terhaar *et al*. (2021) suggested that between 28-51% of current primary production in the Arctic Ocean is fuelled by inputs of nutrients from rivers and coastal erosion. An essential part of this system, involved in the transport of river and coastal erosion derived material to the central Arctic Ocean, is the ESAS region. Nutrients delivered from here are cycled through the central basin and their signal is still detected in the only deep major outflow from the Arctic Ocean, the Fram Strait (Buchanan *et al.*, 2022). However, the little work that has been completed on the terrestrial organic nitrogen delivered to the ESAS involves bulk techniques such as bulk isotope analysis ($\delta^{15}N$), elemental analysis (TOC/TN ratios) and determination of macromolecular component analyses by flash pyrolysis (Sparkes *et al.*, 2016). The latter, for instance, allows the relative proportion of terrestrial vs marine derived OM to be determined, yielding valuable information about the origin/fate of the material. More specifically, the relative proportions of phenols (lignin derived and thus of terrestrial origin) to pyridines (N-rich, mainly from proteins and considered to be a pseudo 'marine N-rich' compound class, which can be found in terrestrial settings but in this instance represents a marine marker) has been applied as a novel ratio for determining the source of macromolecular organic matter. When applied to the ESAS, this shows a clear trend (Fig. 2.9)

offshore from terrestrial to marine derived macromolecular organic matter, which is further supported by elemental data (TOC/TN and $\delta^{15}N$).

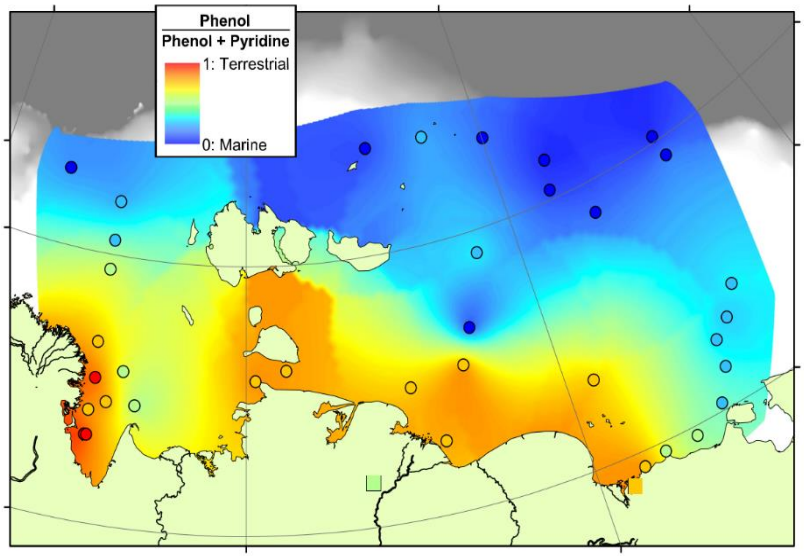

Figure 2.9 Phenol to pyridine ratio along the ESAS, from Sparkes et al., 2016.

$\delta^{15}N_{Bulk}$ of marine sediments has been used as a source indicator alongside $\delta^{13}C_{TOC}$ to determine relative inputs from marine and terrestrial end-members (e.g. Schubert and Calvert, 2001; Gaye *et al.*, 2007; Guo, Ping and Macdonald, 2007; Nagel *et al.*, 2009; Calleja *et al.*, 2013; Tesdal, Galbraith and Kienast, 2013). When dissolved nitrogen is fixed by microbes in the ocean it retains the isotopic composition of the nitrogen source, meaning no isotopic fractionation is imparted and therefore can be used to track sources of nitrogen (Robinson *et al.*, 2012). The nitrogen source can also be influenced by water column processes such as denitrification and remineralization, both of which can have an associated isotopic fractionation. The lighter isotope of nitrogen is preferentially consumed by phytoplankton, in the case of complete nitrate utilisation the isotopic effect is negligible however in the case of incomplete consumption, there are some isotope effects depending on the form of nitrogen being consumed (nitrate, nitrite, ammonium and urea; Sigman and Casciotti, 2001). It is expected that particulate organic matter is lowest in $\delta^{15}N$ at the surface and can be due to

the fixation of N_2 at the surface and the recycling of N_2 by heterotrophic processes. As particles sink through the water column the lighter isotope is preferentially consumed through remineralisation which leads the remaining pool becoming enriched in the heavier isotopes (Sigman and Casciotti, 2001). The shorter the residence time in the water column (e.g. shallow depths) the less time a particulate has to be altered so is more likely to reflect surface values, this is similar for areas of high sedimentation rates such as on continental margins (Robinson *et al.*, 2012). It is also the case for highly productive areas or regions under planktonic blooms in that the effects of depth on the $\delta^{15}N$ of particulates are negligible and reflective of the $\delta^{15}N$ of particulates at the surface (Robinson *et al.*, 2012). Once particles have settled at the sediment water interface and begin sedimentation there is the possibility for further alteration of the $\delta^{15}N$ isoscape, typically a larger isotopic shift is seen in areas with low sedimentation rates compared to those of higher. The isotopic alterations are largely due to the preferential break down of these labile compounds through remineralisation and denitrification. In areas of lower sedimentation there has been shown to be an increases in sedimentary $\delta^{15}N$ due to the preferential consumption of the lighter isotope and subsequent enrichment of the remaining pool by bacteria in the sediments (Robinson *et al.*, 2012; Brahney *et al.*, 2014).

In a high Arctic fjord a strong correlation between $\delta^{15}N_{Bulk}$ and $\delta^{13}C_{TOC}$ was interpreted to be as a consequence of increased autochonthous production which led to heavier $\delta^{13}C_{TOC}$ and subsequently a more complex food web structure and therefore heavier $\delta^{15}N_{Bulk}$ values (Koziorowska et al., 2016). In the Kara Sea, isotopically lighter values in $\delta^{15}N_{Bulk}$ were interpreted as a feature of the increasing contribution of less degraded organic matter from thicker permafrost horizons (Nagel *et al.*, 2009). Across the Siberian coastline, a pattern of decreasing $\delta^{15}N_{Bulk}$ was attributed to permafrost catchment areas and the result of a mixing

with marine organic matter and some degree of diagenesis (Guo *et al.*, 2004). Diagenesis relating to nitrogen is typically associated with the fast break down of labile nitrogen containing compounds such as proteins in comparison to carbon rich compounds which are more refractory.

Within organisms, $\delta^{15}N_{Bulk}$ is used as an indicator of food web structure, trophic position and foraging pathways. This is due to the enrichment of $\delta^{15}N_{Bulk}$ with each successive trophic level (Fig. 2.11; Bowes and Thorp, 2015). In order to successfully determine a trophic position or a food web structure, a well resolved baseline is needed; this is the $\delta^{15}N_{Bulk}$ at the base of the food web from primary producers (also known as the isoscape; West *et al.*, 2010). In the Arctic, this is a particular challenge due to the influence of different water masses and fresh water inputs. There are two distinctly different water masses both in their nutrient composition and physical characteristics, derived from the Atlantic and the Pacific and this is complicated by increasing seasonal contributions of nutrients from terrestrial sources (Terhaar *et al.*, 2021; Buchanan *et al.*, 2022). The Pacific waters tend to have heavier $\delta^{15}N$ values for both inorganic and organic nitrogen than their Atlantic counterpart due to differences in the strength of the biological pump and nitrogen cycling within these basins (Somes *et al.*, 2010; Sigman and States, 2019; Vega *et al.*, 2021). This further supports a case study approach to the Arctic, to resolve baseline variations which could in part be related to true changes in food web structure but also alterations due to changes in varying contributions from water masses (Vega *et al.*, 2021).

The increased river discharge in Arctic rivers due to climate change (Dittmar and Kattner, 2003) will therefore likely cause an increase in the amounts of organic nitrogen delivered to the Arctic shelves, potentially impacting the marine ecosystem. The organic

matter delivered via the Arctic rivers is thought to be almost entirely of terrestrial origin, mainly due to the low autochthonous production in these rivers which does not contribute significantly to the organic matter pool (Dittmar, Fitznar and Kattner, 2001; Dittmar and Kattner, 2003). Shelf sediments also receive marine inputs, typically from decaying phytoplankton in the form of particulate and dissolved nitrogen; these tend to be more enriched in nitrogen relative to carbon when compared to their terrestrial counterparts (Dittmar, Fitznar and Kattner, 2001).

$\delta^{15}N_{Bulk}$ is a very useful tool but like other bulk parameters it has its limitations that should always be considered when interpreting results. Several issues have been identified with this method in marine sediments particularly:

1. The $\delta^{15}N_{Bulk}$ represents marine organic nitrogen, terrestrial organic nitrogen and inorganic nitrogen, and their relative contributions are hard to unravel (Tesdal *et al*., 2013).
2. $\delta^{15}N_{Bulk}$ can fractionate during diagenesis leading to over or under estimations of the nitrogen delivered to the seafloor, sometimes due to selective preservation or removal of certain compound mediated by bacteria (Batista *et al.*, 2014).
3. Depending on utilization of inorganic nitrogen sources by primary producers in surface waters, the isotopic composition of sinking particulate matter that eventually makes its way to the sediments will vary.

Due to these limitations it is important to delve further into the nitrogen pool, principally the organic nitrogen fraction as this can provide insights baseline isoscape variations without interference from inorganic components.

2.5.1 Amino acids

Protein amino acids are important as these account for a large proportion of the total organic nitrogen found in organisms and can be present in significant amounts in recent sediments (Burdige and Martens, 1988; Cowie and Hedges, 1992; Dauwe and Middelburg, 1998; Dittmar, Fitznar and Kattner, 2001; Carstens *et al.*, 2013). The availability of these compounds depends upon the matrix they are in and whether or not they have undergone bacterial remineralization; amino acids that are free and labile will enhance secondary or bacterial productivity in coastal areas, whereas more refractory matter is unlikely to be taken up or metabolised and therefore will persist further offshore (Dittmar, 2004). Typically, marine phytoplankton and POM in the water column are more enriched in amino acids than sediments found at the seafloor (Cowie and Hedges, 1992; Armannsson, 1999). The biggest contributor to sedimenting organic nitrogen is the particulate fraction, hydrolysable amino acids can contribute up to 60% of this (Dittmar and Kattner, 2003).

Early work on amino acids investigated whether different sources of organic matter had different compositions of individual amino acids, but it was found that no amino acid is completely unique to a single origin and protein amino acids in particular are not source indicative (Burdige and Martens, 1988; Cowie and Hedges, 1992; Dauwe and Middelburg, 1998). However, on a broader basis, bacterially derived matter is enriched in D-amino acids and phytoplankton is enriched in L-amino acids. Though this should not be used a definitive indicator of origin as diagenetic reactions in the water column and in terrestrial soils where there is selective preservation can modify these (Burdige and Martens, 1988; Dittmar, Fitznar and Kattner, 2001). The enantiomeric distributions of some amino acids can indicate the extent of diagenetic modification since during diagenesis. D-amino acids are likely to increase

in relative concentration as they form bacterial cell wall constituents and therefore are less accessible to bacterial remineralization (Burdige and Martens, 1988; Cowie and Hedges, 1992; Dauwe *et al.*, 1999; Dittmar, Fitznar and Kattner, 2001). Therefore, elevated concentrations of these enantiomers and non-protein amino acids (e.g. B-Alanine) are associated with a high degree of diagenesis (Cowie and Hedges, 1992).

Amino acids are often split into different groups. Typically for biological samples two groups are identified, essential (EAA; threonine, valine, methionine, leucine, histidine, lysine and phenylalanine) and non-essential amino acids (NEAA; aspartic acid, proline, glutamic acid, serine, glycine, alanine and arginine; e.g. Dauwe and Middelburg, 1998; McMahon and McCarthy, 2016; Webb *et al.*, 2016; Grosse *et al.*, 2021). Essential amino acids are those that cannot be synthesised within most organisms and must be ingested through dietary routes, on the other hand non-essential amino acids are those that can be synthesised from dietary proteins or *via* their *de novo* biosynthesis (Bromke, 2013). Grosse *et al.* (2021) revealed that across the Fram Strait, EAAs were enriched in the particulate fraction and NEAAs were enriched in the dissolved fraction. The partition was explained by the particulate amino acids (PAA) representing live organisms that can synthesise the full suite of amino acids whereas the total dissolved amino acids (TDAA) represented a pool degraded by heterotrophic bacteria.

Earlier studies split amino acids depending on their functionality or charge class; where aspartic acid and glutamic acid form the acidic group; glycine, alanine, valine, isoleucine and leucine the neutral group; histidine and arginine the basic group; tyrosine and phenylalanine the aromatic group; methionine the sulphidic group and serine and threonine the hydroxylic group (e.g. Dauwe and Middelburg, 1998; Fig. 2.10). Grouping amino acids in

this way revealed a dominance of the neutral group across eastern North Sea sediments sites but there was little compositional variance in these groups and furthermore, differences in individual amino acid patterns were obscured (Dauwe and Middelburg, 1998). The final grouping that has been used, particularly in sediments, is the affiliation of certain amino acids to cell constituents. Some amino acids are more concentrated in cell walls (e.g. glycine) and are thought to be more refractory than amino acids which are concentrated in cell plasma (e.g. glutamic acid and phenylalanine; Dauwe and Middelburg, 1998). Studies employing this kind of grouping found glycine to be concentrated in sediments deemed degraded, influenced by terrestrial inputs or at deeper sediment depths where amino acid concentrations decrease (Dittmar, Fitznar and Kattner, 2001; Dittmar and Kattner, 2003; McCarthy *et al.*, 2007). In contrast, the amino acids that are concentrated in cell plasma degraded at a quicker rate and were depleted with increasing degradation and with sediment depth (Dauwe and Middelburg, 1998; Batista *et al.*, 2014).

While amino acids form a large proportion of sedimenting organic nitrogen (Burdige and Martens, 1988), their concentrations typically decrease with depth alongside a decrease in TOC and TN. The concentrations of individual amino acids found in sediments also depends on diagenetic pathways, hence Dauwe *et al.*, (1999) formulated a degradation index (DI) that estimates the extent of diagenetic alteration of organic matter in marine environments using (protein) amino acid concentrations (Eqn. 2.1),

$$DI = \sum \left[\frac{var_i - AVG\ var_i}{STD\ var_i} \right] x\ fac.coef_i \qquad \text{Equation 2.1}$$

In which var_i is the molar percentage of amino acid (i), AVG var_i and STD var_i are its mean and standard deviation in a data set and $Fac.coef_i$ is the factor coefficient for amino acid (i) (Dauwe *et al.,* 1999). A complete description of the variables can be found in Calleja *et al.*, (2013).

When applied to some of the large Arctic Russian Rivers, it was found that dissolved amino acids were more degraded than particulate amino acids found in rivers and nearshore samples. When the DI was compared with D-amino acid trends by Dittmar, Fitznar and Kattner (2001) it became evident that the index does not show set states of diagenesis but instead echoes various routes of degradation. Dittmar, Fitznar and Kattner (2001) found that for the dissolved fraction of amino acids in Arctic rivers that the DI was on average -1 indicating considerably degraded organic matter.

Although these studies are a good indication of the fate of terrestrial organic nitrogen in the Arctic regions, they do not fully explain the source and potential impact on food webs of individual protein amino acids (Fig. 2.10). For this to be fully characterized there is a need for compound specific isotope analysis to decouple effects that bulk parameters encompass.

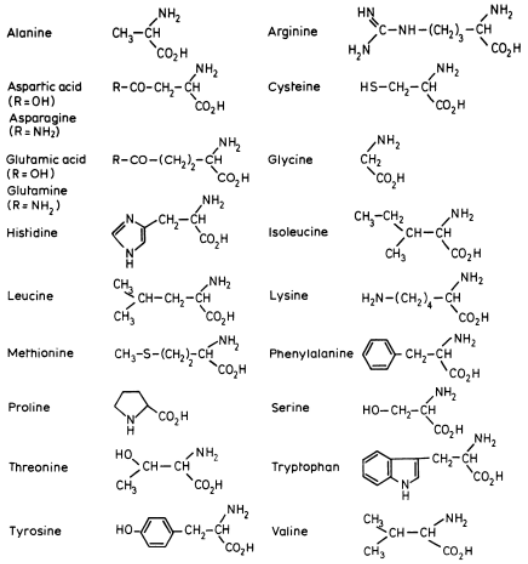

Figure 2.10 Protein amino acids from Hardy, (1985)

2.5.2 Compound Specific Isotope Analysis for Amino Acids (CSIA-AA)

Compound specific isotope analysis of $\delta^{15}N$ in amino acids (CSIA-AA) is a technique that has primarily been used on animal tissue, dissolved and particulate organic matter; there are few studies that focus on marine sediments (McClelland and Montoya, 2002; Chikaraishi *et al.*, 2007; McCarthy *et al.*, 2007; Carstens *et al.*, 2013; Batista *et al.*, 2014). Typically this approach is used to determine the trophic position of a specific organism within a food web (Fig. 2.11; Bowes and Thorp, 2015); hence, some amino acids are isotopically fractionated during trophic transfer or transamination (trophic amino acids or Tr-Aas) while others remain relatively unchanged and represent the baseline of the food web (source amino acids or Src-Aas). Tr-Aas have a carbon-nitrogen bond which cleaves during a trophic transfer, for example glutamic acid and aspartic acid (Carstens *et al.*, 2013), whereas in Src- C-N bonds remain intact during trophic transfer, therefore there is no fractionation effect (Carstens *et al.*, 2013).

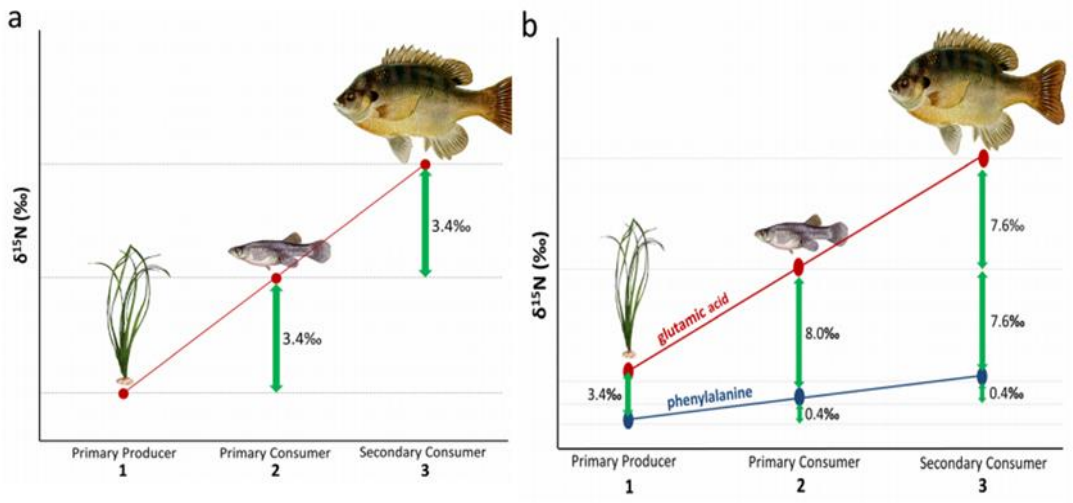

Figure 2.11 $\delta^{15}N$ changes related to changes in trophic position (x-axis). Bulk tissue used in (a) and CSIA-AA used in (b). (Bowes and Thorp, 2015).

McCarthy *et al.*, (2007) first used the isotopic differences between mean $\delta^{15}N$ of source and trophic amino acids to determine the number trophic transfers (ΔTr) undergone (Eqn. 2.2):

$$\Delta \boldsymbol{Tr} = \left[\Delta \boldsymbol{\delta^{15}N_{sample}} - \Delta \boldsymbol{\delta^{15}N_{phytoplankton}}\right] / \mathbf{4.67} \qquad \text{Equation 2.2}$$

ΔTr is calculated using the difference between average amino acid isotopic compositions from the sample and phytoplankton ($\Delta\delta^{15}N$ = AVG $\delta^{15}N$ (Asp, Glu, Leu, Val, Pro) – AVG $\delta^{15}N$ (Phe and Threonine)) and +4.67 is the change in $\delta^{15}N$ for a single trophic transfer (McCarthy *et al.*, 2007). Although this method cannot be used for sediments due to the lack of fresh plankton found in sedimenting organic matter, later Chikaraishi *et al.*, (2009) described a similar equation (Eqn 2.3) which could be applied to sediments. Source AAs provide vital information about the origin of $\delta^{15}N$ at the base of the food web while trophic AAs illustrate the history of trophic transfer (McClelland and Montoya, 2002). Trophic position can be calculated by comparison of the trophic and source AAs $\delta^{15}N$ composition (Chikaraishi *et al.*, 2009). Chikaraishi *et al.* (2009) applied the following trophic position equation (TP; Eqn 2.3) to their studies using phenylalanine and glutamic acid as source and trophic amino acids, respectively:

$$\boldsymbol{TP} = \frac{(\boldsymbol{\delta^{15}N_{Glx}} - \boldsymbol{\delta^{15}N_{Phe}} - \mathbf{3.4}‰)}{\mathbf{7.6}‰} + \mathbf{1} \qquad \text{Equation 2.3}$$

In which 3.4‰ is the difference between $\delta^{15}N$ (Glx) and $\delta^{15}N$ (Phe) for marine autotrophs and 7.6‰ is the trophic enrichment factor (TEF) for nitrogen, this method has also been used in marine sediments (Chikaraishi *et al.*, 2009; Batista *et al.*, 2014).

McCarthy *et al.*, (2007) also suggested another proxy alongside ΔTr known as the 'total heterotrophic amino acid resynthesis' or $\sum V$ (see Eqn. 2.4)

$$\sum \boldsymbol{V} = \frac{\mathbf{1}}{\boldsymbol{n}} \sum |\boldsymbol{X_i}| \qquad \text{Equation 2.4}$$

Where X_i is the difference between individual amino acid $\delta^{15}N$ and average $\delta^{15}N$ ($\delta^{15}N$ -AVG $\delta^{15}N$) and n is the number of amino acids used for calculation (Batista *et al.,* 2014). The proxy uses the deviation of $\delta^{15}N$ of individual trophic amino acids from the average $\delta^{15}N$ of all trophic amino acids and tracks if there has been microbial activity (Batista *et al.*, 2014).

Early studies of marine sediments were concerned about the alteration of amino acid isotopic signatures during transition from water column particulates to sediments, however it has been shown that the signature is well preserved in POM and sedimentary organic matter (SOM) making it possible to do food web studies on detrital and sediment material (McCarthy *et al.*, 2007; Batista *et al.*, 2014). Although Carstens *et al.*, (2013) found that there is some preferential degradation and preservation that occurs during early diagenesis within surface sediments, an increase was observed in $\delta^{15}N$ of individual amino acids surpassing values for $\delta^{15}N_{Bulk}$. This is coupled with a decreasing contribution of amino acids to total organic matter and increasing degradation state possibly demonstrated the preferential degradation of amino acids that causes enrichment in $\delta^{15}N$ (Carstens *et al.*, 2013). Batista *et al.*, (2014) also found a similar trend between $\delta^{15}N_{THAA}$ and $\delta^{15}N_{Bulk,}$ whereby the difference is greatest in freshest samples and decreases through the water column and into the sediments. However, it cannot be excluded that this is caused by the input of isotopically different terrestrial organic and inorganic nitrogen, lowering the $\delta^{15}N_{Bulk}$ (Carstens *et al.*, 2013). Though $\delta^{15}N_{Bulk}$

do not indicate organic nitrogen transport and further work is required to better constrain this.

CSIA-AA could be particularly important in regions like the Arctic, where there are large amounts of fresh water delivered from land, because it examines the principal group of compounds that make up sedimenting organic nitrogen which could impact the food web from the primary producers up (McCarthy *et al.*, 2007; Batista *et al.*, 2014). It also removes effects associated with bulk measurements such as interference from other nitrogen containing compounds (polysaccharides such as chitin, chlorophylls, inorganic nitrogen etc.) which have distinct isotopic signatures (Batista *et al.*, 2014). CSIA-AA of marine sediments has yet to be tested in the Arctic region but provides the capability to understand the contributions of terrestrial organic nitrogen into the Arctic Seas and consequently the food web. This research is vital to generate a baseline for current and future changes of the Arctic food web due to increasing influences of terrestrial organic nitrogen, which has the potential to feed into numerical models and eventually policy making for the Arctic region.

2.6 Aims and objectives of the study

It is clear that a better understanding of the fate of organic matter in the Arctic Ocean is essential, specifically the various sources, its state and fate across the Arctic shelves to the deep Arctic basins. In addition, the origins of organic matter in this region will be particularly important given that there is currently and predicted to be unprecedented change in the amount of organic matter entering the Arctic through changes in primary productivity and terrestrial inputs. There is a strong focus on the organic nitrogen fraction of the sedimentary organic matter as this is far less understood than organic carbon and additionally provides insights in amino acid cycling and baseline isoscape values. Therefore, the overall aim of this project is to better constrain the fate of terrestrial ON during transport across the Arctic Ocean continental coastal shelves using complimentary carbon datasets.

In order to achieve this aim, a number of objectives were identified:

1. Collecting sediment samples on a W-E transect from Svalbard to Greenland on the JR17005 to add to samples previously collected samples (ISSS-08, SWERUS-C3 and JR16006 campaigns).
2. Extending the metadata set from the ESAS to fill in data gaps and analysing JR16006 and JR17005 for $\delta^{13}C_{Bulk}$, $\delta^{15}N_{Bulk}$ and macromolecular analysis using flash pyrolysis (Sparkes *et al.*, 2016).
3. Developing a protocol and setting a method for the analyses of the composition of amino acids in (marine) sediments.
4. Analysing sediments using GC-FID to identify amino acids compositions present in Arctic marine sediments, particularly phenylalanine (Src-AA) and glutamic acid (Tr-AA).

5. Measuring the $\delta^{15}N$ of individual amino acids in surface sediments (0-1cm in ESAS and 0-0.5cm in Barents Sea and Fram Strait) from all viable samples collected
6. Combining new and old data sets of $\delta^{15}N_{Bulk}$, $\delta^{13}C_{Bulk}$, macromolecular data and $\delta^{15}N$ for individual amino acids to interpret cross shelf transport and diagenesis of organic nitrogen in two important Arctic regions.

These objectives will be achieved through two projects, each focussing on a specific Arctic region, that encompass all of the analysis possible during this study to provide a complete overview of both past and new knowledge relating to both study areas.

The research will combine a number of datasets alongside generating a baseline isoscape for specific amino acids in two contrasting regions of the Arctic to enable a better understanding of current change and how this might impact future studies.

Huskies in Longyearbyen, Svalbard, September 2019

Chapter 3

Novel amino acid compositional, isotopic and macromolecular sedimentary analyses provide insights into contrasting biogeochemical regions across the East Siberian Arctic Shelf (ESAS)

Emma C. Burns [1], George A. Wolff [2], Rachel M. Jeffreys [2], Robert B. Sparkes [3], Örjan Gustafsson [4], Bart E. van Dongen [1]

[1]Department of Earth and Environmental Sciences and Williamson Research Centre for Molecular Environmental Science, University of Manchester, Manchester, UK

[2]Department of Earth, Ocean and Ecological Sciences, University of Liverpool, Liverpool, UK

[3]School of Science and the Environment, Manchester Metropolitan University, Manchester, UK

[4]Department of Environmental Science and Analytical Chemistry (ACES) and the Bolin Centre for Climate Research, Stockholm University, Stockholm, Sweden

Manuscript in preparation for submission to Biogeosciences. Supporting information for this manuscript can be found in Appendix 1.

Author Contributions:

E.C.B. wrote the manuscript, carried out the geochemical analyses (py-GCMS, GC-FID and GC-C-IRMS), made the figures and ran all statistical analyses. G.A.W. designed the project, helped with geochemical analyses and the interpretation of the data and edited the manuscript. R.M.J. helped with geochemical analyses, the interpretation of the data and edited the manuscript. R.B.S. carried out previous geochemical analyses on the sample set and aided with interpretation of py-GCMS data. O.G. collected the samples, provided additional geochemical data and aided with interpretation of data. B.v.D. designed the project, collected the samples, helped with geochemical analyses, the interpretation of data and edited the manuscript.

Highlights:

- Novel amino acid compositional and $\delta^{15}N$ sedimentary analyses from the East Siberian Arctic shelf

- $\delta^{15}N$ at bulk and molecular level track terrestrial versus marine contributions across the shelf.

- $\delta^{15}N$ of coastal sediments indicate regional differences in terrestrial sources/degradation.

- Analyses indicate that these differences are not caused by inorganic nitrogen contributions.

- $\delta^{15}N$ of offshore sediments indicate that regional differences persist from the nearshore.

Keywords: Arctic Ocean; Nitrogen isotopes; Amino acids; Amino acid composition; Compound-specific nitrogen isotopes analysis; Isoscape; Marine sediments; Biogeochemistry

3.1 Abstract

The East Siberian Arctic Shelf (ESAS) is a region under-going rapid change as a direct consequence of climate warming. Warming in this region is leading to the mobilisation of vast quantities of terrestrial organic matter, previously locked away in terrestrial permafrost and ice complex deposits (ICD), via fluvial and coastal erosion processes to the ESAS. Of particular concern is the nitrogen delivered to the shelf. Nitrogen is a limiting nutrient in the growth of primary producers, so changes in the amount or composition of nitrogen impose changes for the particulate organic nitrogen in sediments. While bulk nitrogen isotopes have proven to be a useful tool both in sedimentary and ecological studies to look at terrestrial vs marine source apportionment, trophic relationships and food sources, the method does encompass the entire nitrogen pool and potentially contributions from inorganic nitrogen compounds and the effects of post-depositional alterations. An innovative technique to alleviate these issues and look directly at the organic nitrogen fraction is compound specific isotope analysis of individual amino acids (CSIA-AA). Amino acids form a large proportion of sedimenting organic nitrogen in the oceans and can provide unique insights into diagenesis within sediments. They also present an opportunity to look at the baseline isoscape in relation to origin as some amino acids fractionate with trophic transfer (trophic amino acids), whereas some remain relatively unchanged (source amino acids) and represent the baseline isoscape. Here, for the first time in the Arctic, we used sedimentary $\delta^{15}N_{Bulk}$ with CSIA-AA ($\delta^{15}N_{AA}$) in combination with a Py-GCMS method, which characterises the macromolecular component, to better understand drivers in changes of nitrogen compounds across the ESAS and how the delivery of terrigenous derived compounds impacts this. We found that $\delta^{15}N_{Bulk}$ and C/N ratio displayed differences between the nearshore regions of the ESAS, indicating a difference in

the terrestrial material delivered to these areas and this difference persisted into the offshore regions too. As with $\delta^{15}N_{Bulk}$, $\delta^{15}N_{AA}$ also displayed differences across the ESAS both in the nearshore regions and continuing into the offshore regions. The difference between the regions of the ESAS is likely due to a number of factors, including the proximity to riverine input, the amount of coastal erosion and marine organic matter input. The same offset between regions was measured in $\delta^{15}N_{Bulk}$ and $\delta^{15}N_{AA}$ (~3‰; using all amino acids) demonstrating that the offset recorded in the $\delta^{15}N_{Bulk}$ is likely not driven by inorganic nitrogen compounds but organic ones (amino acids). The source amino acids further supported this as these showed differences between the nearshore regions, suggesting a difference in the baseline isoscape of these regions. To further clarify the terrestrial origins of these differences a full suite of terrestrial end-members would need to be analysed alongside a full water column analysis. This method can be applied to different regions within the Arctic to better understand shifts in the baseline isoscape which will be needed to as this region undergoes rapid change.

3.2 Introduction

The Arctic is warming at a rate of up to twice the global average and predictions indicate this trend will continue into the future (IPCC, 2021). The increase in temperature affects many components of the Arctic system, both land, sea and troposphere. The most obvious of these changes is the loss of sea ice, both in summer and winter, with reductions in thickness of multiyear ice (IPCC, 2014). The easing of light limitation in the Arctic Ocean in this way has stimulated marine primary productivity, leading to a 57% increase since 1998 (Lewis et al., 2020).

Arctic warming is also observed in the terrestrial environment; as for the marine system it contains features which are particularly susceptible to warming. A large proportion of the land surrounding the Arctic Ocean is dominated by continuous and discontinuous permafrost. Even small increases in air temperature can lead to the thawing and breakdown of these deposits (Oliva and Fritz, 2018). Permafrost soils are of particular concern as they are estimated to store more than half of the world's soil organic matter, including organic carbon and nitrogen (Tarnocai et al., 2009; Schuur et al., 2015). The Arctic Ocean receives large amounts of freshwater and nutrient inputs from the rivers surrounding it, the drainage basins of many of these is dominated by permafrost. As the permafrost thaws, it drains freshwater and organic matter into these rivers which eventually make their way to the Arctic Ocean. In all scenarios of future climate change (set by the IPCC) river runoff will increase due to thawing permafrost, by up to 28% before the end of the century (Kattsov et al., 2007). Additionally, Ice Complex Deposits (ICD) are found across the Arctic region, particularly along the Siberian coastline; these are permafrost cliffs, known locally as Yedoma, that have a high ice and organic matter contents, and so are susceptible to increases in air and sea

temperatures (Hoque and Pollard, 2016). ICD's are not only susceptible to changes in air/sea temperature but to the increased wave strength and fetch as the Arctic Oceans become increasingly ice-free leading to undercutting and block failure (Hoque and Pollard, 2016).

The fate of the organic matter delivered *via* rivers and coastal erosion has been a key area of research with a particular focus on the organic carbon, as this has been found to degrade close to the point of origin releasing carbon dioxide (CO_2) and acting as a positive feedback to climate change and resulting in ocean acidification which is predominantly occurring in Arctic shelf waters (van Dongen et al., 2008; Semiletov et al., 2016; Martens et al., 2019; Jong et al., 2020).

The East Siberian Arctic Shelf (ESAS) is of particular interest and concern because in addition to having some of the highest rates of coastal erosion of ICD's (up to 10m yr^{-1} in some areas), it contains major rivers which drain water and organic matter from watersheds dominated by continuous permafrost and it is the largest and shallowest continental shelf on the planet extending up to 1,500 Km offshore. Together, these provide an opportunity to study the impacts of Arctic change on a range of interacting systems. Previous studies in the ESAS have mainly focussed on the delivery and fate of carbon compounds which have shown that there is a correlation between the type of material the carbon is associated with and how it is transported across the shelf and degraded (Tesi et al., 2016), indicating at least a partly hydrodynamic control on particle transportation. Further to this, studies have shown that topsoil organic matter is more prone to degradation than organic matter released from coastal erosion of ICDs (up to 90% and 60% degradation, respectively; Karlsson et al., 2016; Tesi et al., 2016; Bröder et al., 2019).

Comparatively less research has focussed on nitrogen delivered by rivers and coastal erosion of ICD's, even though it has been suggested that permafrost soils contain globally significant stores of nitrogen (Abbott and Jones, 2015), and its fate in this region is unknown. It is particularly important to understand nitrogen cycling in the Arctic as it increasingly becomes limiting to primary productivity as light limitation from ice cover reduces (Dittmar et al., 2001). A recent study by Terhaar et al. (2021) suggested that between 28-51% of current primary production in the Arctic Ocean is fuelled by inputs of nutrients from rivers and coastal erosion and in nearshore regions nutrients delivered from these sources has been found to have the greatest control on productivity (Dunton et al., 2006).

Thus far, studies focussing on nitrogen (organic and inorganic) delivered to the ESAS have focused on the use of bulk and macromolecular analyses, the former incorporates the entire nitrogen signal (both organic and inorganic nitrogen). A novel phenol/pyridine ratio, for instance, can distinguish between organic matter of terrestrial and marine origin, phenols are thought to be derived from lignin and therefore terrestrial in origin whereas pyridines are considered to be nitrogen rich from proteinaceous sources and represent a pseudo 'marine N-rich' compound (Sparkes et al., 2016). When applied to the ESAS, this showed a clear trend offshore from terrestrial to marine derived macromolecular organic matter, which is further supported by elemental data (TOC/TN and $\delta^{15}N$). $\delta^{15}N_{Bulk}$ across the ESAS has been shown to become enriched from the West to the East, which is considered to reflect the changing permafrost catchment areas of rivers and the result of mixing with marine organic matter (Guo et al., 2004). However, the underlying mechanism(s) driving the changes from West to East in the nitrogen pool across the ESAS are not well understood. It is important to unravel the drivers to these changes as nutrient delivery to the ESAS increases, potentially becoming more important in fuelling marine primary productivity.

Protein amino acids (AAs) account for a large proportion of total organic nitrogen found within organisms and can be present in significant amounts in recent sediments where particulates from the overlying water column accumulate (Burdige and Martens, 1988; Cowie and Hedges, 1992; Dauwe and Middelburg, 1998; Dittmar, Fitznar and Kattner, 2001; Carstens et al., 2013). Several earlier studies used the distribution of AAs to establish if the composition varied by source (Cowie and Hedges, 1992; Birgit Dauwe et al., 1999). Many concluded that while the data produced did not indicate differences in source of organic matter, there was potential for the degradation state of the organic matter to be indicated by relative enrichment of certain AAs relative to others (Dauwe and Middelburg, 1998; Dauwe et al., 1999). Since these earlier studies, a novel method to further interrogate AAs has been developed, whereby the individual isotopic composition of AAs can be analysed ($\delta^{15}N_{AA}$; McClelland and Montoya, 2002). This has been extensively applied to marine organisms to better constrain their trophic position compared to using $\delta^{15}N_{Bulk}$ as certain AAs have been revealed to fractionate through trophic levels whereas others show little or no fractionation (McClelland and Montoya, 2002; McClelland, Holl and Montoya, 2003; Chikaraishi et al., 2007, 2009). Additionally, variations in $\delta^{15}N_{AA}$ have been linked to heterotrophic bacterial degradation and selective resynthesis of certain AAs (McCarthy et al., 2007; Calleja et al., 2013a). As a large proportion of sinking particulate organic nitrogen is made up of AAs, $\delta^{15}N_{AA}$ in sediments has the unique capability to provide: information relating to the overlying water column, expose the degree of alteration from bacteria and to potentially reveal if the organic nitrogen pool in a region leads variations in $\delta^{15}N_{Bulk}$ (Batista et al., 2014).

Previous studies focussing on the ESAS have identified a shift in the sedimentary bulk nitrogen signal across the shelf but the underlying molecular level causes of this have, to the best of knowledge, never been fully investigated. We hypothesize that the shift in

biogeochemical regime from West to East on the ESAS is caused by the organic nitrogen signal close to the coastline. Further to this, there is a need understand to what extent the transport of organic matter delivered to the coastal shelf shifts the baseline values of the isoscape and what implications this has for future studies. To test this hypothesis we focus on a holistic approach; combining previous $\delta^{15}N_{Bulk}$, $\delta^{13}C_{TOC}$, C/N datasets, improving the spatial resolution of a previously reported macromolecular dataset (Sparkes et al., 2016) and presenting a novel AA compositional and $\delta^{15}N_{AA}$ analyses of sediments across the ESAS.

3.3 Materials and Methods

3.3.1 Study Area

The ESAS is located on the Siberian-Arctic Ocean boundary, is the largest and shallowest continental shelf on Earth and comprises of two distinct biogeochemical regions, the Laptev Sea in the west and the East Siberian Sea to the east with the Dmitry Laptev Strait separating them (Karlsson et al., 2015). The area presents a unique setting, with inputs of fresh water from the Yana and three of the five Great Russian Arctic Rivers (GRARs): the Lena, Indigirka and Kolyma (Fig. 3.1). These rivers have catchment areas dominated by continuous permafrost (Stein and MacDonald, 2004) with layers of ground actively thawing each summer, presenting a distinctly seasonal discharge. The Lena, in the west of the shelf, is by far the largest river in terms of annual discharge (average 588 $km^3\ y^{-1}$; Holmes et al., 2012) and the total suspended matter that it delivers to the shelf (20.7 $10^6\ t{\cdot}y^{-1}$; Gordeev, 2006). The Kolyma River is the second largest in terms of mean annual discharge, followed by the Indigirka and the Yana (122, 54 and 32 $km^3\ y^{-1}$ respectively; Gordeev, 2006).

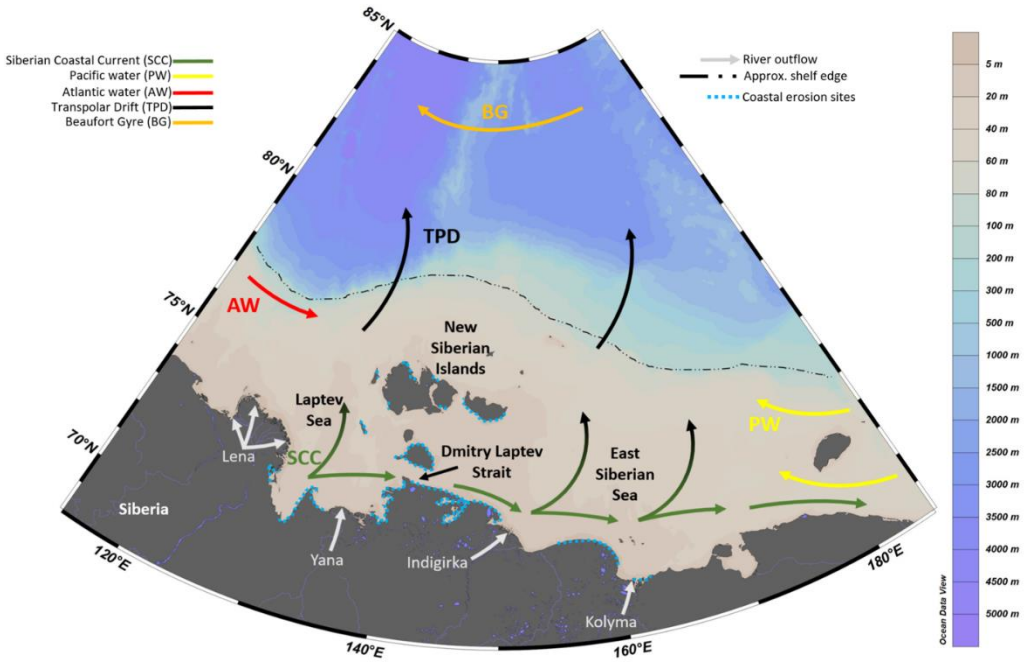

Figure 3.1 Schematic of East Siberian Arctic Shelf (ESAS) indicating general circulation of water masses and river inputs with coloured arrows; Siberian Coastal Current (SCC), Pacific water (PW), Atlantic water (AW), Transpolar Drift (TPD), Beaufort Gyre (BG) and grey arrows labelled with river outflows. Dashed black line indicates the approximate position of the shelf edge. Dashed blue line along coastline indicates areas undergoing enhanced rates of coastal erosion (>1m yr-1, Lantuit et al., 2011). Colour bar represent water depth. Base map created in Ocean Data View

As previously mentioned a large proportion of the ESAS coastline is made up of Pleistocene ice complex deposits (ICDs or Yedoma). These are organic rich, ice wedge dominated deposits that make the coastline more susceptible to erosion and contribute a large proportion of sediment input entering the shelf (Vonk et al., 2012). Rates of erosion along the coastline are up to 10 m y^{-1} and this is expected to increase with the reduction in sea ice and increase in nearshore wave action (Lantuit et al., 2011; Schirrmeister et al., 2011).

Alongside riverine inputs, the shelf also presents a complex hydrographic system, with the Siberian Coastal Current (SCC) flowing along the ESAS coastline from the West to the East, modified Atlantic water from the West and Pacific water to the East (Fig. 3.1). The transpolar drift (TPD) system drives water from the shelf towards the pole where it eventually exits through the Fram Strait, while the Beaufort Gyre (BG) pulls water in towards its centre depending on the strength of the gyre (Fig. 3.1).

As mentioned earlier the region can be split into regions following the same convention used by Sparkes et al. (2016) and based on previous biogeochemical analyses (Vonk et al., 2012; Karlsson et al., 2015; Bischoff et al., 2016; see Fig. 3.2). The 'nearshore Laptev Sea' (NLS) region encompasses stations which are in Buor-Khaya Bay containing Muostakh Island and those that are adjacent to the eastern outflow of the Lena River delta. Sediments in the NLS are rich in organic carbon of terrestrial origin; this was shown through biomarker analyses revealing a dominance of riverine glycerol dialkyl glycerol tetraethers (GDGTs) and substantial organic matter inputs from coastal erosion (Sparkes et al., 2015; Vonk et al., 2012). To the East of the NLS is a strait which has the lowlands of the Yana and Indigirka rivers to the south and the New Siberian Islands to the north, this is the 'Dmitry Laptev Strait' (DLS). The DLS is a region where coastal erosion input is most prominent due to the lack of nearby riverine input; radiocarbon analyses ($\Delta^{14}C$) of sediments revealed erosion of Pleistocene aged Yedoma was a major contributor to the terrestrial organic matter pool in this region (Vonk et al., 2012).

The 'nearshore East Siberian Sea' (NESS) region comprises the area from the DLS, the Indigirka river outflow to past the Kolyma river outflow. Doğrul Selver et al. (2015) used the R'soil (bacteriohopanepolyols index; range 0.07-0.57) and BIT (glycerol dialkyl glycerol tetraethers; range 0.02-0.51) indices compared with bulk stable isotopes to show the difference in sources of organic compounds along the Kolyma River outflow. R'soil had a linear correlation with the bulk stable isotopic composition of sedimentary organic matter ($\delta^{13}C$ and $\delta^{15}N$), indicating a more integrated signal of coastal erosion and riverine input. On the other hand, BIT showed a greater decrease close to the nearshore region representing an almost purely riverine source of GDGTs.

Sparkes et al. (2016) grouped all samples outside of the NLS and NESS together; for this study two separate offshore regions in the west and east have been identified. The 'offshore Laptev Sea' (OLS) region includes all stations to the west of the New Siberian Islands and those that are more than 200 km from river outflows. The 'offshore East Siberian Sea' (OESS) region includes all stations to the East of the New Siberian Islands and those that are more than 200 km offshore from river outflows. Each of these offshore regions shows an increased contribution of marine organic matter and a decrease in terrestrial input to the sediments (Vonk et al., 2012; Doğrul Selver et al., 2015; Sparkes et al., 2015).

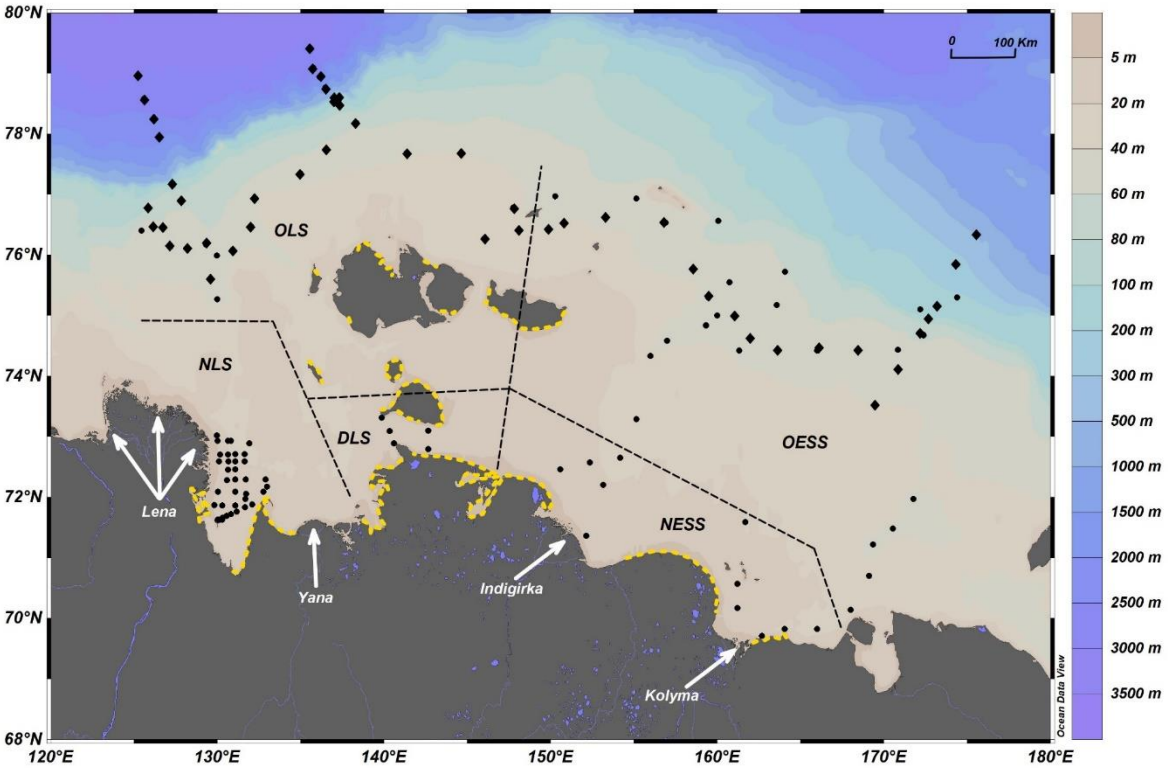

Figure 3.2 Map of the East Siberian Arctic Shelf (ESAS) showing locations of sediment samples from the ISSS-08 cruise (circles) and SWERUS-C3 cruise (diamonds) used in this study. Major river outflows are indicated by white arrows and areas of enhanced coastal erosion (>1my^{-1}, Lantuit et al., 2011) are shown in yellow. Regions of the ESAS referred to in this study are shown by the dashed black line (NLS: nearshore Laptev Sea; OLS: offshore Laptev Sea; DLS: Dmitry Laptev Strait; NESS: nearshore East Siberian Sea; OESS: offshore East Siberian Sea). Bathymetry of the shelf, slope and Arctic Ocean are shown in the colour bar (Ocean Data View, 2021)

3.3.2 Sample Collection

The samples used in this study were collected during two research campaigns to the ESAS: in 2008 and 2014 (Fig. 3.2). The first cruise collected samples during the International Siberian Shelf Study in August-September 2008 on board the H/V Yacob Smirnitskyi (ISSS-08; Semiletov & Gustafsson, 2009) using a van Veen grab sampler and a GEMAX dual gravity corer (top 1cm from cores used). The cruise spanned the length of the ESAS from 125-175°E; including river outflows, areas of enhanced coastal erosion to offshore sites hundreds of kilometres offshore. Detailed reports of sample collection procedures can be found in Sparkes et al. (2015) and Tesi et al. (2014). Briefly, samples were stored in pre-cleaned polyethylene containers and kept frozen before being oven (50°C) or freeze-dried prior to analysis.

The second cruise collected surface sediments as part of the international Swedish-Russian-US collaboration (SWERUS-C3) on-board I/B Oden during the summer of 2014, using an 8-tube multicorer. Unlike the ISSS-08, the SWERUS-C3 sampled stations on the outer part of the shelf, including shelf slope and rise samples. Sediment cores were sectioned (top 1cm used), frozen (-20°C) and stored on-board and then freeze-dried prior to analysis; detailed collection protocols can be found within the cruise report (Semiletov and Gustafsson, 2009).

3.3.3 Geochemical Analyses

3.3.3.1 Elemental analyses and bulk stable isotope analysis

Surface sediments from the ISSS-08 cruise were analysed in duplicate for their elemental composition (total C, N and OC) and bulk stable isotopic composition ($\delta^{13}C$ and $\delta^{15}N$) simultaneously using an elemental analyser isotope ratio mass spectrometer as reported by Vonk et al. (2012) and Karlsson et al. (2011). As per convention, isotopic values are reported using the standard δ-notation and are relative to Vienna PeeDee Belemnite and atmospheric N_2 for $\delta^{13}C_{TOC}$ and $\delta^{15}N_{bulk}$, respectively. Surface sediments from the SWERUS-C3 cruise were

analysed in triplicate using a Carlo Erba NC2500 elemental analyser connected to a Finnigan MAT Delta Plus mass spectrometer, detailed procedures can be found within Salvadó et al. (2016) ($\delta^{15}N$ measurements from SWERUS-C3 stations are unpublished and permission has been given to use these within this publication).

The isotopic compositions of additional samples were analysed using an elemental analyser (Costech) coupled to Delta V isotope ratio mass spectrometer (IRMS; Thermo Fisher Scientific); details of analysis procedures can be found within de la Vega et al. (2021).

3.3.3.2 Pyrolysis gas chromatography mass spectrometry (Py-GCMS)

This study extended an existing Py-GCMS dataset (Sparkes et al., 2016) using samples from the ISSS-08 cruise. An extra 32 stations were added (to a total of 68), improving the spatial resolution of the dataset. Both freeze-dried untreated and solvent-extracted dried samples were analysed using an Agilent GC-MSD which was interfaced with a CDS-5200 Pyroprobe. The analysis method followed that of Sparkes et al. (2016) with minor adjustments. In short, sediments were placed into a clean quartz tube, which is fire polished using a Bunsen burner in between each sample and placed into the pyroprobe ready for Py-GCMS analyses. Sediments were pyrolysed at 700°C for 20 seconds in a flow of helium. Pyrolysis products were passed through a heated transfer line (325°C) using helium as a carrier gas (20 mL min^{-1}, gas saver mode active) to an Agilent 7980A GC in split mode (split ratio 20:1, GC interface at 280°C) fitted with a HP-5 GC column (30 m and 0.25 mm (i.d.), film thickness 0.25 µm, non-polar stationary phase of 5%-phenyl-methylpolysiloxane). The GC oven was set from 40°C (held for 5 minutes) to 250°C at 4°C min^{-1}, then heated to 300°C at 20°C min^{-1} and held for 1 minute at this temperature (61 minute total run time). The eluent from the GC was

transferred *via* a transfer line (325°C) to an Agilent 5975 MSD single quadrupole mass spectrometer in electron ionisation (EI) mode (ionisation potential 70 eV; scanning range of m/z 50 to 650 at 2.7 scans s^{-1}; EI source at 230°C; MS quadrupole at 150°C). Chromatograms were processed using Enhanced ChemStation, Agilent Technologies software. Samples were analysed in duplicate at a minimum and precision ranged from 0 to 0.2 for the phenol to pyridine ratio. Samples reported by Sparkes et al. (2016) were re-analysed to check reproducibility and new samples were analysed at least in duplicate. As noted by Sparkes et al. (2016), the chromatograms produced from Py-GCMS are complex and therefore a number of 'pyrolysis moieties' (Guo et al., 2009) were determined (Fig. 3.3). Hence, the major fragment ions were used to determine peak areas in the appropriate single ion current chromatograms. For the purpose of this study, two of the nine representative moieties were used as they formed a proxy for terrestrial and marine input (phenols/pyridines ratio index, PPRI; Eqn. 3.1; phenols major ion m/z 94 and pyridines m/z 79 and 93; Fig. 3.3; a full list of ions can be found in Sparkes et al., 2016). This method does not characterise all of organic compounds generated by pyrolysis of the sediments but is a tool for inter-sample comparison across a land to sea gradient.

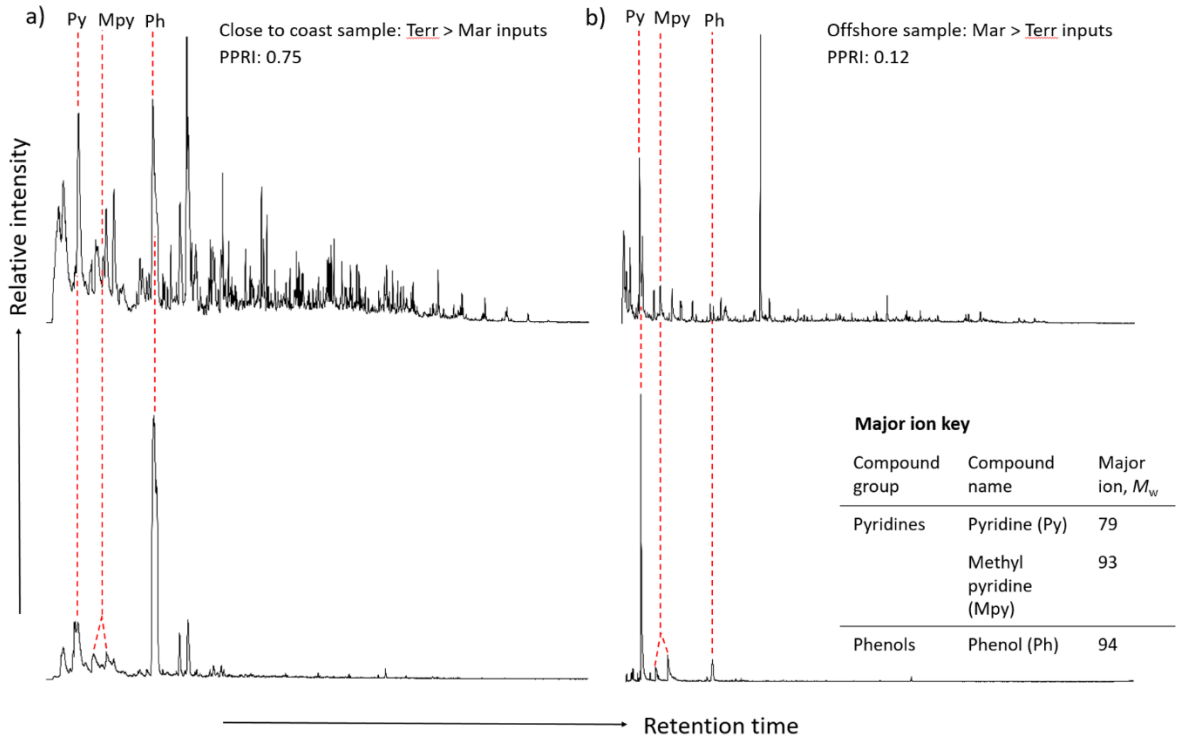

Figure 3.3 Representative chromatograms from Py-GCMS analysis (top) with chromatograms produced by using single ion filtering (SIF; bottom). a) Sample close to the coast with a PPRI of 0.75 and a single ion filter chromatogram displaying relatively higher proportions of phenols compared to pyridines. b) Sample offshore with a PPRI of 0.12 and single ion filter chromatogram displaying relatively higher proportions of pyridines compared to phenols. The major ion key specifies ions used for SIF's following Sparkes et al. (2016) method.

3.3.3.3 Amino acid isotope analysis

For compound specific isotope analyses (CSIA; $\delta^{15}N$) of individual amino acids both fresh freeze-dried sediments and solvent-extracted residues were used, which increased the amount of samples available for the study (see supplementary information). As initial experiments found sedimentary amino acids to be in low concentrations within some of the sediments studied almost all of the available sediment (from 2-10 g) was used for CSIA.

Prior to hydrolysis, an internal standard (L-norleucine, Sigma-Aldrich) of known concentration was added. In 20 mL culture tubes, fitted with Pyrex lids to ensure no evaporation, approximately 10-12 mL of 6N HCL was added to each sample and then a shaker

bed was used to fully mix the slurry. Samples were transferred to a pre-heated oven at 110°C under an N_2 atmosphere for a minimum of 21 hours. It should be noted that during acid hydrolysis, asparagine and glutamine were converted to aspartic acid and glutamic acid, respectively.

Once hydrolysed the samples were cooled, transferred to a NanoSep centrifugal device to ensure all hydrolysates were collected and transferred into clean vials. A mixture of dichloromethane (DCM): *n*-heptane (3:2) was added to each sample and the lipid layer was removed by drawing off the top layer with a Pasteur pipette, this was repeated (x3) to ensure its complete removal. Following Styring et al. (2012), a cation exchange column was prepared to ensure all exchange sites within the resin were occupied by H^+ ions prior to sample addition. Approximately 1 mL of Dowex 50WX8 (200–400 mesh) was added into a Pasteur pipette and washed with 12 mL of deionised water. Samples were transferred to the column and salts were eluted with deionised water; finally amino acids were eluted into clean vials with NH_4OH solution (4N) and centrifuged to ensure no particulates from the resin remained. Sample were frozen (-80°C) in preparation for freeze-drying prior to derivatisation.

Amino acids were propylated using acetyl chloride: anhydrous isopropanol (1:4, v/v, 0.25 mL) for 1 hour at 100°C; the reaction was quenched in a freezer (-20°C) and reagents evaporated to dryness under N_2. A small amount of DCM was added and evaporated (x3) to ensure complete removal of any remaining reagents. To acetylate the amino acids, a mixture of acetone: triethylamine: acetic anhydride (5:2:1, v/v, 1 mL) was added to the amino acid propyl esters and heated for 10 minutes at 60°C. All reagents were evaporated to dryness under N_2 before being dissolved in 2 mL of ethyl acetate and 1 ml of saturated NaCl solution. Samples were then placed into a vortex mixer to create phase separation and the organic

phase was collected; this was repeated (x2) and the organic phases collected. A Pasteur pipette plugged with glass wool and packed with anhydrous $MgSO_4$ removed any remaining

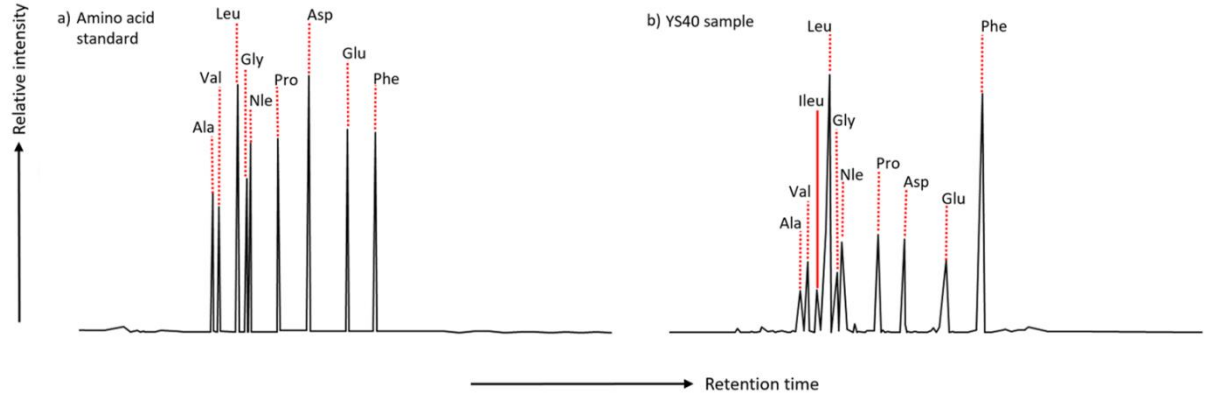

Figure 3.4 Representative GC-FID chromatograms for a) amino acid standard and b) a representative sample from the outflow of the Kolyma River (YS40). Amino acids detected: alanine (ala), valine (val), isoleucine (Ileu), leucine (leu), glycine (gly), norleucine (nle, internal standard), proline (pro), aspartic acid (asp), glutamic acid (glu) and phenylalanine (phe).

water. Lastly, samples were evaporated to dryness under N_2, dissolved in DCM and stored at -20°C prior to analysis. Following this procedure, a total of 8 amino acids could be identified from associating peaks with standard runs; Alanine (Ala), Valine (Val), Leucine (Leu), Glycine (Gly), Proline (Pro), Aspartic Acid (Asp), Glutamic Acid (Glu) and Phenylalanine (Phe; Fig. 3.4).

The mole percent of individual amino acids were determined prior to $\delta^{15}N$ amino acid analysis ($\delta^{15}N_{AA}$) using a GC-FID (gas chromatograph-flame ionization detector; Agilent Technologies 7890A GC System). The GC was fitted with a HP-INNOWax Agilent column (30 m x 0.25 mm (i.d.), film thickness 0.5 µm, high polarity stationary phase of polyethylene glycol) using helium as a carrier gas (1.1 mL min^{-1}, splitless mode) and the injector set at 250°C. The GC oven was programmed after 2 minutes from 50°C to 180°C at 10°C min^{-1}, then from 180°C to 260°C at 6°C min^{-1} and held at 260°C for 20 minutes. The FID operating conditions were as follows: detector heater 220°C; H_2 40 mL min^{-1}; air flow 400 mL min^{-1}; N_2 25 mL min^{-1}.

$\delta^{15}N_{AA}$ values were determined using GC-C-IRMS (Thermo Scientific Trace Ultra gas chromatograph 1310 coupled to a GC Isolink and Delta V Advantage isotope ratio mass spectrometer with a ConFlo IV interface). A HP-INNOWax Agilent column (30 m x 0.25 mm (i.d.), film thickness 0.5 µm, high polarity stationary phase of polyethylene glycol) fitted to the GC was used for amino acid separation, helium as a carrier gas (flow 1.4 $mL.min^{-1}$) and the injector set at 260°C. After separation the eluents were passed through a combustion reactor (Cu/Ni, 1000°C, Thermo Fisher) followed by a liquid nitrogen trap to remove CO_2 from the samples. The GC oven was programmed after 2 minutes from 50°C to 180°C at 10°C min^{-1}, then from 180°C to 260°C at 6°C min^{-1} and held at 260°C for 16.7 minutes. The molecular ions of N_2 (*m/z* 28, 29 & 30) were detected and the resulting $\delta^{15}N$ of each amino acid peak was determined by comparison with a standard reference N_2 gas (measure 4 times at the start and finish of each sample analysis) using Isodat software (version 3.0, Thermo Fisher).

All $\delta^{15}N_{AA}$ results are reported in per mill notation (‰) relative to atmospheric N_2 (e.g. McCarthy *et al.*, 2007; Batista *et al.*, 2014). Each sample was analysed in duplicate, any sample that had a greater difference between sample runs than expected (>2.0‰) was not included in the dataset. A mixed standard of 8 amino acids with known $\delta^{15}N$ were analysed at the start of every run and every 4 samples to determine precision and accuracy (University of Indiana, United States and SI Science, Japan). The mean precision of all standards was ± 1.0‰ and ranged from ± 0.4‰ for proline and ± 2.4‰ for alanine (*n* = 25 and 36, respectively). The mean accuracy of all standards was ± 1.4‰ and ranged from ± 0.7‰ for aspartic acid to ± 2.2‰ for glutamic acid (*n* = 36).

3.3.4 Amino acid groupings and definitions

Amino acids can be separated into a variety of groupings, depending on sample type, the type of data produced from the analysis (mol% or $\delta^{15}N_{AA}$) and aims of the study. Studies using the molar percent contribution of sedimentary amino acids usually investigate their behaviour in the substrate and links to diagenetic processes (e.g. Dauwe et al., 1999). There are some amino acids that are apparently more easily degraded or more refractory due to either their chemical structure or the type of organic matter fraction they are typically associated with. Dauwe & Middelburg (1998) split protein amino acids up by their functional group and associated charge: neutral (Gly, Ala, Val and Leu); acidic (Glu and Asp); and aromatic (Phe). Glycine is usually higher in its relative concentration in diatom and bacterial cell walls (Yamashita and Tanoue, 2003) and previous studies have found it to preferentially accumulate compared to more labile constituents such as cell plasma, which are rich in phenylalanine and glutamic acid (Cowie and Hedges, 1992). Additionally, higher concentrations of glycine have been linked to heterotrophic reworking in marine sediments, as glycine can be synthesized from many precursor amino acids and has a relatively lower food value (e.g. zooplankton) due to its short chain length, which leads to an enriched pool relative to other amino acids (Dauwe and Middelburg, 1998; Birgit Dauwe et al., 1999; McCarthy et al., 2013).

When using $\delta^{15}N_{AA}$ amino acids are typically split into groups based on their behaviour in a food web, for biological samples two groups are used (trophic and source amino acids) consistent with the existing literature (e.g. Batista et al., 2014). Trophic amino acids (Ala, Val, Leu, Pro, Asp and Glu) are those that become enriched in ^{15}N with each trophic transfer and are reflective of the consumer. Source amino acids (Gly and Phe) are those that have little or

no enrichment in ^{15}N with trophic transfer and are thought to represent the base of the food web (Chikaraishi et al., 2007; McClelland & Montoya, 2002).

3.3.5 Source and Diagenetic indicators/proxies

A number of metrics can be used based on the above analyses to assess both the source and quality of OM:

The Phenol to Pyridine Ratio (PPRI; Sparkes et al., 2016) as obtained by Py-GCMS shows nearshore to offshore trends in the relative abundance of two representative compound classes. Pyridines are used as a pseudo-marine proxy and phenols used as a pseudo-terrestrial proxy (pseudo as both compounds can be found across marine and terrestrial environments); values of the PPRI that are close of 0 are deemed marine in origin and values closer to 1 are predominantly terrestrial:

Equation 3.1

$$\frac{Phenol}{Phenol + Pyridine}$$

A proxy for the total $\delta^{15}N$ of proteinaceous material ($\delta^{15}N_{THAA}$) was proposed by McCarthy et al. (2013). This is calculated as the mole percent weighted sum of each $\delta^{15}N_{AA}$ and it is noted that as not every amino acid is analysed within the sample that this is a representative proxy and not the absolute value:

Equation 3.2

$$\delta^{15}N_{THAA} = \Sigma\ (\delta^{15}N_{AA} \cdot mol\%_{AA})$$

Amino acid $\delta^{15}N$ values can be normalised to the $\delta^{15}N_{THAA}$, providing intra sample comparison and removing inorganic N influences (McCarthy et al., 2013).

The degradation index (DI) is used as an indicator of organic matter quality and uses the protein amino acid composition of each sample following Dauwe et al. (1999):

Equation 3.3

$$DI = \Sigma \left[\frac{\text{var}_i - \text{AVGvar}_i}{\text{STDvar}_i}\right] \times \text{Fac. coef}_i$$

Where var_i is the mole percent of amino acid *i*; AVGvar_i and STDvar_i are the mean and standard deviation of amino acid *i* in the study from Dauwe et al. (1999) and fac. coef_i is the factor coefficient of amino acid *i* based on the first axis of the principle component analysis in Dauwe et al. (1999).

The ∑V parameter, first proposed by McCarthy et al. (2007), is a proxy used to determine total heterotrophic resynthesis by looking at the scatter of $\delta^{15}N_{AA}$ values around the mean of total values:

Equation 3.4

$$\Sigma V = \frac{1}{n} \Sigma Abs(\chi_i)$$

Whereχ_i, is the deviation in each AA $\delta^{15}N$ I from the average ($\delta^{15}N_i$—AVG $\delta^{15}N_i$) and n is the number of AA used total for the calculation. The amino acids used are those representing the 'trophic' group, for this study Ala, Leu, Pro, Asp and Glu were used.

3.3.5 Statistical tests

All statistical analyses were performed in R version 4.0.2 (R Core Team, 2021) with RStudio interface version 1.3.959. To explore patterns between the different regions of the ESAS and transects from nearshore to offshore within a region, a variety of statistical tests were performed. Primarily one-way ANOVA (analysis of variance) with post hoc Tukey honestly significant difference (HSD) pair-wise test, this tested the differences in each region for a given variable measured (e.g. mol percent of each amino acid in each region) and the differences within each of those groups, respectively. Before using statistical analysis the data was tested for normality using a visual check of the quantile-quantile plots followed by a studentised Breusch-Pagan test to test for heteroscedasticity. Due to the small number of data points for some analyses and regions (e.g. n=3), there are some inherent limitations of using parametric tests however ANOVA is considered acceptable for data that does not rigorously fit a Gaussian distribution (McCarthy et al., 2007). A 95% confidence interval is used for all test results, both ANOVA and Tukey HSD post-hoc.

Some indices also warranted correlation tests to be performed, where initial scatter plots were created alongside a linear model which was then tested for normality and then subjected to Pearson and Spearman Rank correlation tests. The first of these solely interrogates linear correlations, whereas the second tested for monotonic correlations. Monotonic correlations do not have to conform to a linear relationship as the test recognises positive or negative correlations even if the rate of change of each variable is not the same, for instance an exponential correlation. By using both tests the correlations can be assigned to a linear or monotonic relationship depending on the strength of the *r* and *p* values they produce.

R coding scripts (5,387 lines of code used to create figures and run statistical analysis) related to these statistical analyses can be found in appendix 1.

3.4 Results

3.4.1 Bulk elemental and isotopic composition

Across the ESAS, C/N ratios in surface sediments ranged from 5.24 (YS-86) to 16.21 (TB-48, Fig. 3.5a). The lowest values were in the offshore regions and the highest close to the Lena outflow in the Buor Khaya Bay. The average C/N for the nearshore regions in the Laptev Sea, East Siberian Sea and Dmitry Laptev Strait were 11.93 ± 1.49, 7.77 ± 1.21 and 8.67 ± 0.87, respectively. This decreased in the offshore regions to 7.33 ± 1.00 in the Laptev Sea and 5.98 ± 0.48 in the East Siberian Sea. There was strong evidence of a significant difference in C/N between regions (ANOVA, $F_{4, 127} = 89.27$, $P < 0.0001$). A post-hoc Tukey's HSD test revealed that the difference was between both the two nearshore regions (NLS & NESS, $P < 0.0001$, 95% C.I. = -5.32, -2.95; Fig. 3.5a) and offshore regions (OLS & OESS, $P < 0.0001$, 95% C.I. = -2.54, -1.03; Fig. 3.6a). Bulk $\delta^{13}C$ ranged from -21.2 (YS-86) to -27.4‰ (YS-22, 22B and 24), the lightest values being in the Dmitry Laptev Straight and heaviest in offshore region of the East Siberian Sea (Fig. 3.5b). There was strong evidence of a significant difference in $\delta^{13}C$ between the regions (ANOVA, $F_{4, 127} = 57.38$, $P < 0.0001$). A post-hoc Tukey's HSD test revealed that the differences were in the nearshore to offshore regions of the Laptev and East Siberian Seas (NLS & OLS, $P < 0.0001$, 95% C.I. = 1.49, 2.71; NESS & OESS, $P < 0.0001$, 95% C.I. = 1.99, 3.81; Fig. 3.6b). Bulk $\delta^{15}N$ ranged from 1.4‰ (TB-46) in the nearshore Laptev Sea region to 10.2‰ (YS-88) in the offshore East Siberian Sea region (Fig. 3.5c). The average bulk $\delta^{15}N$ for the nearshore regions of the Laptev Sea, East Siberian Sea and Dmitry Laptev Strait were 2.8 ± 0.6‰, 5.8 ± 0.8‰ and 4.8 ± 0.2‰, respectively. The average bulk $\delta^{15}N$ for the offshore

regions of the Laptev Sea and the East Siberian Sea were 5.4 ± 0.8‰ and 8.6 ± 1.0‰, respectively. There was strong evidence of differences in $\delta^{15}N$ between the regions (Kruksal-Wallis, (H (2) = 113.93, df = 4, P <0.0001). A post-hoc Tukey's HSD test revealed similar differences to those found with the C/N ratios, in that there were differences in the nearshore areas of the Laptev and East Siberian Seas (NLS & NESS, P <0.0001, 95% C.I. = 2.29, 3.81; NLS & DLS, P <0.0001, 95% C.I. = 1.14, 2.89; Fig. 3.6c). There was also strong evidence of a difference in the nearshore to offshore areas of both regions (NLS & OLS, P <0.0001, 95% C.I. = 2.60, 3.60; NESS & OESS, P <0.0001, 95% C.I. = 1.99, 3.47; Fig. 3.6c). Individual station data (C/N, $\delta^{13}C$ and $\delta^{15}N$) as well as complete ANOVA, Kruksal-Wallis and Tukey's HSD statistical analysis results can be found in appendix 1.

3.4.2 Distribution of phenols and pyridines across the ESAS

The phenol to pyridine ratio (PPRI) as determined by Py-GCMS decreased across the shelf from near to offshore regions in all transects, the relative proportion of phenols decreased while the pyridines increased towards the offshore regions (Fig. 3.5d). The highest phenol to pyridine ratio was found in the nearshore Laptev Sea region (0.88, YS-15) and the lowest in the offshore region of the East Siberian Sea (0.04, YS-88 and 100). The average PPRI for the nearshore region in the Laptev Sea, East Siberian Sea and Dmitry Laptev Strait was 0.68 ± 0.12, 0.60 ± 0.14 and 0.71 ± 0.07, respectively. This decreased in the offshore regions to 0.26 ± 0.11 in the Laptev Sea and 0.22 ± 0.16 in the East Siberian Sea. There was strong evidence of differences in the PPRI between regions (ANOVA, $F_{4, 64} = 44.96$, P <0.0001). A post-hoc Tukey's HSD test revealed no differences between the nearshore regions but instead differences in the nearshore to offshore areas of each region (NLS & OLS, P <0.0001, 95% C.I. = -0.65, -0.19; NESS & OESS, P <0.0001, 95% C.I. = -0.52, -0.23; Fig. 3.6d). Individual station data of PPRI as

well as complete ANOVA and Tukey's HSD statistical analysis results can be found in appendix 1.

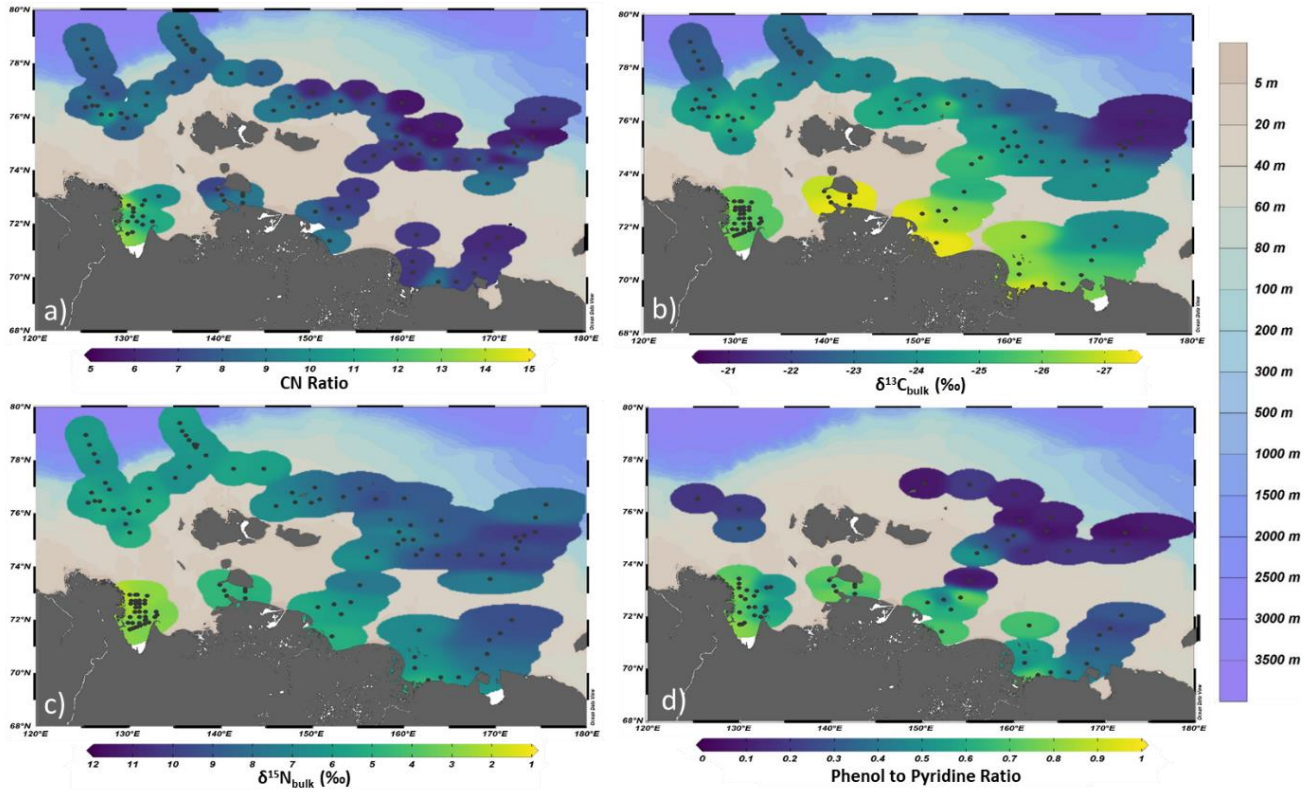

Figure 3.5 Map panel showing a) C/N ratio, b) δ13C, c) δ15N and d) Phenol to Pyridine Ratio (PPRI) across the ESAS, indicating nearshore to offshore trends and changes from West to East. Created using weighted average gridding in Ocean Data View

Using a ANOVA/ Kruksal-Wallis tests followed by Tukey's HSD for each analysis and by region enables a pattern to emerge whereby differences West-East in the nearshore regions are reflected in the $\delta^{15}N$ and C/N ratios but not in the $\delta^{13}C$ and PPRI (Fig. 3.6).

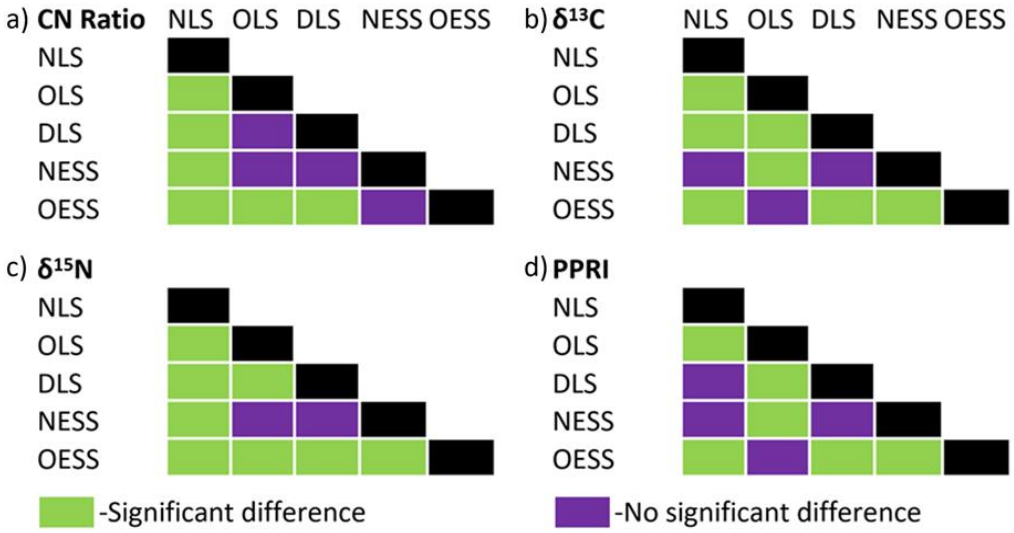

Figure 3.6 Indicating differences found between regions for C/N ratio, $\delta^{13}C$, $\delta^{15}N$ and PPRI using ANOVA or Kruksal-Wallis tests followed by Tukey's HSD post-hoc test with significant difference being defined as a P-value smaller than <0.01 at a 95% confidence interval. This demonstrates that in the nearshore regions (NLS, NESS and DLS) that there are differences in the C/N ratio and δ15N but not in the $\delta^{13}C$ and PPRI.

3.4.3 Amino acid composition (GC-FID)

Leucine is the dominant amino acid in surface sediments across all regions of the ESAS (28.5 - 34.0 mol %) followed by phenylalanine (16.2 - 26.3 mol %) whereas all other amino acids exhibit lower mol% values; glycine (9.91 - 15.43); alanine (8.5 - 13.1); valine (7.8 - 8.5); glutamic acid (7.4 - 9.7); aspartic acid (6.5 - 9.4; Fig. 3.4 and 3.7).

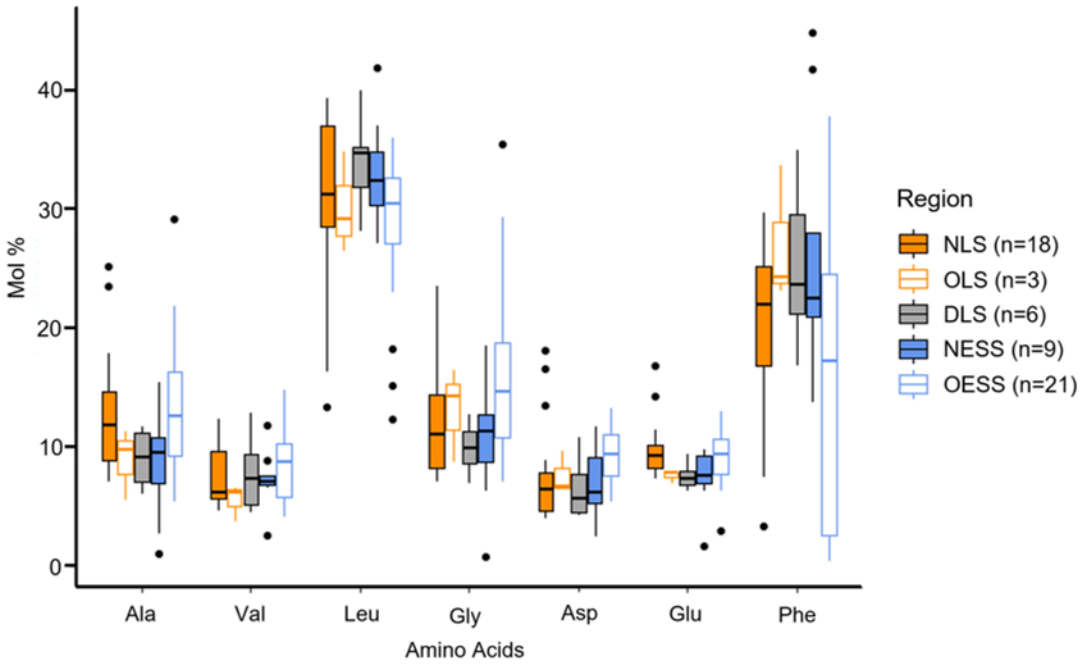

Figure 3.7 Distribution of mol% amino acids (AA) across ESAS regions, NLS (nearshore Laptev Sea), OLS (offshore Laptev Sea), DLS (Dmitry Laptev Strait), NESS (nearshore East Siberian Sea) and OESS (offshore East Siberian Sea). Changes in region do not modify the compositions of AA in sediments significantly with the most dominant amino acid being leucine across each region. The median is the horizontal line through each box and the 25% to the 75% quartile are the bottom and top of the boxes. The line extending below and above each box represent the 5% and 95% quartiles. Closed circles represent data points that fall below or above the 5% and 95% quartiles.

There was weak evidence of a difference in glutamic acid and phenylalanine between regions (ANOVA; $F_{4, 52} = 2.51$, $P = 0.05$; and, $F_{4, 52} = 3.13$, $P = 0.02$, for Glutamic acid and Phenylalanine respectively). In the case of Phenylalanine, a post-hoc Tukey's HSD test revealed that the difference was between the nearshore and offshore of the East Siberian Sea (NESS-OESS; $P < 0.05$, 95% C.I. = -22.12, -0.31; filled blue to open blue boxes, Fig. 3.7). To better understand the relationship between individual amino acid mol% two types of correlation tests were performed, Pearson's and Spearman's rank (using both can indicate

the kind of relationship present rather than just if there is one; a full list of correlation test results can be found within appendix 1). Two groups of amino acids are identified from these correlation tests, the first is leucine and phenylalanine (leu and phe) which display the same kind of relationship to the other amino acids. For example leu and phe mol% display negative correlations with the mol% of aspartic acid (asp) while the other amino acids measured all display positive correlations with asp, this kind of grouping is present for all of the amino acids measured (Fig. 3.8). The correlation of the amino acid mol% data to other indices (C/N, bulk $\delta^{15}N$, PPRI and DI) also reveals the same pattern, in that leu and phe had opposite relationships to the other amino acids have with the indices (Fig. 3.8).

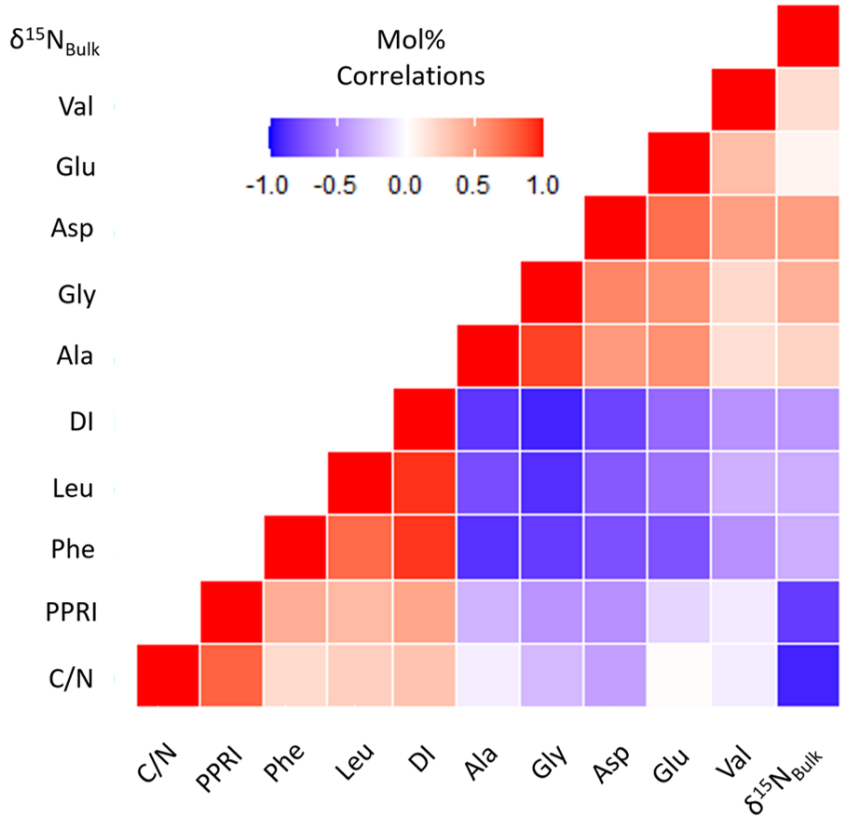

Figure 3.8. A correlation heat map displaying the positive (red) or negative (blue) relationships between individual amino acid mol% and indices measured as part of this study. Here the grouping of leu and phe becomes more apparent compared to the other amino acids. Created using 'ggplot2' within RStudio 1.3.959.

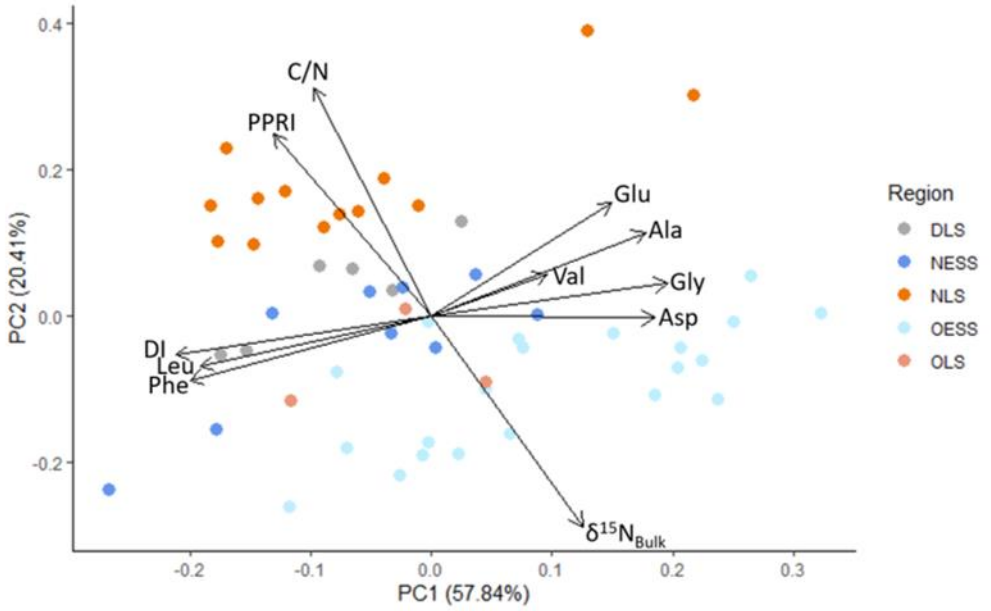

Figure 3.9 Principle component analysis (PCA) of amino acid mol%, C/N, $\delta^{15}N_{Bulk}$, Phenol to Pyridine ratio (PPRI) and degradation index (DI). Sample location regions are represented by colours, nearshore Laptev Sea (NLS), offshore Laptev Sea (OLS), Dmitry Laptev Strait (DLS), nearshore East Siberian Sea (NESS) and offshore East Siberian Sea (OESS). Showing grouping of Leu and Phe on opposite sides of PC1 to other amino acids, likely signifying the degradation index proposed by Dauwe et al. (1999). PCA was conducted using 'prcomp' within the 'R Stats Package' and displayed using 'ggplot2' autoplot function in RStudio 1.3.959

These patterns were also confirmed through principle component analysis of mol% of each amino acid compared to the DI, C/N ratio, PPRI, $\delta^{15}N_{bulk}$ and the associated region (PCA; Fig. 3.9). The analysis presented 11 principle components with the first two of these (PC1 and PC2) explaining 78.3% of the total variance. The DI, Leu and Phe are negatively correlated to Val, Glu, Ala, Gly and Asp along PC1. Whereas PPRI and C/N are negatively correlated to 15Nbulk along PC2 and regions spread along PC2 more so than PC1 (Fig. 3.9).

3.4.4 Amino acid nitrogen isotope composition

The trophic amino acids (Ala, Leu, Pro, Asp and Glu) on the whole display more enriched $\delta^{15}N$ values compared to those of the source amino acids (Gly and Phe; Fig. 3.10). There is an enrichment in $\delta^{15}N$ from near to offshore regions for each amino acid measured, however this was less pronounced in Phe (Fig. 3.10). $\delta^{15}N$ values of Phe remain similar between nearshore and offshore in the Laptev Sea region (Tukey's HSD, $P > 0.05$, 95% C.I. = -2.04, 3.55; Fig. 3.10). There was weak to strong evidence for differences in the $\delta^{15}N$ of each amino acid between regions (ANOVA and Tukey's HSD post-hoc test, Table 3.1). The most noteworthy are those between the nearshore regions (NLS, DLS and NESS) and from the near to offshore in both the Laptev and East Siberian Seas (Table 3.1). Generally, sedimentary amino acids in the Laptev Sea (NLS and OLS) were more depleted in $\delta^{15}N$ compared to the East Siberian Sea (NESS and OESS), whilst the Dmitry Laptev Strait (DLS) sedimentary amino acid $\delta^{15}N$ values fell between the two regions, (Fig. 3.10; Table 3.1).

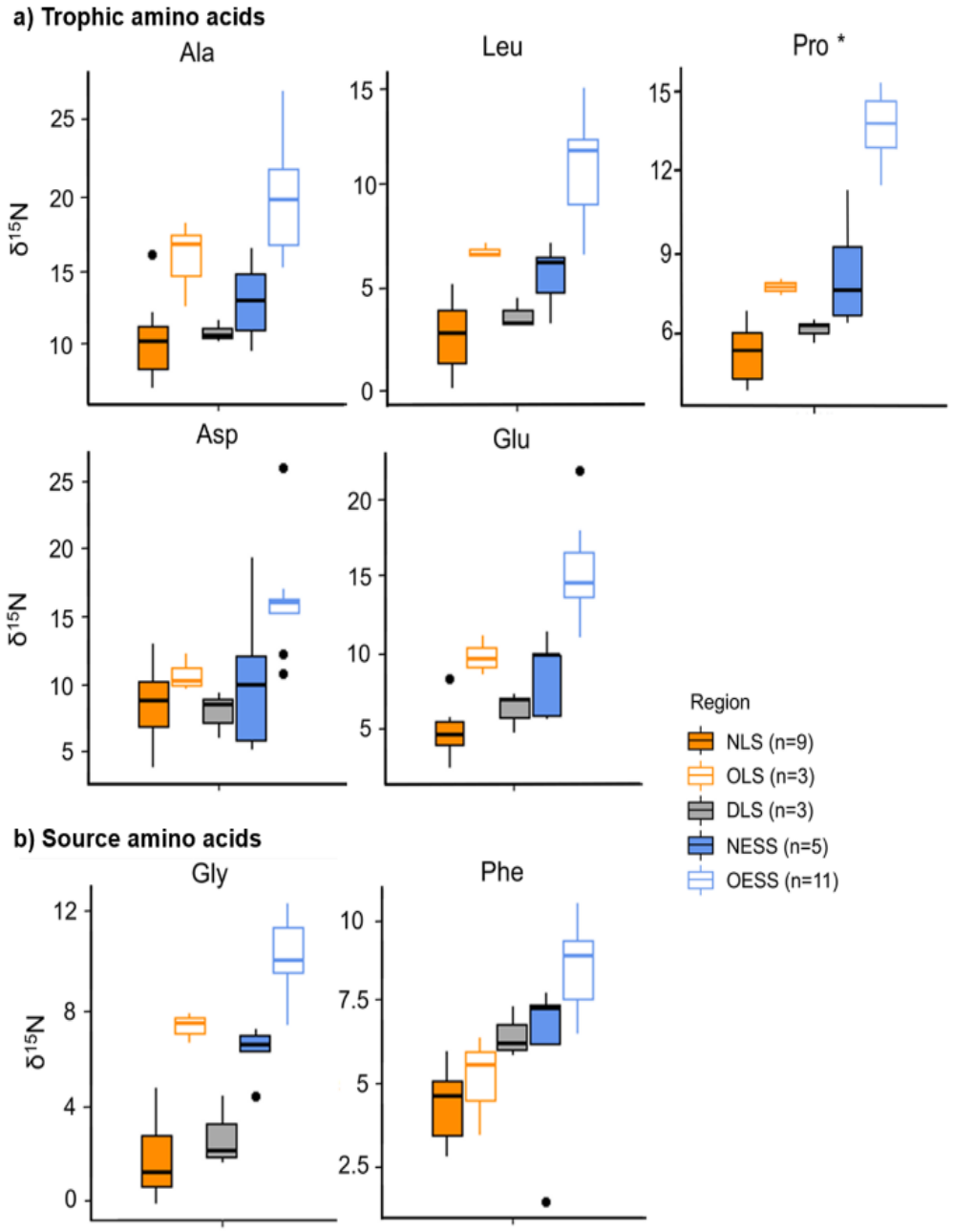

Figure 3.10 $\delta^{15}N_{AA}$ values of sediments in the ESAS split by region, NLS (nearshore Laptev Sea), OLS (offshore Laptev Sea), DLS (Dmitry Laptev Strait), NESS (nearshore East Siberian Sea) and OESS (offshore East Siberian Sea). More enriched values tend to be in the offshore regions in the case of Ala, Leu, Gly, Pro, Asp and Glu and to a lesser extent in the case of Phe. Closed circles represent individual data that falls below or above the 5% and 95% quartiles. *as Pro was not present in all amino acid standards the number of measurements per region are as follows: NLS (n=5), OLS (n=3), DLS (n=3), NESS (n=4) and OESS (n=9).

Table 3.1 Statistical analysis results using ANOVA and post-hoc Tukeys HSD pair-wise test on amino acids from sediments across the ESAS regions. NLS (nearshore Laptev Sea), OLS (offshore Laptev Sea), DLS (Dmitry Laptev Strait), NESS (nearshore East Siberian Sea) and OESS (offshore East Siberian Sea). No significant difference was found between regions in Alanine and Aspartic acid using Tukeys HSD.

Amino acid	ANOVA (F statistics and P values)	Tukey's HSD, noteworthy relationships (regions, *P*-value, 95% C.I. = lower, upper)
Alanine	$F_{4,27}$ = 14.19, P <0.0001	NESS-OESS, <0.05, 95% C.I. = 1.94, 11.61
Leucine	$F_{4,27}$ = 25.28, P <0.0001	NLS-OLS, <0.01, 95% C.I. = 0.40, 7.98 NESS-OESS, <0.001, 95% C.I. = 2.2, 8.4
Glycine	$F_{4,27}$ = 53.22, P <0.0001	NLS-OLS, <0.0001, 95% C.I. = 2.88, 8.25 NLS-NESS, <0.0001, 95% C.I. = 2.30, 6.77 NESS-DLS, <0.01, 95% C.I. = 0.57, 6.53 DLS-OLS, <0.01, 95% C.I. = -7.91, -1.24 NESS-OESS, <0.001, 95% C.I. = 1.75, 6.15 OESS-OLS, <0.05, 95% C.I. = 0.27, 5.59
Proline	$F_{4,19}$ = 38.44, P <0.0001	NLS-NESS, <0.05, 95% C.I. = 0.2, 5.94 OLS-OESS, <0.0001, 95% C.I. = 3.26, 8.96 NESS-OESS, <0.0001, 95% C.I. = 2.98, 8.12
Aspartic acid	$F_{4,27}$ = 6.65, P <0.001	N/A
Glutamic acid	$F_{4,27}$ = 29.18, P <0.0001	NLS-OLS, <0.05, 95% C.I.= 0.45, 9.35 OLS-OESS, <0.01, 95% C.I. = 1.18, 9.98 NESS-OESS, <0.0001, 95% C.I. = 3.14, 10.43
Phenylalanine	$F_{4,27}$ = 10.91, P <0.0001	OLS-OESS, <0.05, 95% C.I. = 0.55, 6.07 NESS-OESS, <0.05, 95% C.I. = 0.16, 4.74

3.4.5 Amino acid indices

The degradation index (DI; Dauwe et al., 1999) ranged from -1.21 to 0.91 (OESS and NESS, respectively); and there is no evidence of a difference between regions (ANOVA, $F_{4,52}$ = 2.4, P >0.05; Fig. 3.11). The ∑V proxy for heterotrophic reworking (McCarthy et al., 2007) ranged from 1.5 to 4.1‰ (NESS/NLS and OESS, respectively); and again there was no evidence of a difference between regions (ANOVA, $F_{4,19}$=1.8, P > 0.05; Fig. 3.11).

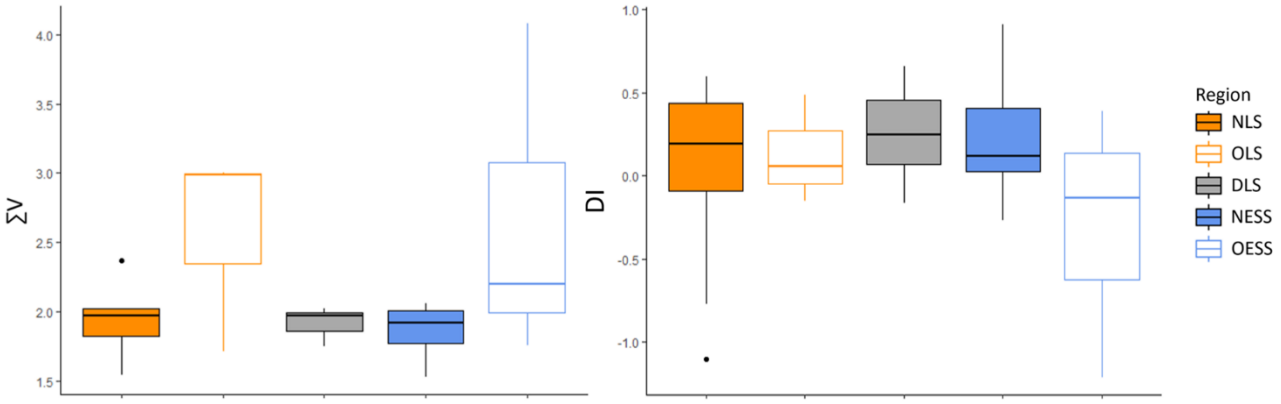

Figure 3.11 Heterotrophic reworking proxy (∑V) values calculated following McCarthy et al., 2007 study with the exception that isoleucine was not measured in the current study. n= for ∑V : NLS (5), OLS (3), DLS (3), NESS (4), OESS (9) . The Degradation index (DI) values calculated following Dauwe et al., 1999 study. n= for DI : NLS (18), OLS (3), DLS (6), NESS (9), OESS (21). Both indices indicating no differences between the regions across the shelf. Closed circles represent individual data that falls below or above the 5% and 95% quartiles.

3.5 Discussion

3.5.1 Comparison of bulk nitrogen and carbon

C/N ratios of marine sediments have been commonly employed to give an indication of organic matter origin; terrestrial OM exhibits higher C/N ratios (>15) than marine OM (~6; Hedges and Oades, 1997; Stein, 2008). The C/N ratios across the ESAS exhibited greater values close to the coastline (NLS, DLS and NESS) which became progressively lower in an offshore direction (OLS and OESS).

In the nearshore Laptev Sea, sediments close to coast and near to the Lena river outflow have elevated C/N values in comparison to the nearshore samples of the DLS and those near to the Indigirka and Kolyma outflows in the NESS region. These results suggest a difference in the terrestrial organic matter delivered to these coastal regions in line with previous studies (Karlsson *et al.*, 2015; Sparkes *et al.*, 2015; Salvadó *et al.*, 2016) Previous studies have, for instance, used the BIT index (branched glycerol dialkyl glycerol tetraethers to crenarchaeol ratio; Doğrul Selver et al., 2015; Sparkes et al., 2015) to show that riverine input was highest close to river outflows and to a lesser extent in ICD dominated areas. In the NESS, the BIT index was much lower than that of the NLS and Lena outflow samples (Sparkes *et al.*, 2015), displaying similar trends W-E as with the C/N ratio reported in present study. Additionally, bacteriohopanepolyols (BHPs) concentrations, and the associated R'Soil index (*terrestrial-marine* proxy; Bischoff *et al.*, 2016), did not display this W-E discrepancy indicating, that at least for these compounds, there is a wide-ranging terrestrial signal characterised unlike the primarily riverine tracking BIT index (Bischoff et al., 2016). Others have linked this pattern to the higher contributions of 'ancient' terrestrial organic matter from mature permafrost soils and ICDs in the DLS and NESS compared to the NLS, using the radiocarbon age of organic

carbon in sediments and contribution of aromatics to the macromolecular fraction (Vonk et al., 2012; Sparkes et al., 2016). This divergence from West to East has been previously shown to illustrate a change in degradation regimes in combination with increased marine organic matter inputs in the East Siberian Sea, if compared to the Laptev Sea, likely driven by the input of Pacific water entering the shelf from the East (Karlsson et al., 2015).Furthermore, the NLS showed elevated C/N ratios if compared to its offshore counterpart (OLS), supporting the increased addition of marine organic matter to the sediment in the OLS. The shift to a less terrestrial dominated system in the OLS is similarly reflected in the BIT, R'Soil index and radiocarbon age of the sediments, where they signify a reduction in terrestrial organic matter contribution compared to the NLS (Vonk et al., 2012; Doğrul Selver et al., 2015; Sparkes et al., 2015, 2016).

Unlike the Laptev Sea, the East Siberian Sea did not exhibit as large a difference from the nearshore to offshore regions. This is in line with previous BIT index analyses in this region (Doğrul Selver et al., 2015; Sparkes et al., 2015) linked to rapidly reducing riverine input close to the coast and increasing amounts of marine organic matter from Pacific water influxes (Vonk et al., 2012; Karlsson et al., 2015; Sparkes et al., 2015; Karlsson et al., 2016). Moreover, there was a difference in the offshore regions of the Laptev and East Siberian Seas (OLS and OESS) which supports the transference of a terrestrial signal difference W-E into the far offshore sediments of the shelf in combination with influx of Pacific water in the OESS. This is also reflected in the R'Soil index displaying markedly reduced terrestrial input in the OESS (Bischoff et al., 2016).

To further investigate this trend, carbon and nitrogen isotopic compositions ($\delta^{13}C_{TOC}$ and $\delta^{15}N_{Bulk}$) obtained from across the ESAS were analysed in more detail. Isotopically lighter

values of $\delta^{13}C_{TOC}$ close to the coastline were consistent across the nearshore regions and then transitioned to heavier values in the offshore regions. Unlike the C/N the $\delta^{13}C_{TOC}$ did not have distinct differences between the NLS and NESS. There were, however, differences between the nearshore and offshore regions (NLS-OLS and NESS-OESS), supporting an increased contribution of marine organic matter as shown by, for instance, the strong correlation to the R'Soil index (Bischoff et al., 2016). However, this is not the case for $\delta^{15}N_{Bulk}$ where there where clear differences found between the two nearshore regions, while the DLS had similar values to the NESS. This suggests that, as with the C/N ratio, there is a difference in the terrestrial matter delivered, and in particular the nitrogen fraction, to the nearshore regions in the Laptev and East Siberian Seas. Consistent with previously reported *terrestrial-marine* proxies (e.g. BIT and R'Soil) the ^{15}N exhibited enriched isotopic values with increasing distance from the coastline, again supporting a transition to a more marine dominated system. Similar to the nearshore regions, the ^{15}N in offshore regions likewise display differences, indicating either a transference of the differences found in nearshore regions or a difference in marine endmember compositions with a potential input of pacific derived inputs in the OESS. However, as $\delta^{15}N_{Bulk}$ measurements encapsulate the entire nitrogen pool indication that a potential difference in contribution of terrestrial inorganic nitrogen cannot be excluded. This means that it remains unclear from $\delta^{15}N_{Bulk}$ whether this shift from west to east is solely driven by organic nitrogen contributions.

When ^{13}C and ^{15}N are compared to regional end members proposed by Tesi et al. (2016), the NLS region again fits closer to a vegetation end member whereas the DLS and ESS a Yedoma end member (Fig. 3.12). Earlier observations have identified some coastal areas around the DLS and ESS as receiving relatively greater contributions of ICD organic matter compared to the NLS (Vonk et al., 2012; Sparkes et al., 2016). This further supports a

difference in the organic matter delivered from the different catchment areas, which remains towards the offshore region where the ESS interacts with the Pacific inflow. The DLS region, for instance, likely incorporates organic matter partly from the Lena River driven by the eastward flowing Siberian Coastal Current but also Yedoma from the eroding coastline (Schuur et al., 2015). This, combined with an elevated BIT in the DLS compared to the NESS demonstrates a major contribution from fluvial transported terrestrial derived OM directly into the DLS (Sparkes et al., 2015), while the large depletion in ^{14}C around the DLS compared to the Lena river outflow as well as the relative high amounts of aromatic moieties as shown by Py-GCMS (Vonk et al., 2012; Sparkes et al., 2018) indicate a substantial Yedoma input, hence the relatively transitional position the DLS sits in when using elemental and bulk isotopic data comparisons (Fig. 3.12). Like the C/N ratio, the $\delta^{15}N_{Bulk}$ had differences in the nearshore and offshore regions of the Laptev and East Siberian Seas, which further supports a difference in the nitrogen pool driving the shifts from the Laptev to East Siberian Seas (Fig. 3.12).

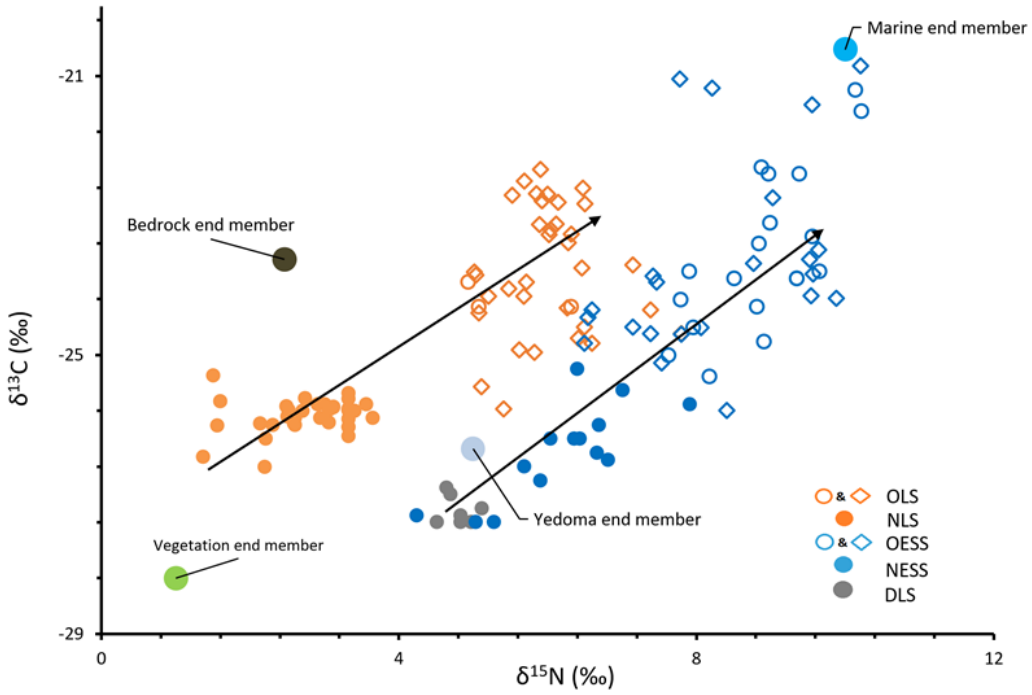

Figure 3.12 Plot of $\delta^{13}C_{Bulk}$ vs. $\delta^{15}N_{Bulk}$ with samples grouped by region (colour) and cruise (shape) as follows: nearshore Laptev Sea (NLS), offshore Laptev Sea (OLS), Dmitry Laptev Strait (DLS), nearshore East Siberian Sea (NESS) and offshore East Siberian Sea (OESS). Circles specify ISSS-08 and diamonds SWERUS-C3 samples. Arrows indicate a near to offshore transect in both regions. End members from Tesi et al. (2016) and are larger filled circles. Note the difference in the nitrogen nearshore values for the NLS and NESS are separated indicating a difference in the nitrogen source between the regions.

3.5.2 Phenol to pyridine ratios across the ESAS

To advance our understanding of the trends on the ESAS we employed the PPRI developed by Sparkes et al. (2016). The additional samples in this study alongside those obtained previously gives a more detailed ESAS wide picture supporting the nearshore to offshore trends in the relative abundance of phenols and pyridines across the whole ESAS. All nearshore regions exhibited a dominance of phenols which in combination with the ^{14}C data was thought to signify a modern source of terrestrially derived organic matter (Sparkes et al., 2016). Tesi et al. (2014) determined the lignin concentrations, using the CuO oxidation method (Goñi and Montgomery, 2000), and analyses indicate a strong correlation between the presence of lignin and relative amounts of phenols in the pyrolysates, suggesting that the latter predominately sourced from surface soils containing lignin (Tesi et al., 2014; Sparkes et

al., 2016). This dominance of phenols relative to pyridines diminishes with increasing distance from the coast and major river inputs. Pyridines can originate from terrestrial and marine sources but an increased abundance in offshore samples is interpreted as an increased input of marine primary produced organic matter to the sediments (Sparkes et al., 2016). The PPRI therefore moves closer to 0 as distance from terrestrial influences increases, a pattern illustrated across the ESAS. If compared to the $\delta^{13}C_{TOC}$ and $\delta^{15}N_{Bulk}$ (Fig. 3.13); a negative correlation and the same trends offshore suggests that both the PPRI and isotopes are tracking similar organic matter inputs. As with $\delta^{13}C_{TOC}$, the PPRI does not display differences in the NLS and NESS regions (Fig. 3.6) where previous studies have documented a change due to contrasting biogeochemical regimes, however these used molecular level analyses (Karlsson et al., 2016). Though, a macromolecular analyses approach characterises different parts of the organic matter material present in the sediments so it might be expected that this pattern is not apparent. Feng et al. (2013), for instance, presented compound specific ^{14}C data for a range of phenol and wax lipids across the ESAS and found that phenols originated from modern surface soils and their export to the ESAS was predominantly controlled by river run off, while plant wax lipids, present in the same sediments, mainly originated from (old) permafrost deposits predominantly controlled by thaw processes, highlighting why we may not see distinct W-E gradients in our own dataset.

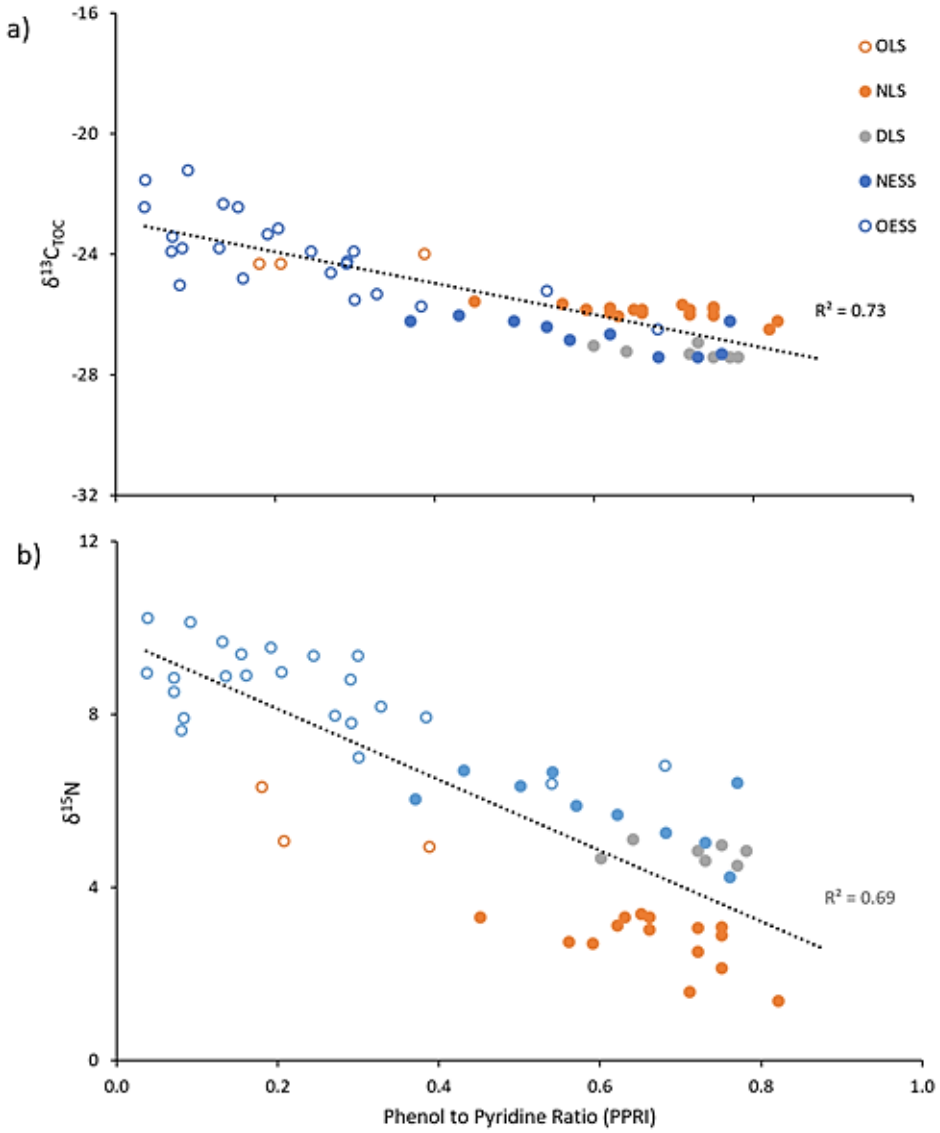

Figure 3.13 Plot a) $\delta^{13}C_{Bulk}$ vs. PPRI. Plot b) $\delta^{15}N_{Bulk}$ vs. PPRI. Samples are grouped by region (colour) as follows: nearshore Laptev Sea (NLS), offshore Laptev Sea (OLS), Dmitry Laptev Strait (DLS), nearshore East Siberian Sea (NESS) and offshore East Siberian Sea (OESS). Both isotopes correlate well with the PPRI indicating they are likely tracking similar inputs of organic matter.

3.5.3 Amino acid composition

To better understand the diagenetic processes in sediments, amino acid compositions are a widely used tool in marine geochemistry, but previous studies have indicated that the abundance of amino acids is not source indicative (Cowie and Hedges, 1992; Dauwe and Middelburg, 1998), which is in line with the outcomes of present study. Correlation tests of the amino acid mol% data (Fig. 3.8 and 3.9) revealed a grouping of leu and phe, displaying the same kind of relationship to the other amino acids and indices measured. PCA analysis, for instance, shows clear grouping with Leu and Phe being grouped together, away from the other amino acids. This is predominantly a reflection of the degradation index established by Dauwe et al. (1999; PC1) with some impact linked to the regions, in particular the nearshore to offshore transects (PC2). This kind of grouping has been noted in other regions of the Arctic (Fram Strait) in both particulate and dissolved amino acids, whereby Leu and Phe were concentrated in the particulate phase, i.e. associated with an actively growing plankton community, while the other amino acids were concentrated in the dissolved phase (Grosse et al., 2021), signifying heterotrophic reworking by bacteria.

Leu and Phe are essential amino acids, meaning they cannot be biosynthesised by some organisms, unlike Ala, Gly, Asp and Glu which are non-essential amino acids (Grosse et al., 2021). Valine, another essential amino acid, did correlate with the non-essential group but it is a minor constituent of the amino acid pool and there were often insignificant relationships or no relationships when tested (Fig. 3.8). The grouping of Leu and Phe and their correlations to other *terrestrial-marine* proxies, such as the C/N ratio and PPRI, could indicate that the terrestrial component present in these sediments is simply enriched in these amino acids compared to their marine counterparts. However, analysis indicates that Phe is the only

amino acid that differs in the nearshore to offshore regions of the East Siberian Sea indicating that a simple terrestrial-marine impact on the amino acid compositions remains undecided. For this to be assessed, a fully characterised terrestrial end-member needs to be analysed confirming whether it is enriched in Leu and Phe. In addition, the amino acid mol% trend could be a result of fluvial-derived organic matter, or some mix of this and terrestrial sources, where in-situ production is driving increases in Leu and Phe mol%, though this would likewise need to be tested riverine water column samples. Finally, in order to fully elucidate whether the AA mol% pattern observed is caused by the relative enrichment of Leu and Phe in sinking particulate matter a full water column analysis would be needed, as shown by Grosse *et al.* (2021).

The DI also did not provide any evidence of differences between regions and the ranges reported here are analogous with other marine sediment studies (e.g. Dauwe et al., 1999; Calleja et al., 2013b; Gaye et al., 2022). When the DI is plotted against the C/N and PPRI there is a positive relationship rather than negative one, as might be expected because large DI values are associated with planktonic material while higher C/N and PPRI values are associated with terrestrial material (Dauwe et al., 1999; appendix. 1). The different techniques used to determine the amino acid composition, e.g. GCMS versus high performance liquid chromatography (HPLC; Dauwe et al., 1999), could have impacted the DI, since more of the protein amino acids can be detected by HPLC. However, it is likely that the presence of permafrost in the drainage basins and the impact this has on the degradation status of the terrestrial OM (Karlsson et al., 2015) combined with the way the terrestrial OM is transported to the ESAS sediments, e.g. fluvial and/or coastal erosion, has also impacted the 'freshness' of terrestrial derived material and thus the DI. Karlsson et al. (2015) for instance, showed that specific OM sources behave differently in the water column, causing

an offset between particulate, colloidal and sedimentary OM compositions. Particularly, coastal erosion derived OM is relatively enriched in surface sediments if compared to concentrations in the water column. In addition, Karlsson et al. (2015) showed different modes of terrestrial OM degradation in different parts of the ESAS, potentially impacting the amino acid distributions.

3.5.4 Amino acid nitrogen isotope composition

Amino acids in sediments can be further investigated, past the compositional level and into the isotopic level using CSIA-AA. This has the capability to decouple potential variations/contamination exhibited in bulk analysis such as the in-mixing of inorganic nitrogen and other compounds that dilute or mask the isotopic signal. Here, we measured the $\delta^{15}N_{AA}$ in surface sediment samples to investigate whether the organic nitrogen fraction drives the changes in bulk elemental and isotopic compositions across the ESAS. Source amino acid ^{15}N (Phe and Gly) are typically regarded as representing the 'baseline' of the food web as they have minimal fractionation associated with trophic level transfer (McClelland and Montoya, 2002; McClelland et al., 2003). Variations in their isotopic composition are viewed as variations in the 'food' source at the base of the food web and a well constrained base across a region provides an isoscape with which to calculate trophic levels more accurately (McClelland and Montoya, 2002; McClelland et al., 2003). As is the case with the $\delta^{15}N_{Bulk}$, the source amino acids exhibit a relative enrichment both from the W-E nearshore regions and from coast to offshore samples, suggesting that the organic nitrogen fraction (amino acids) played a dominant control over the variations presented in the C/N ratio and $\delta^{15}N_{Bulk}$ rather than the inorganic nitrogen deviations.

The variations in the source amino acids between the regions in this study highlight the major differences that can be present in the isoscape, even in regions where it might be assumed that there would be none or little variation in the baseline due to their geochemical similarities and proximity to one another (Bischoff et al., 2016; Semiletov et al., 2016; Sparkes et al., 2016). As the difference originates in the nearshore region it is probable that there is a terrestrial driver in these deviations and, as climate warming advances, we expect an increased amount of terrestrial organic nitrogen to be delivered to the ESAS which will further alter the isoscape presented here.

Across the trophic amino acids (Ala, Leu, Pro, Asp and Glu) there is a general trend of enrichment in $\delta^{15}N$ from the nearshore to offshore regions in both the Laptev and East Siberian Seas, with some of these forming substantial differences between them. This could be caused by a number of reasons, although it is likely that some combination of all them has caused the observed changes in trophic $\delta^{15}N_{AA}$. Firstly, this pattern could be due to terrestrial inputs in the nearshore areas, which transitions to a more 'marine' dominated system offshore, where primary producers fix nitrogen from dissolved inorganic nitrogen sources in the water column (which tend to be more enriched compared to it terrestrial counter parts in ^{15}N; Batista et al., 2014).

The enrichment in trophic ^{15}N offshore could also reflect an increased amount of heterotrophic bacterial reworking (McCarthy et al., 2007). However, while the $\sum V$ proxy does show some increases from the nearshore to offshore regions, there are no significant differences between the two, so can only account, in part, for some of the increases in $\delta^{15}N$ of trophic amino acids. Furthermore, marine food webs are known to be more intricate than

terrestrial ones, with more trophic levels leading to relatively enriched $\delta^{15}N$ values (Webb et al., 2016; Ohkouchi et al., 2017).

A helpful proxy to use is the total hydrolysable amino acid ^{15}N values, or the $\delta^{15}N_{THAA}$, this combines the total molar weighted average $\delta^{15}N$ of all of the amino acids measured and has been used in previous studies to give an overall ^{15}N value for proteinaceous material in a sample (McCarthy et al., 2013; Batista et al., 2014; Yamaguchi and McCarthy, 2018). When the $\delta^{15}N_{Bulk}$ to $\delta^{15}N_{THAA}$ is compared across the ESAS (Fig. 3.14; Batista et al., 2014) in the Laptev and East Siberian Seas, there is a good positive correlation (r^2 = 0.8 and 0.87, respectively; Fig. 3.14), which implies that changes in $\delta^{15}N_{Bulk}$ are likely driven by changes in the $\delta^{15}N_{THAA}$ and therefore excluding inorganic nitrogen as a driver of change across the regions. $\delta^{15}N_{THAA}$ is almost consistently enriched relative to $\delta^{15}N_{Bulk}$ in all regions of the ESAS (Fig. 3.14 and 3.15) comparable to a previous study in marine sediments from the Santa Barbara Basin (Batista et al., 2014). Batista et al. (2014) concluded that this offset was not caused by a terrestrial input due to the similarity in $\delta^{15}N_{Bulk}$ between both 'fresh' planktonic material (where no terrestrial signal should be present) and sedimentary samples. However, as discussed previously, it is clear that the coastal regions of the ESAS are dominated by a terrestrial input and therefore the offset reported here is not predominantly due to the influx of planktonic material to the nearshore regions (e.g. Vonk et al., 2012; Sparkes et al., 2016; Tesi et al., 2016). However, similar to the amino acid compositions, to fully confirm this we would, ideally, have endmember analysis of plankton and terrestrial samples.

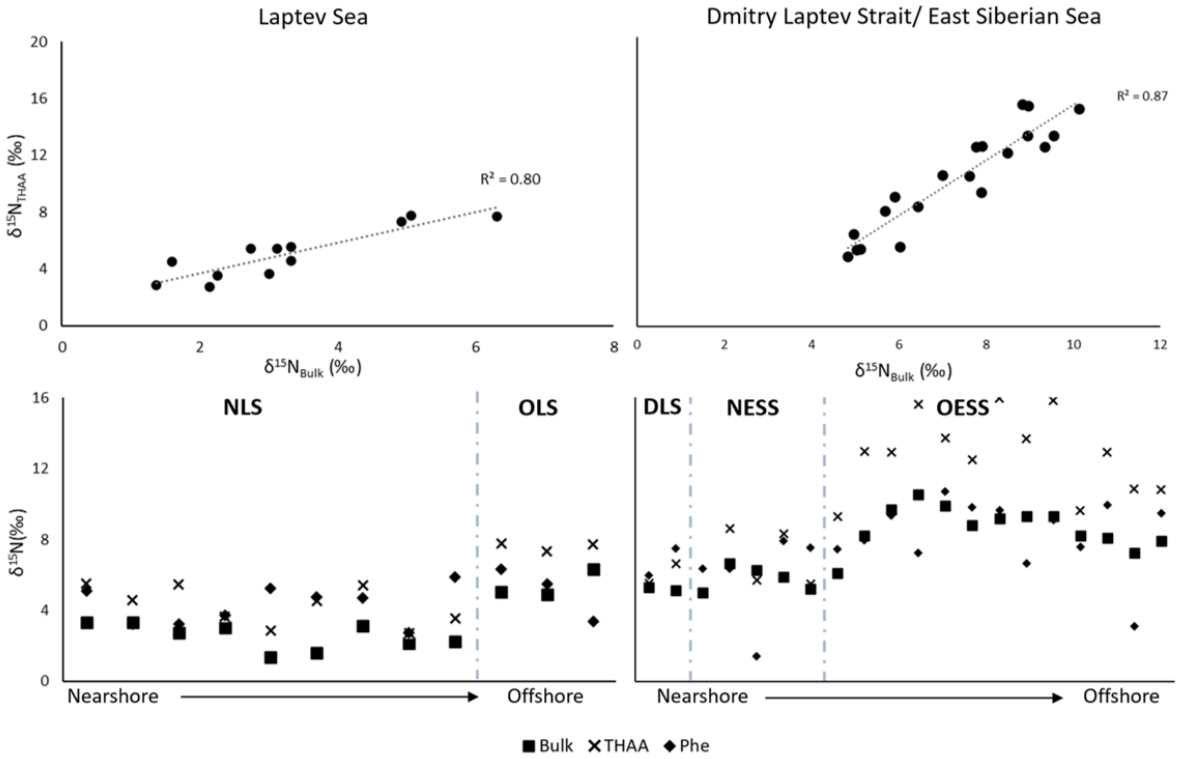

Figure 3.14 Correlation plots (top) showing the $\delta^{15}N_{Bulk}$ vs. $\delta^{15}N_{THAA}$ (total hydrolysable amino acids) for the Laptev Sea samples (right) and Dmitry Laptev Strait and East Siberian Sea (left) samples and comparison plots (bottom) between the $\delta^{15}N_{Bulk}$, $\delta^{15}N_{THAA}$ and $\delta^{15}N_{Phe}$ in the same regions illustrating a consistent enrichment of $\delta^{15}N_{THAA}$ to $\delta^{15}N_{Bulk}$ across the region and indicating varying baseline values from the $\delta^{15}N_{Phe}$. NLS (nearshore Laptev Sea), OLS (offshore Laptev Sea), DLS (Dmitry Laptev Strait), NESS (nearshore East Siberian Sea) and OESS (offshore East Siberian Sea).

The offsets we report earlier in $\delta^{15}N_{Bulk}$ between the nearshore regions of the Laptev and East Siberian Seas was ~3.3‰ this is consistent with differences we also find in $\delta^{15}N_{THAA}$ between the same regions (~3.3‰; Fig. 3.15), indicating again that the organic nitrogen pool is causing the E-W difference in nitrogen isotopes rather than inorganic sources. It is, therefore, reasonable to assume that the offset we present in the C/N ratio, $\delta^{15}N_{Bulk}$, $\delta^{15}N_{Phe}$, $\delta^{15}N_{THAA}$ is a direct consequence of a shift in the organic nitrogen pool from the Laptev to the East Siberian Seas.

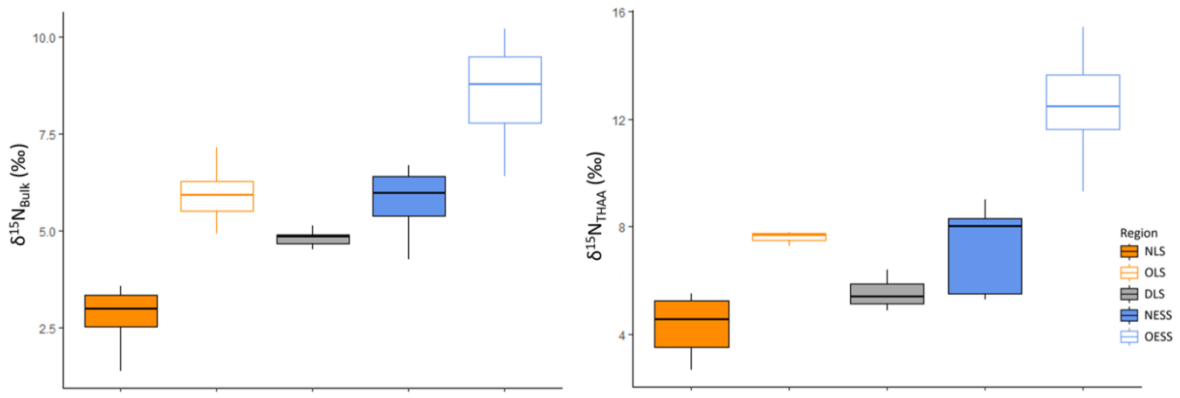

Figure 3.15 Bulk ^{15}N and $^{15}N_{THAA}$ split by region indicating clear offsets between the nearshore regions of both the Laptev and East Siberian Seas. NLS (nearshore Laptev Sea), OLS (offshore Laptev Sea), DLS (Dmitry Laptev Strait), NESS (nearshore East Siberian Sea) and OESS (offshore East Siberian Sea). Closed circles represent individual data that falls below or above the 5% and 95% quartiles. Bulk ^{15}N NLS n=34, OLS n=36, DLS n=7, NESS n=10 and OESS n=42. $^{15}N_{THAA}$ NLS n=10, OLS n=3, DLS n=3, NESS n=5 and OESS n=12.

Overall these results show that in the coastal regions of the ESAS there is a difference in the organic matter delivered to the sediments, by using a multi-proxy approach it becomes apparent that this difference is driven by nitrogen containing compounds and more specifically the organic nitrogen fraction, as our CSIA-AA reveals. As we move offshore this difference persists, indicating that there are also differences between the offshore regions across the ESAS, like the nearshore regions this was revealed to be in the organic nitrogen pool. By using CSIA-AA in this region we can, for the first time, utilise the ^{15}N of source amino acids to better constrain the isoscape of the region. This has considerable implications for assessing the status of the region as variations in the isoscape can be an indicator of changes in source of organic matter which has implications for organic matter degradation and subsequent degradation to carbon dioxide or carbon sequestration.

3.6 Conclusions and implications

To summarise, analyses of surface sediments from across the ESAS indicate that the $\delta^{15}N_{Bulk}$ is, comparable to other proxies such as the C/N ratio, PPRI and molecular indices, tracking the terrestrial versus marine contributions across the ESAS, with clear differences between the Laptev and East Siberian regions. This is likely reflecting a difference in terrestrial contributions across both regions. Amino acid distribution patterns show no distinct patterns across the whole ESAS although the abundance of Leu and Phe (the essential amino acids) correlated well with C/N ratios and PPRI. This is likely caused by a combination of the presence of large amounts of permafrost in the drainage basins, different degradation rates for the terrestrial OM contributors and the distinctly different modes of degradation in different parts of the ESAS. The ^{15}N isotopic compositions of the amino acids do show distinct differences across the ESAS. Like the $\delta^{15}N_{Bulk}$, there are clear differences between the coastal regions, implying that changes in $\delta^{15}N_{Bulk}$ are driven by changes in the $\delta^{15}N_{THAA}$ and not caused by contributions of inorganic nitrogen across the shelf. Furthermore, distinct enriched $\delta^{15}N_{THAA}$ values are observed in the more offshore regions also following the trends in the $\delta^{15}N_{Bulk}$. These results, for the first time, not only give us a more detailed understanding of changes in sedimentary nitrogen (amino acid compositional and $\delta^{15}N$) across this region but also has wide ranging implications for assessing food web status and future climate induced changes. The baseline isoscape presented here varies between the regions which needs to be factored into trophic level determination from primary producers at the base to apex predators at the top of the food chain. As the Arctic becomes increasingly ice–free and more nutrient than light limited, an accurate understanding of the impacts on sedimentary organic matter will be crucial. The Arctic, and in particular the ESAS, is known to be undergoing rapid

change which is leading to increased amounts of organic matter delivered to the shelf, there will likely be further alterations of the isoscape as a direct result of this, making it vital to have a current baseline to work from.

References

Abbott, B. W. and Jones, J. B. (2015) 'Permafrost collapse alters soil carbon stocks, respiration, CH4, and N2O in upland tundra', *Global Change Biology*, 21(12), pp. 4570–4587. doi: 10.1111/gcb.13069.

Batista, F. C. *et al.* (2014) 'Compound specific amino acid δ15N in marine sediments: A new approach for studies of the marine nitrogen cycle', *Geochimica et Cosmochimica Acta*. Elsevier Ltd, 142, pp. 553–569. doi: 10.1016/j.gca.2014.08.002.

Bischoff, J. *et al.* (2016) 'Source, transport and fate of soil organic matter inferred from microbial biomarker lipids on the East Siberian Arctic Shelf', *Biogeosciences*, 13(17), pp. 4899–4914. doi: 10.5194/bg-13-4899-2016.

Bröder, L. *et al.* (2019) 'Quantifying Degradative Loss of Terrigenous Organic Carbon in Surface Sediments Across the Laptev and East Siberian Sea', *Global Biogeochemical Cycles*, 33(1), pp. 85–99. doi: 10.1029/2018GB005967.

Burdige, D. J. and Martens, C. S. (1988) 'Biogeochemical cycling in an organic-rich coastal marine basin: 10. The role of amino acids in sedimentary carbon and nitrogen cycling', *Geochimica et Cosmochimica Acta*, 52(6), pp. 1571–1584. doi: 10.1016/0016-7037(88)90226-8.

Calleja, M. L. *et al.* (2013a) 'Changes in compound specific δ15N amino acid signatures and d/l ratios in marine dissolved organic matter induced by heterotrophic bacterial reworking', *Marine Chemistry*. Elsevier B.V., 149, pp. 32–44. doi: 10.1016/j.marchem.2012.12.001.

Calleja, M. L. *et al.* (2013b) 'Changes in compound specific δ15N amino acid signatures and d/l ratios in marine dissolved organic matter induced by heterotrophic bacterial reworking', *Marine Chemistry*. Elsevier B.V., 149, pp. 32–44. doi: 10.1016/j.marchem.2012.12.001.

Carstens, D. *et al.* (2013) 'Amino acid nitrogen isotopic composition patterns in lacustrine sedimenting matter', *Geochimica et Cosmochimica Acta*. Elsevier Ltd, 121, pp. 328–338. doi: 10.1016/j.gca.2013.07.020.

Chikaraishi, Y. *et al.* (2007) 'Metabolic control of nitrogen isotope composition of amino acids in macroalgae and gastropods: Implications for aquatic food web studies', *Marine Ecology*

Progress Series, 342(2003), pp. 85–90. doi: 10.3354/meps342085.

Chikaraishi, Y. *et al.* (2009) 'Determination of aquatic food-web structure based on compound-specific nitrogen isotopic composition of amino acids', *Limnology and Oceanography: Methods*, 7(11), pp. 740–750. doi: 10.4319/lom.2009.7.740.

Cowie, G. and Hedges, J. (1992) 'Sources and reactivities of amino acids in a coastal marine environment', *Limnology and Oceanography*, 37(4), pp. 703–724.

Dauwe, Birgit *et al.* (1999) 'Linking diagenetic alteration of amino acids and bulk organic matter reactivity', *Limnology and Oceanography*, 44(7), pp. 1809–1814. doi: 10.4319/lo.1999.44.7.1809.

Dauwe, B. *et al.* (1999) 'Linking diagenetic alteration of amino acids and bulk organic matter reactivity', *Limnology and Oceanography*, 44(7), pp. 1809–1814. doi: 10.4319/lo.1999.44.7.1809.

Dauwe, B. and Middelburg, J. J. (1998) 'Amino acids and hexosamines as indicators of organic matter degradation state in North Sea sediments', *Limnology and Oceanography*, 43(5), pp. 782–798. doi: 10.4319/lo.1998.43.5.0782.

Dittmar, T., Fitznar, H. P. and Kattner, G. (2001) 'Origin and biogeochemical cycling of organic nitrogen in the eastern Arctic Ocean as evident from D-and L-amino acids', *Geochimica et Cosmochimica Acta*, 65(22), pp. 4103–4114. Available at: http://linkinghub.elsevier.com/retrieve/pii/S0016703701006883.

Doğrul Selver, A. *et al.* (2015) 'Distributions of bacterial and archaeal membrane lipids in surface sediments reflect differences in input and loss of terrestrial organic carbon along a cross-shelf Arctic transect', *Organic Geochemistry*, 83–84, pp. 16–26. doi: 10.1016/j.orggeochem.2015.01.005.

van Dongen, B. E. *et al.* (2008) 'Contrasting lipid biomarker composition of terrestial organic matter exported from across the Eurasian Arctic by the five great Russian Arctic rivers', *Global Biogeochemical Cycles*, 22(1), p. n/a-n/a. doi: 10.1029/2007GB002974.

Dunton, K. H., Weingartner, T. and Carmack, E. C. (2006) 'The nearshore western Beaufort Sea ecosystem: Circulation and importance of terrestrial carbon in arctic coastal food webs',

Progress in Oceanography, 71(2–4), pp. 362–378. doi: 10.1016/j.pocean.2006.09.011.

Feng, X. *et al.* (2013) 'Differential mobilization of terrestrial carbon pools in Eurasian Arctic river basins', *Proceedings of the National Academy of Sciences of the United States of America*, 110(35), pp. 14168–14173. doi: 10.1073/pnas.1307031110.

Gaye, B. *et al.* (2022) 'What can we learn from amino acids about oceanic organic matter cycling and degradation?', pp. 807–830.

Goni, M. A. and Montgomery, S. (2000) 'Alkaline CuO Oxidation with a Microwave Digestion System : Lignin Analyses of Geochemical Samples', 72(14), pp. 3116–3121.

Gordeev, V. V. (2006) 'Fluvial sediment flux to the Arctic Ocean', *Geomorphology*, 80(1–2), pp. 94–104. doi: 10.1016/j.geomorph.2005.09.008.

Grosse, J. *et al.* (2021) 'Summertime Amino Acid and Carbohydrate Patterns in Particulate and Dissolved Organic Carbon Across Fram Strait', *Frontiers in Marine Science*, 8(July). doi: 10.3389/fmars.2021.684675.

Guo, L. *et al.* (2004) 'Characterization of Siberian Arctic coastal sediments: Implications for terrestrial organic carbon export', *Global Biogeochemical Cycles*, 18(1). doi: 10.1029/2003gb002087.

Guo, L. *et al.* (2009) 'Chemical and isotopic composition of high-molecular-weight dissolved organic matter from the Mississippi River plume', *Marine Chemistry*. Elsevier B.V., 114(3–4), pp. 63–71. doi: 10.1016/j.marchem.2009.04.002.

Hedges, J. I. and Oades, J. M. (1997) 'Comparative organic geochemistries of soils and marine sediments', *Organic Geochemistry*, 27(7).

Holmes, R. M. *et al.* (2012) 'Seasonal and Annual Fluxes of Nutrients and Organic Matter from Large Rivers to the Arctic Ocean and Surrounding Seas', *Estuaries and Coasts*, 35(2), pp. 369–382. doi: 10.1007/s12237-011-9386-6.

Hoque, M. A. and Pollard, W. H. (2016) 'Stability of permafrost dominated coastal cliffs in the Arctic', *Polar Science*. Elsevier B.V. and NIPR, 10(1), pp. 79–88. doi: 10.1016/j.polar.2015.10.004.

IPCC (2014) *Climate Change 2013*, *the Fifth Assessment Report*.

Jong, D. *et al.* (2020) 'Nearshore Zone Dynamics Determine Pathway of Organic Carbon From Eroding Permafrost Coasts', *Geophysical Research Letters*, 47(15). doi: 10.1029/2020GL088561.

Karlsson, E., Gelting, J., Tesi, T., van Dongen, B., *et al.* (2016) 'Different sources and degradation state of dissolved, particulate, and sedimentary organic matter along the Eurasian Arctic coastal margin', *Global Biogeochemical Cycles*, 30(6), pp. 898–919. doi: 10.1002/2015GB005307.

Karlsson, E. S. *et al.* (2011) 'Carbon isotopes and lipid biomarker investigation of sources, transport and degradation of terrestrial organic matter in the Buor-Khaya Bay, SE Laptev Sea', *Biogeosciences*, 8(7), pp. 1865–1879. doi: 10.5194/bg-8-1865-2011.

Karlsson, E. S. *et al.* (2015) 'Contrasting regimes for organic matter degradation in the East Siberian Sea and the Laptev Sea assessed through microbial incubations and molecular markers', *Marine Chemistry*. Elsevier B.V., 170, pp. 11–22. doi: 10.1016/j.marchem.2014.12.005.

Kattsov, V. M. *et al.* (2007) 'Simulation and Projection of Arctic Freshwater Budget Components by the IPCC AR4 Global Climate Models', *Journal of Hydrometeorology*, 8(3), pp. 571–589. doi: 10.1175/JHM575.1.

Lantuit, H. *et al.* (2011) 'Coastal erosion dynamics on the permafrost-dominated Bykovsky Peninsula, north Siberia, 1951-2006', *Polar Research*, 30(SUPPL.1). doi: 10.3402/polar.v30i0.7341.

Lewis, K. M., Dijken, G. L. Van and Arrigo, K. R. (2020) 'Changes in phytoplankton concentration now drive increased Arctic Ocean primary production', 202(July), pp. 198–202.

Martens, J. *et al.* (2019) 'Remobilization of Old Permafrost Carbon to Chukchi Sea Sediments During the End of the Last Deglaciation', *Global Biogeochemical Cycles*, 33(1), pp. 2–14. doi: 10.1029/2018GB005969.

Masson-Delmotte, V., P. Zhai, A. Pirani, S. L., Connors, C. Péan, S. Berger, N. Caud, Y. Chen, L. Goldfarb, M.I. Gomis, M. Huang, K. Leitzell, E. Lonnoy, J.B.R. Matthews, T. K. and Maycock, T. Waterfield, O. Yelekçi, R. Yu, and B. Z. (2021) *IPCC, 2021: Summary for Policymakers. In: Climate Change 2021: The Physical Science Basis. Contribution of Working Group I to the Sixth*

Assessment Report of the Intergovernmental Panel on Climate Change.

McCarthy, M. D. *et al.* (2007) 'Amino acid nitrogen isotopic fractionation patterns as indicators of heterotrophy in plankton, particulate, and dissolved organic matter', *Geochimica et Cosmochimica Acta*, 71(19), pp. 4727–4744. doi: 10.1016/j.gca.2007.06.061.

McCarthy, M. D., Lehman, J. and Kudela, R. (2013) 'Compound-specific amino acid δ15N patterns in marine algae: Tracer potential for cyanobacterial vs. eukaryotic organic nitrogen sources in the ocean', *Geochimica et Cosmochimica Acta*. Elsevier Ltd, 103, pp. 104–120. doi: 10.1016/j.gca.2012.10.037.

McClelland, J. W., Holl, C. M. and Montoya, J. P. (2003) 'Relating low δ15N values of zooplankton to N 2-fixation in the tropical North Atlantic: Insights provided by stable isotope ratios of amino acids', *Deep-Sea Research Part I: Oceanographic Research Papers*, 50(7), pp. 849–861. doi: 10.1016/S0967-0637(03)00073-6.

McClelland, J. W. and Montoya, J. P. (2002) 'Trophic Relationships and the Nitrogen Isotopic Composition of Amino Acids in Plankton', *Ecology*, 83(8), pp. 2173–2180. doi: 10.1890/0012-9658(2002)083[2173:TRATNI]2.0.CO;2.

Ohkouchi, N. *et al.* (2017) 'Advances in the application of amino acid nitrogen isotopic analysis in ecological and biogeochemical studies', *Organic Geochemistry*. Elsevier Ltd, 113, pp. 150–174. doi: 10.1016/j.orggeochem.2017.07.009.

Oliva, M. and Fritz, M. (2018) 'Permafrost degradation on a warmer Earth: Challenges and perspectives', *Current Opinion in Environmental Science & Health*. Elsevier Ltd, 5, pp. 14–18. doi: 10.1016/j.coesh.2018.03.007.

Salvadó, J. A., Tesi, T., Sundbom, M., Karlsson, E., Krusä, M., *et al.* (2016) 'Contrasting composition of terrigenous organic matter in the dissolved, particulate and sedimentary organic carbon pools on the outer East Siberian Arctic Shelf', *Biogeosciences*, 13(22), pp. 6121–6138. doi: 10.5194/bg-13-6121-2016.

Schirrmeister, L. *et al.* (2011) 'Sedimentary characteristics and origin of the Late Pleistocene Ice Complex on north-east Siberian Arctic coastal lowlands and islands - A review', *Quaternary International*. Elsevier Ltd and INQUA, 241(1–2), pp. 3–25. doi: 10.1016/j.quaint.2010.04.004.

Schuur, E. A. G. *et al.* (2015) 'Climate change and the permafrost carbon feedback', *Nature*, 520(7546), pp. 171–179. doi: 10.1038/nature14338.

Semiletov, I. *et al.* (2016) 'Acidification of East Siberian Arctic Shelf waters through addition of freshwater and terrestrial carbon', *Nature Geoscience*, 9(5), pp. 361–365. doi: 10.1038/ngeo2695.

Semiletov, I. and Gustafsson, Ö. (2009) 'East Siberian shelf study alleviates scarcity of observations', *Eos*, 90(17), pp. 145–146. doi: 10.1029/2009eo170001.

Sparkes, R. B. *et al.* (2015) 'GDGT distributions on the East Siberian Arctic Shelf: Implications for organic carbon export, burial and degradation', *Biogeosciences*, 12(12), pp. 3753–3768. doi: 10.5194/bg-12-3753-2015.

Sparkes, R. B. *et al.* (2016) 'Macromolecular composition of terrestrial and marine organic matter in sediments across the East Siberian Arctic Shelf', *Cryosphere*, 10(5), pp. 2485–2500. doi: 10.5194/tc-10-2485-2016.

Sparkes, R. B. *et al.* (2018) 'Carbonaceous material export from Siberian permafrost tracked across the Arctic Shelf using Raman spectroscopy', *Cryosphere*, 12(10), pp. 3293–3309. doi: 10.5194/tc-12-3293-2018.

Stein, R. (2008) *Arctic Ocean Sediments: Processes, Proxies, and Paleoenvironment*. Elsevier.

Stein, R. and MacDonald, R. W. (2004) *The Organic Carbon Cycle in the Arctic Ocean*. Heidelberg: Springer-Verlag Berlin Heidelberg.

Styring, A. K. *et al.* (2012) 'Practical considerations in the determination of compound-specific amino acid δ15N values in animal and plant tissues by gas chromatography-combustion-isotope ratio mass spectrometry, following derivatisation to their N-acetylisopropyl esters', *Rapid Communications in Mass Spectrometry*, 26(19), pp. 2328–2334. doi: 10.1002/rcm.6322.

Tarnocai, C. *et al.* (2009) 'Soil organic carbon pools in the northern circumpolar permafrost region', *Global Biogeochemical Cycles*, 23(2), p. n/a-n/a. doi: 10.1029/2008GB003327.

Team", "R Core (no date) 'R: A language and environment for statistical computing. R Foundation for Statistical Computing'. Austria, Vienna: R Core Team. Available at: https://www.r-project.org/.

Terhaar, J. *et al.* (2021) 'Around one third of current Arctic Ocean primary production sustained by rivers and coastal erosion', *Nature Communications*. Springer US, 12(1), pp. 1–10. doi: 10.1038/s41467-020-20470-z.

Tesi, T. *et al.* (2014) 'Composition and fate of terrigenous organic matter along the Arctic land-ocean continuum in East Siberia: Insights from biomarkers and carbon isotopes', *Geochimica et Cosmochimica Acta*, 133, pp. 235–256. doi: 10.1016/j.gca.2014.02.045.

Tesi, T. *et al.* (2016) 'Matrix association effects on hydrodynamic sorting and degradation of terrestrial organic matter during cross-shelf transport in the Laptev and East Siberian shelf seas', *Journal of Geophysical Research: Biogeosciences*, 121(3), pp. 731–752. doi: 10.1002/2015JG003067.

de Vega, C. *et al.* (2021) 'Biomarkers in Ringed Seals Reveal Recent Onset of Borealization in the High- Compared to the Mid-Latitude Canadian Arctic', 8(September), pp. 1–11. doi: 10.3389/fmars.2021.700687.

Vonk, J. E. *et al.* (2012) 'Activation of old carbon by erosion of coastal and subsea permafrost in Arctic Siberia', *Nature*, 489(7414), pp. 137–140. doi: 10.1038/nature11392.

Webb, E. C. *et al.* (2016) 'Compound-specific amino acid isotopic proxies for distinguishing between terrestrial and aquatic resource consumption', *Archaeological and Anthropological Sciences*. Archaeological and Anthropological Sciences, pp. 1–18. doi: 10.1007/s12520-015-0309-5.

Yamaguchi, Y. T. and McCarthy, M. D. (2018) 'Sources and transformation of dissolved and particulate organic nitrogen in the North Pacific Subtropical Gyre indicated by compound-specific δ15N analysis of amino acids', *Geochimica et Cosmochimica Acta*. Elsevier Ltd, 220, pp. 329–347. doi: 10.1016/j.gca.2017.07.036.

Yamashita, Y. and Tanoue, E. (2003) 'Distribution and alteration of amino acids in bulk DOM along a transect from bay to oceanic waters', *Marine Chemistry*, 82(3–4), pp. 145–160. doi: 10.1016/S0304-4203(03)00049-5.

Photo taken by author while on Royal Research Ship James Clark Ross JR17006. Megacorer being deployed to collect marine sediment cores in Fram Strait

Chapter 4

Organic Matter Cycling in Barents Sea and Fram Strait Sediments: using a novel multiproxy approach to decipher its sources

Emma C. Burns [1], George A. Wolff [2], Rachel M. Jeffreys [2], Robert B. Sparkes [3], Bart E. van Dongen [1]

[1]Department of Earth and Environmental Sciences and Williamson Research Centre for Molecular Environmental Science, University of Manchester, Manchester, UK

[2]Department of Earth, Ocean and Ecological Sciences, University of Liverpool, Liverpool, UK

[3]School of Science and the Environment, Manchester Metropolitan University, Manchester, UK

Manuscript in preparation for submission to Global Biogeochemical Cycles. Supporting information for this manuscript can be found in Appendix 2.

Author Contributions:

E.C.B. wrote the manuscript, collected the samples, carried out the geochemical analyses (EA-IRMS, py-GCMS, GC-FID and GC-C-IRMS), made the figures and ran all statistical analyses. G.A.W. designed the project, helped with geochemical analyses and the interpretation of the data and edited the manuscript. R.M.J. helped with geochemical analyses, the interpretation of the data and edited the manuscript. R.B.S. aided with interpretation of py-GCMS data. B.v.D. designed the project, helped with geochemical analyses, the interpretation of data and edited the manuscript.

Highlights:

- Novel amino acid compositional and $\delta^{15}N$ sedimentary analyses from the Barents Sea and Fram Strait

- C/N ratio, $\delta^{15}N_{Bulk}$ and PPRI tracks the inputs of OM associated to the polar front, marginal ice zones and terrestrial inputs

- $\delta^{15}N$ at bulk level is decoupled from $\delta^{15}N_{THAA}$ due to the inmixing of inorganic nitrogen.

- $\delta^{15}N$ of coastal sediments indicate terrestrial input.

- $\delta^{15}N$ of offshore sediments indicate the polar front and marginal ice zones control organic matter input to sediments.

- $\delta^{15}N$ variations highlights importance for organic matter cycling in a changing Arctic.

Keywords: Arctic Ocean; Nitrogen isotopes; Amino acids; Amino acid composition; Compound-specific nitrogen isotopes analysis; Isoscape; Marine sediments; Biogeochemistry

4.1 Abstract

The continued intrusion of warm Atlantic water and increasing atmospheric temperatures due to climate warming has led to a shift northwards of the polar front (PF) and the associated marginal ice zone (MIZ), earlier sea ice thaw periods and decreasing extent and thickness of sea ice in the Barents Sea and Fram Strait region. PF and MIZ areas are known to be highly productive due to the advection of nutrients, particularly nitrate, and the subsequent melting of sea ice leading to more light penetrating the surface layers indicating that a shift northwards could lead to an increase in productivity and transport of organic matter to underlying sediments. Particularly amino acids and (bulk) ^{15}N analyses have been used to better understand the source of organic matter, determine the baseline isoscape and interrogate the degradation state of the sediments. However, the limited surface sediment data available from the Barents Sea and Fram Strait region, particularly baseline sedimentary amino acid composition and isotopic data, has proved difficult to interpret due to the complicated interplay of water masses, sea-ice, terrestrial inputs and diagenesis.

Here, for the first time, a combined approach of bulk elemental (carbon, nitrogen and $\delta^{15}N_{Bulk}$), macromolecular, amino acid compositional and ^{15}N amino acid isotope analysis of surface sediments from the Barents Sea and Fram Strait is presented to better understand the influence of these changing parameters on the underlying sediments. The $\delta^{15}N_{Bulk}$, C/N ratio and the phenol to pyridine ratio obtained from across this region indicated that the relative position to the PF and MIZ coupled to influx of terrestrial derived inputs from river run off and glacial terminus plays a major role in the sedimentary composition of organic matter present. Amino acid distribution patterns across the study area do not show any distinct trends relating to the MIZ or PF and are generally dominated by elevated

concentrations of leucine (Leu) and phenylalanine (Phe) likely due to their abundance in actively growing phytoplankton communities in the water column, suggesting that this pattern is transferred into the underlying sediments in this region. The ^{15}N of amino acids revealed similar source amino acids across the whole region indicating that a comparable $\delta^{15}N\text{-}NO_3$ source is being utilised regardless of water mass influence. The total $\delta^{15}N$ of proteinaceous material ($\delta^{15}N_{THAA}$) was consistently enriched relative to $\delta^{15}N_{Bulk}$, primarily caused by the inmixing of inorganic nitrogen in the sediments which dilutes the bulk signal. This highlights the limitations of using $\delta^{15}N_{bulk}$ analyses where there is a significant amount of inorganic nitrogen present in the sediments and the valuable information $\delta^{15}N_{THAA}$ can provide in de-coupling these effects. This will be particularly important going forward as the region continues to become more Atlantified due to climate change, altering the positions of the polar front and marginal ice zones and the nitrate sources to primary producers. Combined, this indicates that compound specific isotope nitrogen analysis of amino acids has the potential to become an invaluable technique to correctly determine baseline isoscape values and decipher sources of organic matter which will be important in a rapidly changing Arctic region.

4.2 Introduction

The Arctic is undergoing rapid transformations as a direct consequence of climate change, most notable in the cryosphere (IPCC, 2019). Sea ice in the Arctic plays a crucial role in ocean circulation and primary productivity, and has been reducing in thickness and extent for several decades. This trend is only set to continue with the Arctic predicted to be ice free during the summer months by the mid-century (Notz and Stroeve, 2016; IPCC, 2019). The loss of sea ice in the Arctic over the last two decades has reduced the amount of light limitation and triggered a 57% increase in marine primary productivity (Lewis et al., 2020). Instead, the Arctic Ocean is becoming more nutrient limited, particularly by nitrate (Codispoti et al., 2013; Arrigo and van Dijken, 2015; Lewis et al., 2020). Nitrate is an important and limiting food source at the base of the food web to organisms like phytoplankton, the Atlantic inflow to the Barents Sea is the primary source of nitrate to organisms (Tuerena et al., 2021).

On short timescales the rapid changes in sea ice are attributed to the increase in atmospheric temperatures and the reduction in export of sea ice across the central Arctic basin (Sorteberg and Kvingedal, 2006). However, the long term trend of decreasing amounts of annual sea ice, at least in the Barents Sea and Fram Strait, are attributed to the growing intrusion of warm and saline Atlantic Water (AW) into the Arctic. This encroachment of AW has contributed to higher sea surface temperatures and a northward shift of the polar front (PF; Onarheim et al., 2015). The PF is the region where AW meets Arctic Water (ArW) flowing south through the Barents Sea and through the centre of the Fram Strait where Polar Surface Water (PSW) meets AW (Fig. 4.1; Oziel et al., 2016; Barton et al., 2018). Associated with the PF is a marginal ice zone (MIZ); here sea ice retreats northwards during summer melt periods and leads to regions with increased availability of nutrients in the surface layers and higher

productivity rates (Engelsen et al., 2002). Further, the increasing extent of open Arctic Ocean due to the annual loss of summer sea ice has led to an increased absorption of sunlight and consequently warming of the ocean and the atmosphere above it through longwave radiation being released, both contributing to further melting (Dai et al., 2019). The higher rates of productivity lead to a substantial increase in marine particulate organic matter in the water column, which usually undergoes some level of degradation and remineralization before settling and accumulating in the underlying sediments.

The organic matter composition of marine surface sediments in the Barents Sea and Fram Strait have been revealed to mirror, at least in part, their location relative to the PF, MIZ and terrestrial inputs (Knies and Martinez, 2009; Stevenson and Abbott, 2019). Terrestrial inputs are an important source of organic matter in sediments close to the coast of Svalbard, and include fjords that contain rivers and glacial termini at the coast (Knies and Martinez, 2009). These inputs become less significant with increasing distance from land and sediments far offshore are characterised by a dominance of marine organic matter. Previous studies in this region have focussed on bulk ($\delta^{13}C_{Bulk}$, $\delta^{15}N_{Bulk}$, C/N ratio) techniques to understand different organic matter contributions to surface sediments (e.g. Knies and Martinez, 2009). While bulk techniques are a useful and efficient method they characterise the entire inorganic and organic fractions of the sediment, particularly in the case of $\delta^{15}N_{Bulk}$, which does not separate the two phases and makes interpretation difficult with many caveats. Isotopic compositions can also be applied to nutrients and particulates in the water column, such as studying nutrient supply through isotopic compositions of nitrate ($\delta^{15}N\text{-}NO_3$) and particulate nitrogen ($\delta^{15}N$-PN). This is an important part of the nitrogen cycle to consider as forming a large part of the sedimenting matter are marine organisms sinking through the water column, which utilise these nutrient sources (Arrigo and van Dijken, 2015). The Atlantic inflow to the

Barents Sea has a distinct isotopic composition of $\delta^{15}N\text{-}NO_3$ (~5‰; Tuerena et al., 2021) compared to that of the Pacific inflow (~3‰ greater in comparison; Somes et al., 2010) and as phytoplankton ^{15}N usually reflects the $\delta^{15}N\text{-}NO_3$ it consumes, it underpins baseline values for sediments (Schubert and Calvert, 2001). Previous analyses revealed there to be a strong correlation between the ^{15}N of organic nitrogen ($\delta^{15}N_{org}$) in the sediments in the Arctic Ocean and the nitrate concentrations in the overlying water column (Altabet and Francois, 1994). This is mainly attributed to the preferential biological uptake of the lighter isotope in nitrate, as nitrogen becomes more limited the ^{15}N of the organisms consuming it becomes heavier (Schubert and Calvert, 2001).

More recently a macromolecular approach has been applied to sediments in the region, as this is usually an overlooked portion compared to the solvent-extractable fraction (Stevenson and Abbott, 2019). The non-extractable, macromolecular, material is thought to form a large amount of the organic matter transported to the Arctic Ocean and contains lignin (associated with phenolic pyrolysis products) and marine proteins (associated with pyridine pyrolysis products; Sparkes et al., 2016). Stevenson and Abbott (2019) followed a South to North (S-N) transect in the Barents Sea identifying variability in macromolecular composition linked to the relative positon of the PF and MIZ. They found that across the transect all surface sediments were characterised by a dominance of marine macromolecular compositions, with terrestrial sources ruled our due the stations distance from land.

A large proportion of organic nitrogen in living organisms is made up of protein amino acids and they can accumulate in significant amounts within modern sediments (Burdige and Martens, 1988; Cowie and Hedges, 1992; Dauwe and Middelburg, 1998; Dittmar et al., 2001; Carstens et al., 2013). Previous work using sedimentary amino acids sought to understand if

the molar distribution of individual amino acids was source indicative, however this is not the case. Nevertheless, their distributions do provide an opportunity to assess the degradation state of the organic matter through the preferential accumulation of certain amino acids (Dauwe and Middelburg, 1998; Birgit Dauwe et al., 1999). More recently a method has been developed to analyse the individual isotopic composition of amino acids (CSIA-AA; $\delta^{15}N_{AA}$; McClelland and Montoya, 2002). Since its development the CSIA-AA technique has been widely used to study the trophic position (TP) of marine organisms within a food web, as some amino acids fractionate with increasing trophic level while others do not, providing a more suitable baseline to calculate TP than $\delta^{15}N_{Bulk}$ (McClelland and Montoya, 2002; McClelland, Holl and Montoya, 2003; Chikaraishi et al., 2007, 2009). The amino acids which do not fractionate with trophic transfer (<1%; McMahon and McCarthy, 2016) therefore trace the ^{15}N of the baseline of the food web which also indicates the nutrient source ($\delta^{15}N\text{-}NO_3$; de Vega *et al.*, 2021). These baseline values measured over a region can be referred to as the isoscape or baseline isoscape. Furthermore, McCarthy et al. (2007) found variations in $\delta^{15}N_{AA}$ can be the result of reworking by bacteria and the resynthesis of specific amino acids. As amino acids form a significant fraction of particulate organic nitrogen settling though the water column the CSIA-AA method is a poweful tool in that it can: a) provide foodweb structure and baseline isoscape ^{15}N values for the water column, b) indicate if any bacterial degradation has occurred and c) help resolve and interpret variations in $\delta^{15}N_{Bulk}$ (Batista et al., 2014).

The limited data set of $\delta^{15}N_{Bulk}$ of surface sediments has proved difficult to interpret due to the complicated interplay of water masses, sea-ice and terrestrial inputs. Here we present a combination of bulk and macromolecular analyses alongside amino acid composition and $\delta^{15}N_{AA}$ with the aim to (i) determine to what extent bulk and

macromolecular datasets confirm patterns observed previously, with composition related to relative positions of the PF and MIZ; (ii) assess if this pattern is reflected in the sedimentary amino acid compositions; (iii) assess the baseline sedimentary ^{15}N isoscape ($\delta^{15}N_{AA}$) and; (iv) determine how this relates to previous work in both the water column and within sediments and diagenetic state of the sediments.

4.3 Materials and Methods

4.3.1 Study area

The Barents Sea Opening (BSO) and Fram Strait act as one of the two major corridors for water entering the Arctic Ocean basin, the other being the Bering Strait where water flows in from the Pacific. AW enters in the east of the Fram Strait where it flows along the west coast of Svalbard as part of the West Spitsbergen Current and enters the Arctic Ocean north of Svalbard (Fig. 4.1). The BSO provides an inflow of AW from the south-west which is mixed with the Norwegian Coastal Current (NCC) flowing along the north coast of Norway. ArW flows into the Barents Sea from the north and east, and where it meets the Atlantic inflow the PF forms which is observed as a gradient in sea surface temperature. The PF is relatively stable year to year since it is largely determined by the bathymetry and topography of the basin (Harris et al., 1998; Knies, 2005). The East Greenland Current (EGC), which flows south along the western side of the Fram Strait, transports ArW which has been influenced by the transference of Pacific water inflows and signatures of continental shelf inputs (Torres-Valdés et al., 2013).

The southern Barents Sea remains ice free all year around due to the warmer AW inflow while the northern Barents Sea is covered seasonally with ice, with a maximum usually in March-April and a minimum in August-September (Faust et al., 2020). The eastern Fram Strait remains ice free for most of the year while the western side freezes due to the influence of cold Arctic Polar water (Paquette et al., 1985). These regions also receive fresh water injections from the melting of sea ice, glacial melt and rivers, all of which can be associated with the input of terrestrial organic matter (Rudels et al., 1996).

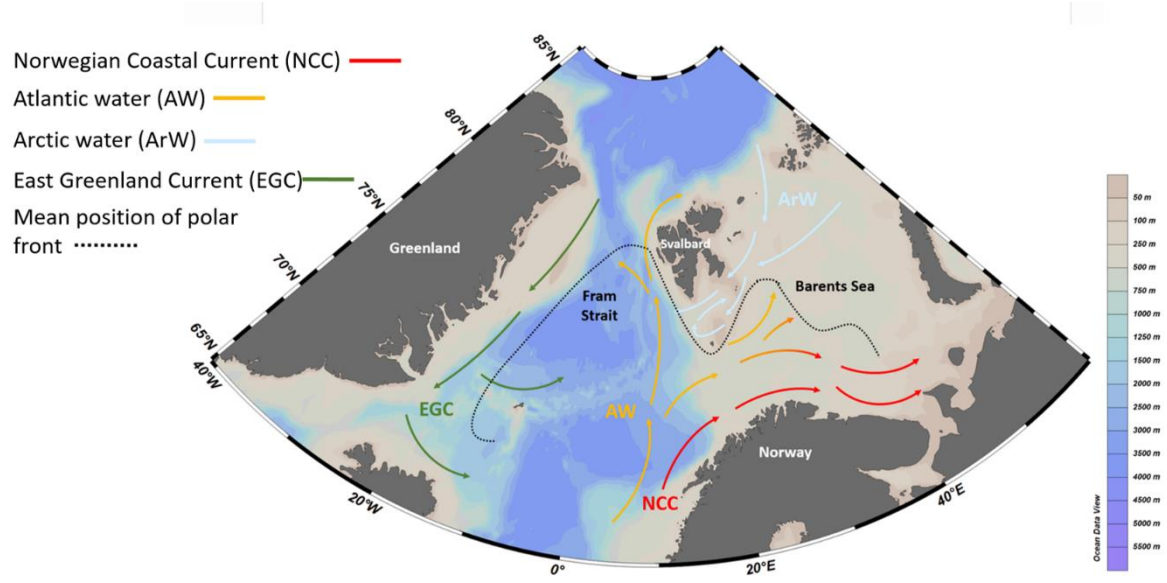

Figure 4.1 Schematic of Fram Strait and Barents Sea study area indicating general circulation of water masses with coloured arrows; Norwegian Coastal Current (NCC), Atlantic Water (AW), Arctic Water (ArW) and the East Greenland Current (EGC). Dashed black line indicates mean position of polar front, Barents Sea front from Stevenson et al. (2020) and Fram Strait front from Perner et al. (2019). Bathymetry of the region are shown in the colour bar. Base map and bar created using Ocean Data View.

4.3.2 Fieldwork

Samples were collected on two cruises both on board the RRS James Clark Ross; the first took place in July 2017 (JR16006; Hopkins, 2018) to the Barents Sea and the second in May 2018 (JR17005; Pond, 2018) to the Fram Strait. A full list of station identifiers can be found in appendix 2. These formed part of the field campaign for the ARISE (ARctic Isotopes and SEals) project which was funded by the Natural Environment Research Councils (NERC) Changing Arctic Ocean Programme. A total of 10 stations were selected during the 2017 fieldwork campaign, capturing the full extent of the Barents Sea opening (Fig. 4.2). The JR17005 stations selected from the Fram Strait cover a transect from the Greenland shelf to the central Fram Strait encompassing both AW inflow and the Arctic outflow. Stations are grouped based on known water masses (Tuerena et al., 2021a; Tuerena et al., 2021b) and consideration of the relative position of the polar front (Perner et al., 2019; Stevenson and Abbott, 2019; Fig. 4.2). A multicorer was deployed at each station, sediment cores collected

were sub-sectioned and the top 0.5 cm used for this study. Core slices were placed into foil, which had been previously ashed (400°C, 12 h), and frozen at -80°C on board the vessel. Samples were kept at -80°C until they were freeze-dried at which point they were homogenised and stored at -20°C prior to analysis.

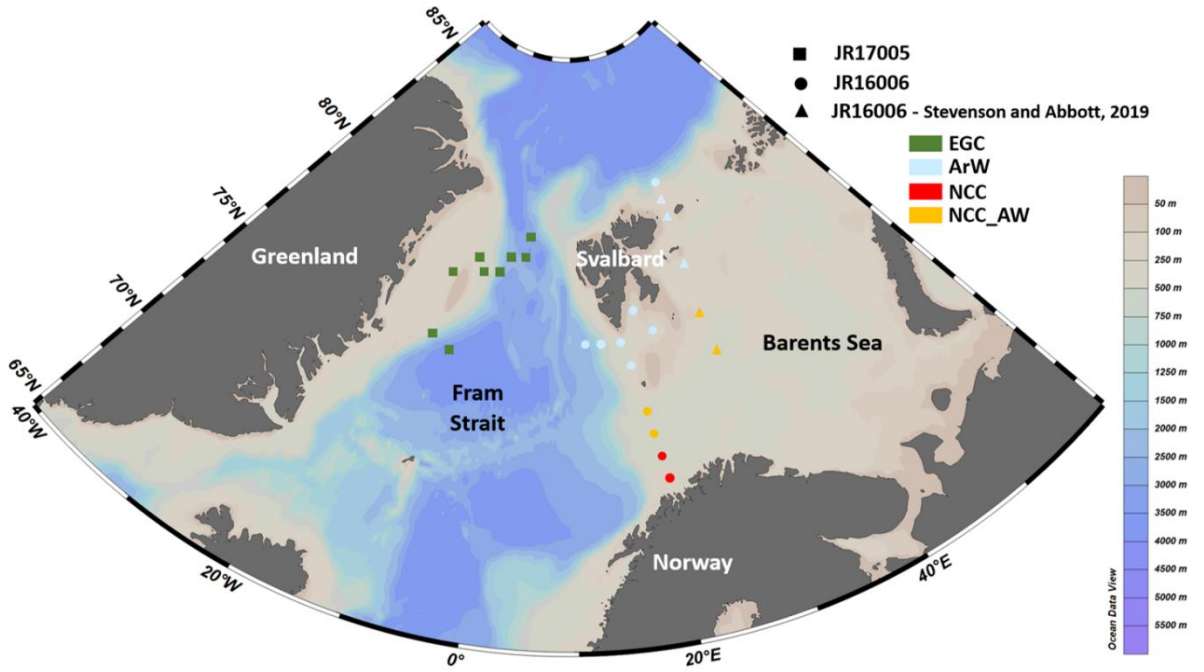

Figure 4.2. Map of the Fram Strait and Barents Sea showing locations of sediment sampling from the JR16006 (circles and triangles) and JR17005 (squares) used in this study. Station colour denotes the water mass group it has been assigned; green and the East Greenland Current (EGC); light blue and Arctic Water (ArW), red and the Norwegian Coastal Current (NCC); orange and the intermediate waters where the Atlantic and Norwegian Coastal Currents mix (NCC_AW). Bathymetry of the region are shown in the colour bar. Base map and bar created using Ocean Data View.

4.3.3 Geochemical analyses

4.3.3.1 Elemental and bulk stable isotopic analysis

Surface sediments were analysed for their elemental compositions (TC, TOC & TN) using Thermo Scientific FlashSmart Elemental Analyser and Thermo Scientific EagerSmart data handling software. Each sample was run in duplicate for TC, TOC and TN. Stable isotope composition of N ($\delta^{15}N$) were determined using an elemental analyser (Costech) coupled to

Delta V isotope ratio mass spectrometer (IRMS; Thermo Fisher Scientific). The amount of sediment required for analysis was calculated from the TN of a sample and the minimum nitrogen content the instrument required (30 µg nitrogen). All isotope results are reported in standard δ-notation (‰) relative to atmospheric N_2 (e.g. de Vega et al., 2021). Precision was monitored using a homogenized prawn (*Penaeus vannamei*) after every 10 samples which has well constrained $\delta^{15}N$ values (6.8‰) and precision was <0.2‰. Accuracy was determined using international reference materials, USGS40 and USGS41a, which have known $\delta^{15}N$ values (USGS40: $\delta^{15}N = -4.52‰$ and USGS41a: $\delta^{15}N = 47.55‰$). Accuracies for reference material USGS40 was 0.03 ± 0.11 for $\delta^{15}N$ and for USGS41a was 0.01 ± 0.15 for $\delta^{15}N$.

4.3.3.2 Pyrolysis gas chromatography mass spectrometry (Py-GCMS)

Freeze-dried sediments were analysed by Py-GCMS analysis following the method of Sparkes et al. (2016), with minor adjustments. Sediments were analysed using an Agilent GC-MSD which was interfaced with a CDS-5200 Pyroprobe. In short, sediments were placed into a clean quartz tube, which is fire polished using a Bunsen burner in between each sample, placed into the pyroprobe and pyrolysed at 700°C for 20 seconds in a flow of helium. Pyrolysis products were passed through a heated transfer line (325°C) using helium as a carrier gas (20 mL min^{-1}, gas saver mode active) connected to an Agilent 7980A GC in split mode (split ratio 20:1, GC interface set at 280°C) fitted with a HP-5 GC column (30 m and 0.25 mm (i.d.), film thickness 0.25 µm, nonpolar stationary phase of 5%-phenyl-methylpolysiloxane). The GC oven was set from 40°C (held for 5 minutes) to 250°C at 4°C min^{-1}, then heated to 300°C at 20°C min^{-1} and held for 1 minute at this temperature (61 minute total run time). The eluent from the GC was transferred *via* a transfer line (325°C) to an Agilent 5975 MSD single quadrupole mass spectrometer in electron ionisation (EI) mode (ionisation potential 70 eV; scanning

range of *m/z* 50 to 650 at 2.7 scans s^{-1}; EI source at 230°C; MS quadrupole at 150°C). Chromatograms were processed using Enhanced ChemStation, Agilent Technologies software. Samples were analysed in duplicate at a minimum and precision ranged from 0 to 0.2 for the phenol to pyridine ratio. As noted by Sparkes et al. (2016), the chromatograms produced from Py-GCMS are complex and therefore a number of 'pyrolysis moieties' were determined (Guo et al., 2009; Fig. 4.3). Hence, the major fragment ions were used to determine peak areas in the appropriate single ion current chromatograms. For the purpose of this study, two of the nine representative moieties were used as they formed a proxy for terrestrial and marine input (phenols/pyridines ratio index, PPRI; phenols major ion *m/z* 94 and pyridines *m/z* 79 and 93; Fig. 4.3; a full list of characteristic ions can be found in Sparkes et al., 2016). This method does not characterise all of organic compounds generated by pyrolysis of the sediments but is a tool for inter-sample comparison across a land to sea gradient. Additional samples from Stevenson and Abbott (2019) which were collected on-board the JR16006 cruise are included for comparison to enhance spatial resolution (stations B13-B17; see appendix 2 for full sample list).

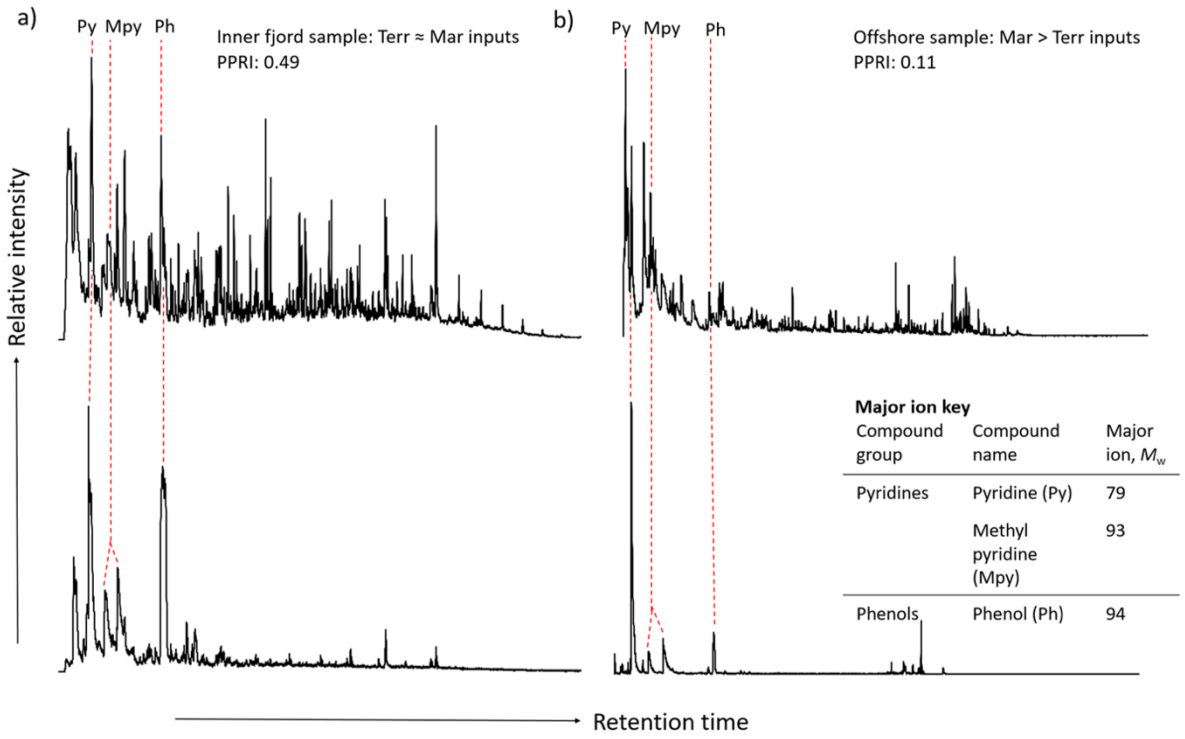

Figure 4.3 Representative chromatograms from Py-GCMS analysis (top) with chromatograms produced by using single ion filtering (SIF; bottom). a) Sample from within a large fjord (ST1) with a PPRI of 0.49 and SIF chromatogram displaying relatively larger proportions of phenols compared to (b). b) Sample from central Fram Strait (F21) with a PPRI of 0.11 and SIF chromatogram displaying relatively larger proportions of pyridines to phenols. The major ion key specifies ions used for SIF's following Sparkes et al. (2016) method.

4.3.3.3 Amino acid isotope analysis

For compound specific isotope analyses (CSIA; $\delta^{15}N_{AA}$) of individual amino acids freeze-dried and homogenised sediments were used. In most cases almost all of the available sediment (from 2-10 g) was used as amino acid concentrations were low in some of the studied sediments.

Prior to hydrolysis, an internal standard (L-norleucine, Sigma-Aldrich) of known concentration was added. In 20 mL culture tubes, fitted with Pyrex lids to ensure no evaporation, approximately 10-12 mL of 6N HCL was added to each sample and a shaker bed was used to fully mix the slurry. Samples were transferred to a pre-heated oven at 110°C under a N_2 atmosphere for a minimum of 21 hours. It should be noted that during acid

hydrolysis, asparagine and glutamine were converted to aspartic acid and glutamic acid, respectively.

Once hydrolysed the samples were cooled, transferred to a NanoSep centrifugal device to ensure all hydrolysates were collected and transferred into clean vials. A mixture of dichloromethane (DCM): *n*-heptane (3:2) was added to each sample and the lipid layer was removed, this was repeated (x3) to ensure its complete removal. Following Styring et al. (2012), a cation exchange column was prepared to ensure all exchange sites within the resin were occupied by H^+ ions prior to sample addition. Approximately 1 mL of Dowex 50WX8 (200–400 mesh) was added into a Pasteur pipette and washed with 12 mL of deionised water. Samples were transferred to the column and salts were eluted with deionised water; finally amino acids were eluted into clean vials with NH_4OH solution (4N) and centrifuged to ensure no particulates from the resin remained. Sample were frozen (-80°C) in preparation for freeze-drying prior to derivatisation.

Amino acids were propylated using acetyl chloride: anhydrous isopropanol (1:4, v/v, 0.25 mL) for 1 hour at 100°C; the reaction was quenched in a freezer (-20°C) and reagents evaporated to dryness under N_2. A small amount of DCM was added and evaporated (x3) to ensure complete removal of any remaining reagents. To acetylate the amino acids, a mixture of acetone: triethylamine: acetic anhydride (5:2:1, v/v, 1 mL) was added to the amino acid propyl esters and heated for 10 minutes at 60°C. All reagents were evaporated to dryness under N_2, being dissolved in 2 mL of ethyl acetate and 1 mL of saturated NaCl solution. Samples were placed into a vortex mixer to create phase separation and the organic phase was collected; this was repeated (x2) and the organic phases collected. A Pasteur pipette plugged with glass wool and packed with anhydrous $MgSO_4$ removed any remaining water.

Lastly, samples were evaporated to dryness under N_2, dissolved in DCM and stored at -20°C prior to analysis. Following this procedure, a total of 8 amino acids could be identified; Alanine (Ala), Valine (Val), Leucine (Leu), Glycine (Gly), Proline (Pro), Aspartic Acid (Asp), Glutamic Acid (Glu) and Phenylalanine (Phe; Fig. 4.4).

The mole percent contributions of individual amino acids were determined prior to $\delta^{15}N$ amino acid analysis ($\delta^{15}N_{AA}$) using a GC-FID (gas chromatograph-flame ionization detector; Agilent Technologies 7890A GC System; Fig. 4.4). The GC was fitted with a HP-INNOWax Agilent column (30 m x 0.25 mm (i.d.), film thickness 0.5 µm, high polarity stationary phase of polyethylene glycol) using helium as a carrier gas (1.1 mL min^{-1}, splitless mode) and the injector set at 250°C. The GC oven was programmed after 2 minutes from 50°C to 180°C at 10°C min^{-1}, from 180°C to 260°C at 6°C min^{-1} and held at 260°C for 20 minutes. The FID operating conditions were as follows: detector heater 220°C; H_2 40 mL min^{-1}; air flow 400 mL min^{-1}; N_2 25 mL min^{-1}.

$\delta^{15}N_{AA}$ values were determined using GC-C-IRMS, Thermo Scientific Trace Ultra gas chromatograph 1310 coupled to a GC Isolink and Delta V Advantage isotope ratio mass spectrometer with a ConFlo IV interface. A HP-INNOWax Agilent column (30 m x 0.25 mm (i.d.), film thickness 0.5 µm, high polarity stationary phase of polyethylene glycol) fitted to the GC was used for amino acid separation, helium as a carrier gas (flow 1.4 mL.min^{-1}) and the injector set at 260°C. After separation the eluents were passed through a combustion reactor (Cu/Ni, 1000°C, Thermo Fisher) followed by a liquid nitrogen trap to remove CO_2 from the samples. The GC oven was programmed after 2 minutes from 50°C to 180°C at 10°C min^{-1}, from 180°C to 260°C at 6°C min^{-1} and held at 260°C for 16.7 minutes. The molecular ions of N_2 (m/z 28, 29 & 30) were detected and the resulting $\delta^{15}N$ of each amino acid peak was

determined by comparison with a standard reference N_2 gas (measure 4 times at the start and finish of each sample analysis) using Isodat software (version 3.0, Thermo Fisher).

All $\delta^{15}N_{AA}$ results are reported in per mill notation (‰) relative to atmospheric N_2 (e.g. McCarthy et al., 2007; Batista et al., 2014). Each sample was analysed in duplicate, any sample that had a greater difference between sample runs than expected (>2.0‰) was not included in the dataset. A mixed standard of 8 amino acids with known $\delta^{15}N$ were analysed at the start of every run and every 4 samples to determine precision and accuracy (University of Indiana, United States and SI Science, Japan). The mean precision of all standards was ± 1.0‰ and ranged from ± 0.6‰ for proline and ± 2.6‰ for alanine (*n* = 38 and 46, respectively). The mean accuracy of all standards was ± 1.4‰ and ranged from ± 0.4‰ for aspartic acid to ± 2.1‰ for proline (*n* = 48 and 38, respectively).

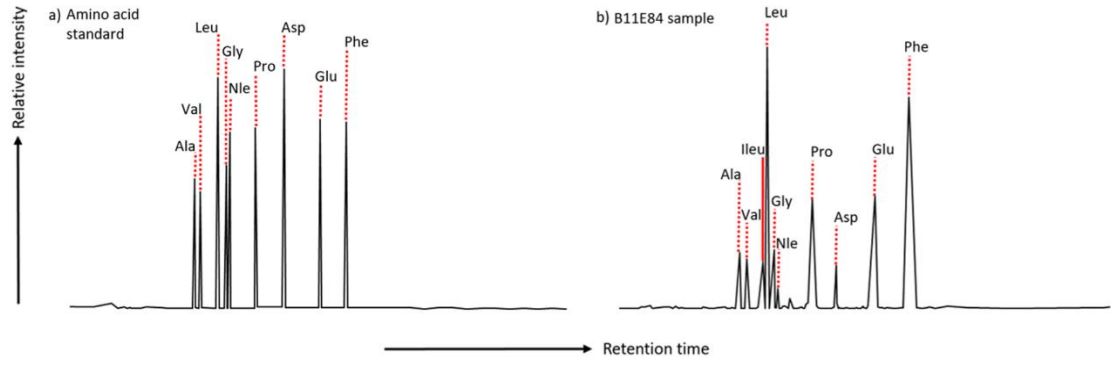

Figure 4.4 Representative GC-FID chromatograms for a) amino acid standard and b) a presentative sample from station B11 south of Svalbard. Amino acids detected: alanine (ala), valine (val), isoleucine (ileu), leucine (leu), glycine (gly), norleucine (nle, internal standard), proline (pro), aspartic acid (asp), glutamic acid (glu) and phenylalanine (phe).

4.3.4 Amino acid groupings and definitions

It is common practice to group amino acids according to the type of analysis used and their various characteristics and associations. Protein amino acids have previously been grouped by their side chain functionality and associated charge; acidic (Asp and Glu), neutral

or aliphatic (Ala, Val, Leu, Gly and Pro) and aromatic (Phe; Dauwe and Middelburg, 1998). Early sedimentary amino acid studies looked at the molar percent contribution of amino acids to investigate degradation state (e.g. Dauwe et al., 1999). Certain amino acids apparently degrade easier or are more refractory due to the type of organic matter matrix they originate from or their chemical structure. Cell walls of bacteria and diatoms are usually enriched in the amino acid glycine, leading it to preferentially accumulate as it is less susceptible to degradation due to the matrix it is protected within (Yamashita and Tanoue, 2003). Leucine and Phenylalanine are usually enriched in comparatively more labile matrices such as cell plasma, which leads to a relative decrease in these amino acids in sediments (Cowie and Hedges, 1992). Glycine found in high concentrations in sediments has been linked to heterotrophic bacterial reworking, due to its ability to be synthesised from other amino acids, moreover its comparatively lesser food value (e.g. to zooplankton) due to its short chain length also tends to concentrate it relative to other amino acids (Dauwe and Middelburg, 1998; Dauwe et al., 1999; McCarthy et al., 2013).

The ability of an organism to synthesize certain amino acids from their diet can also be used to group them; essential amino acids that must be obtained from diet (Val, Leu and Phe) and non-essential that can be synthesized within an organism (Ala, Gly, Pro, Asp and Glu). Typically for $\delta^{15}N_{AA}$ analysis and as per Batista et al. (2014), amino acids are separated into two groups (trophic and source amino acids) which is consistent with the existing literature for samples in the marine environment. Trophic amino acids (Ala, Val, Leu, Pro, Asp and Glu) are those that become enriched in ^{15}N with each trophic transfer and are reflective of the consumer. Source amino acids (Gly and Phe) are those that have little or no enrichment in ^{15}N with trophic transfer and are thought to represent the baseline of the food web (Chikaraishi et al., 2007; McClelland & Montoya, 2002).

4.3.5 Source and Diagenetic indicators/proxies

A number of metrics can be used based on the analyses above to assess both the source and quality of OM:

The Phenol to Pyridine Ratio (PPRI) was conceptualised in the Sparkes et al. (2016) study after a macromolecular investigation showed nearshore to offshore trends in the relative abundance of two representative compound classes on the East Siberian Arctic Shelves. Pyridines are used as a pseudo marine marker and phenols used as a pseudo terrestrial marker; values of the PPRI that are close of 0 are deemed marine in origin and values closer to 1 are predominantly terrestrial:

Equation 4.1

$$\frac{Phenol}{Phenol + Pyridine}$$

A proxy for the total $\delta^{15}N$ of proteinaceous material ($\delta^{15}N_{THAA}$) was proposed by McCarthy et al. (2013). This is calculated as the mole percent weighted sum of each $\delta^{15}N_{AA}$ and it is noted that as not every amino acid is analysed within the sample that this is a representative proxy and not the absolute value:

Equation 4.2

$$\delta^{15}N_{THAA} = \Sigma\ (\delta^{15}N_{AA}\ \cdot\ \mathrm{mol}\%_{AA})$$

Amino acid $\delta^{15}N$ values can be normalised to the $\delta^{15}N_{THAA}$, providing intra sample comparison and removing inorganic N influences (McCarthy et al., 2013).

The degradation index (DI) is used as an indicator of organic matter quality and uses the protein amino acid composition of each sample following Dauwe et al. (1999):

Equation 4.3

$$DI = \Sigma \left[\frac{\mathrm{var}_i - \mathrm{AVGvar}_i}{\mathrm{STDvar}_i} \right] \times \mathrm{Fac.\ coef}_i$$

Where var_i is the mole percent of amino acid *i*; AVGvar_i and STDvar_i are the mean and standard deviation of amino acid *i* in the study from Dauwe et al. (1999) and fac. coef_i is the factor coefficient as determine by principle component analysis (PCA). Certain amino acids were found to be enriched or depleted in concentration depending on the degradation state of the organic matter, the divergent behaviour was attributed to the association of a particular amino acid to more labile sources such as cell plasma and less labile sources such as cell walls (Dauwe and Middelburg, 1998).

The ∑V parameter, first proposed by McCarthy et al. (2007), is a proxy used to determine total heterotrophic resynthesis by looking at the scatter of $\delta^{15}N_{AA}$ values around the mean of total values:

Equation 4.4

$$\Sigma V = \frac{1}{n} \Sigma Abs(\chi_i)$$

Where χ_i, is the deviation in each AA $\delta^{15}N$ I from the average ($\delta^{15}N_i$—AVG $\delta^{15}N_i$) and n is the number of AA used for the calculation. The amino acids used are those representing the 'trophic' group, for this study Ala, Leu, Pro, Asp and Glu were used.

4.3.6 Statistical analysis

All statistical analyses were performed in R version 4.0.2 (R Core Team, 2021) with RStudio interface version 1.3.959. To explore patterns between the different water mass interactions in the region, a variety of statistical tests were performed. One-way ANOVA (analysis of variance) with post hoc Tukey honestly significant difference (HSD) pair-wise tests determined the differences in each region for a given variable measured (e.g. mol% of each amino acid in each region) and the differences within each of those groups, respectively. Before using statistical analysis, the data was tested for normality using a visual check of the quantile-quantile plots followed by a studentised Breusch-Pagan test for heteroscedasticity. Due to the small number of data points for some analyses and regions (e.g. n=3), there are some inherent limitations of using parametric tests however ANOVA is considered acceptable for data that does not rigorously fit a Gaussian distribution (McCarthy et al., 2007). A 95% confidence interval is used for all test results, both ANOVA and Tukey HSD post-hoc.

Some indices also warranted correlation tests to be performed, where initial scatter plots were created alongside a linear model which was then tested for normality and then subjected to Pearson and Spearman Rank correlation tests. The first of these solely interrogates linear correlations, whereas the second tested for monotonic correlations. Monotonic correlations do not have to conform to a linear relationship as the test recognises positive or negative correlations even if the rate of change of each variable is not the same,

for instance an exponential correlation. By using both tests the correlations can be assigned to a linear or monotonic relationship depending on the strength of the *r* and *p* values they produce.

R coding scripts (4,298 lines of code used to create figures and run statistical analysis) related to these statistical analyses can be found in appendix 2.

4.4 Results

4.4.1 Bulk elemental and isotopic composition

Molar C/N ratios were measured across the Barents Sea and Fram Strait and ranged from 5.86 (B1, close to the coast of Norway) to 10.62 (ST1, a Fjord location near Svalbard; Fig. 4.5a). The lowest C/N ratios were found closest to the Norwegian coast (5.86, B1) and on the East Greenland shelf edge (6.25, F15; Fig. 4.5a). The highest C/N (10.62, station ST1) is found in Storfjorden, an embayment at the southern tip of the archipelago with an opening to the south where Atlantic and Polar waters mix (Fig. 4.5a). There is a trend of increasing C/N with increasing distance from the north coast of Norway towards Svalbard (B1-ST1, 5.86 - 10.62; Fig. 4.5a). The average C/N for each region is as follows; NCC 6.6 ± 1.1; NCC_AW 8 ± 0.6; ArW 8.6 ± 1.3; EGC 8.1 ± 1.1. There was no evidence of significant differences in C/N between water mass regions (ANOVA, $F_{3, 21} = 1.64$, $P > 0.05$).

Bulk $\delta^{15}N$ of surface sediments ranged from 4.1 (B1 and B4) to 7.1‰ (B15), most depleted values are found along the transect from Norway to Svalbard, whilst the most enriched are found off the East coast of Svalbard and the East Greenland shelf edge (Fig. 4.5b). Unlike the C/N, the bulk $\delta^{15}N$ did not display any trend across the Norway to Svalbard transect, although there is a general enrichment towards the archipelago, it is not

pronounced (Fig. 4.5b). The average bulk $\delta^{15}N$ for each region is as follows; NCC 4.7 ± 0.9; NCC_AW 4.3 ± 0.3; ArW 5.3 ± 0.8; EGC 5.7 ± 0.7). There was no evidence of differences in bulk $\delta^{15}N$ between water mass regions (ANOVA, $F_{3, 17} = 2.42$, $P > 0.05$).

4.4.2 Distribution of phenols and pyridine

The PPRIs of sediments collected as part of this study are combined with data from Stevenson and Abbott (2019; stations B13-17; Fig. 4.5c). The highest PPRI value was at station ST1 (0.49, also the highest C/N) whilst the lowest was at F21 (0.11, Fig. 4.5c). As for C/N, there is a decreasing trend in the relative contributions of pyridines to phenols from Norway to Svalbard (PPRI 0.28-0.49; Fig. 4.5c). The average PPRI for each water mass region is as follows: NCC 0.29 ± 0.01; NCC_AW 0.3 ± 0.05; ArW 0.3 ± 0.09; EGC 0.17 ± 0.05 and there is significant evidence of a difference between them (ANOVA, $F_{3, 21} = 6.48$, $P < 0.01$); a post-hoc Tukey's HSD test revealed that the differences originated from the EGC compared to the NCC_AW and the ArW (EGC-NCC_AW, $P < 0.05$, 95% C.I. = -0.24, -0.009; EGC-ArW, $P < 0.01$, 95% C.I. = -0.21, -0.04).

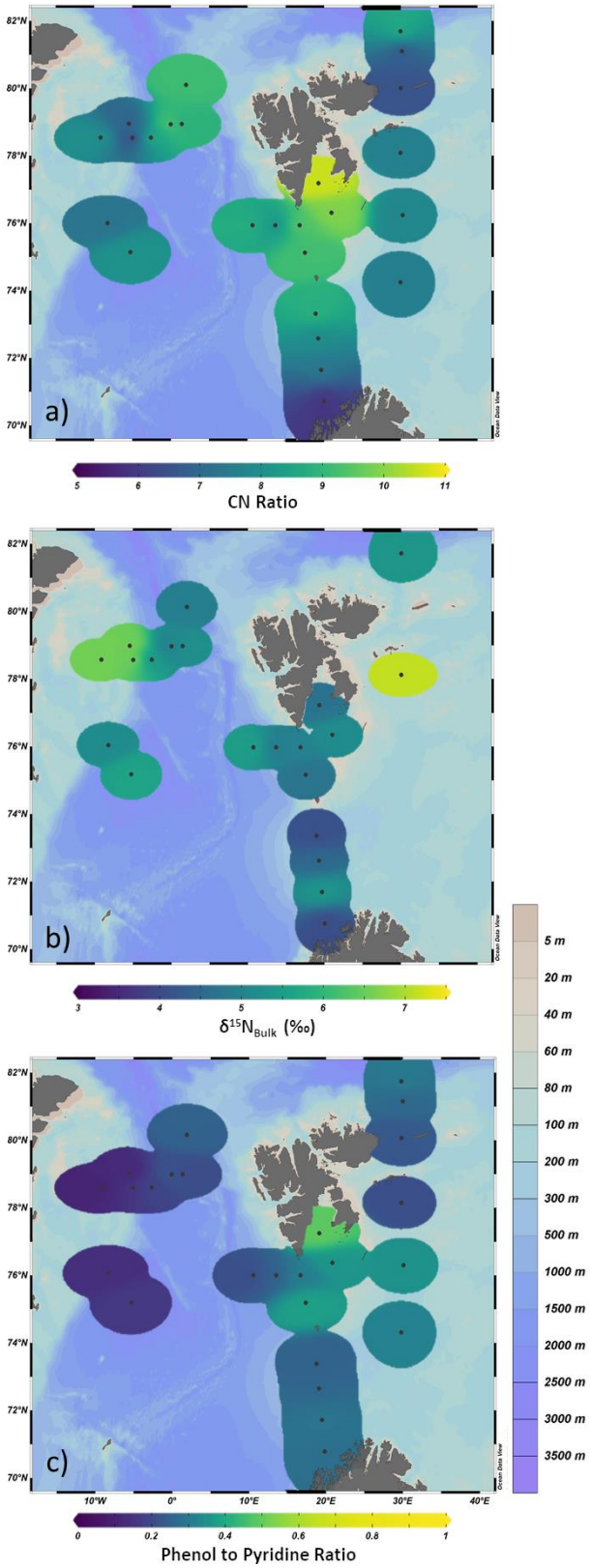

Figure 4.5 Map panel showing a) C/N ratio, b) $\delta^{15}N$ and c) Phenol to Pyridine Ratio (PPRI) across the Barents Sea and Fram Strait. Additional samples from Stevenson and Abbott (2019) have been added to the C/N and PPRI. Colour bar below each plot indicates value of indices for each station and colour bar to the right indicates bathymetry of region. Created using weighted average gridding in Ocean Data View.

4.4.3 Amino acid composition

Leucine was the dominant amino acid across the study area (22.9 – 38.4 mol %) followed by phenylalanine (14.3 – 32.1 mol %); all other amino acids exhibit lower mol% values; glycine (5.1 - 14.8); glutamic acid (5.1 – 14.1); alanine (5.1 – 13.2); aspartic acid (1.8 – 9.7); valine (3.8 – 9.5; Fig. 4.4 and Fig. 4.6).

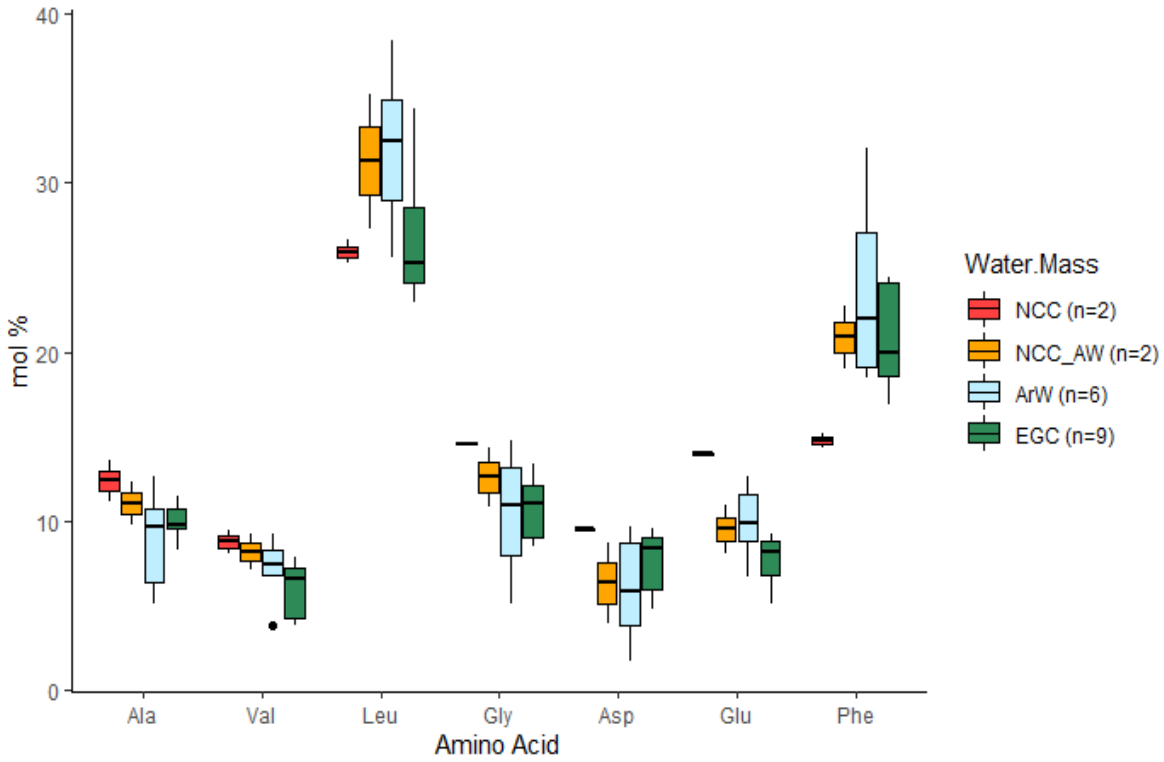

Figure 4.6 Distribution of mol% amino acids (AA) across the Barents Sea and Fram Strait regions, NCC (Norwegian Coastal Current, NCC_AW (Norwegian Coastal Current with Atlantic Water), ArW (Arctic Water) and EGC (East Greenland Current). Changes in water mass appear to not modify the compositions of AA in the sediments, with the most dominant amino acid being leucine across all regions. The median is the horizontal line through each box and the 25% to the 75% quartile are the bottom and top of the boxes. The line extending below and above each box represent the 5% and 95% quartiles. Closed circles represent data points that fall below or above the 5% and 95% quartiles.

Of all amino acids, only glutamic acid displayed evidence of a strong difference between water mass regions (ANOVA; $F_{3, 15} = 7.72$, $P = 0.002$). A post-hoc Tukey's HSD test revealed that this difference is between the Norwegian Coastal Current and the East Greenland Current (NCC-EGC; $P < 0.005$, 95% C.I. = 2.42, 10.53; Fig. 4.6).

To better understand the relationship between individual amino acid mol %, different correlation tests were performed, Pearson's and Spearman's rank (using both can indicate

the kind of relationship there is; a full list of correlation test results can be found in Appendix 2). Two groups of amino acids were identified from these correlation tests, namely leucine and phenylalanine (Leu and Phe), which display negative correlations with the mol% of Glycine (Gly), while the second group of all other amino acids display positive correlations with Gly (Fig. 4.7). The correlation of Leu and Phe mol% data with C/N reveals the same pattern, in that the other amino acids had the opposite relationship with C/N (Fig. 4.7).

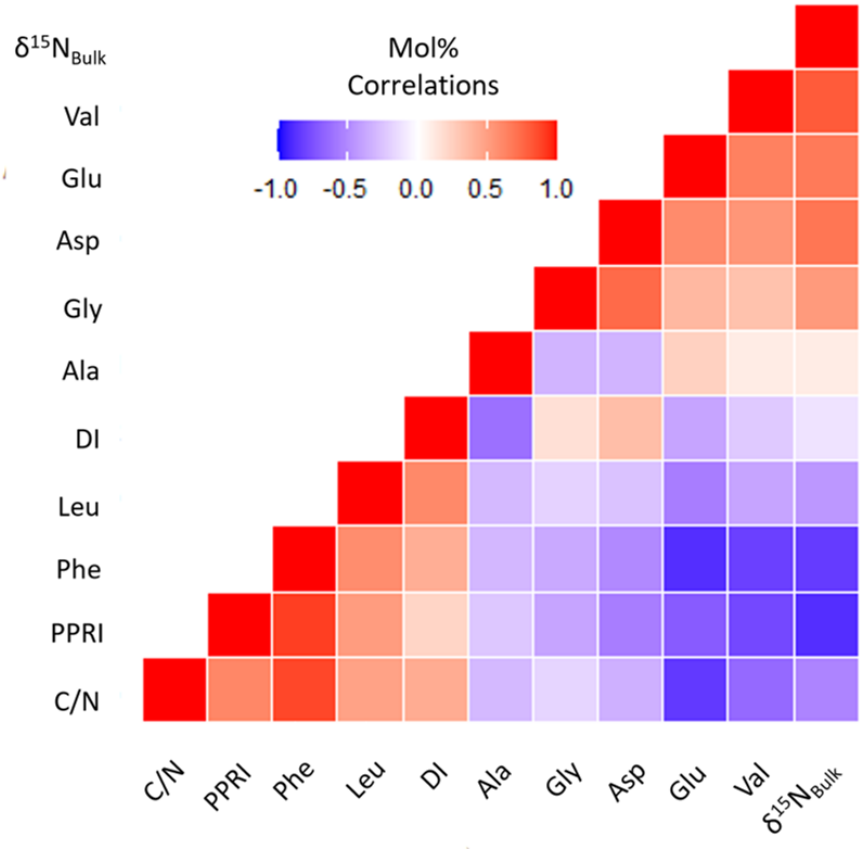

Figure 4.7 A correlation heat map displaying the positive (red) or negative (blue) relationships between individual amino acid mol% and indices measured as part of this study. Here the grouping of Leu and Phe becomes more apparent compared to other amino acids analysed. Created using 'ggplot2' within RStudio 1.3.959

A principle component analysis (PCA) was performed using the 'prcomp' function with RStudio which is a singular value decomposition method. This was to further investigate the correlations of individual mol% amino acids with other proxies and the effects of water mass groupings (Fig. 4.8). The analysis produced 11 components and the first two (PC1 and PC2)

accounted for 76.1% of the variance found. The first axis (PC1) separated Phe, Leu, DI and C/N from Asp, Ala and Gly, whilst the second axis (PC2) separated $\delta^{15}N_{Bulk}$ and the PPRI. Water mass groupings formed a more complicated picture but the ArW, NCC and EGC groups did distinctly separate although not along the same principle component.

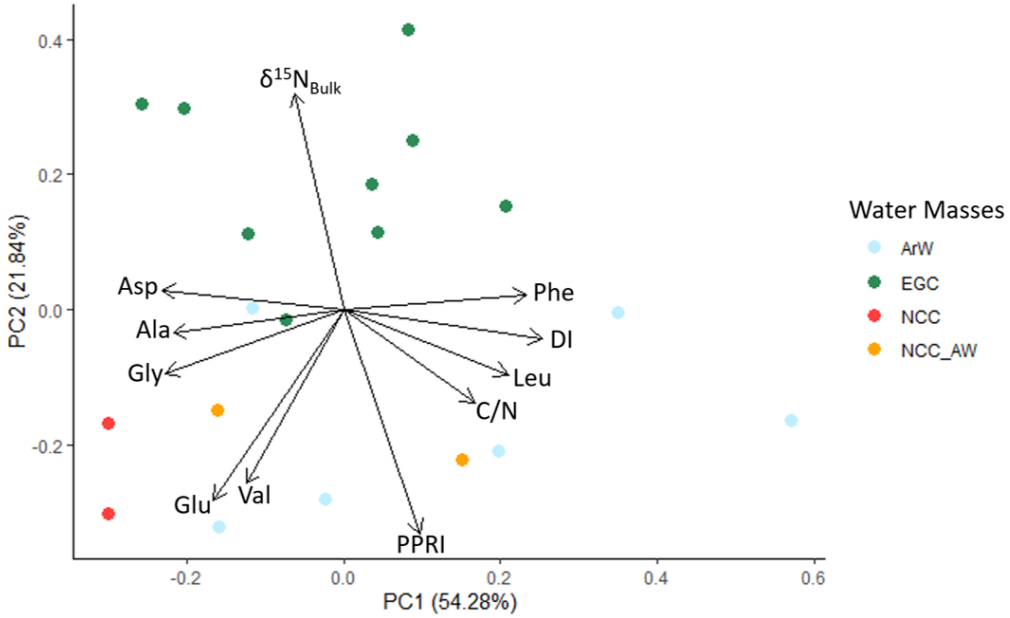

Figure 4.8 PCA biplot of loadings of amino acid mol% distribution (Ala, alanine; Val, valine; Leu, leucine; Gly, glycine; Asp, aspartic acid; Glu, glutamic acid; Phe, phenylalanine), degradation index (DI; Dauwe et al., 1999), C/N ratio, phenol to pyridine ratio (PPRI; Sparkes et al., 2016) and $\delta^{15}N_{Bulk}$. Colour represent water mass groupings: ArW Arctic Water, EGC East Greenland Current, NCC Norwegian Coastal Current and NCC_AW Norwegian Coastal Current mixed with Atlantic Water.

4.4.4 Amino acid nitrogen isotopic composition

The trophic amino acids (Ala, Leu, Pro, Asp and Glu) on the whole display more enriched $\delta^{15}N$ values compared to the source amino acids (Gly and Phe; Fig. 4.9). As source amino acids, Gly and Phe also display less variation between regions in $\delta^{15}N$ values compared to the trophic amino acids (Fig. 4.9). Pro is the only amino acid that displayed moderate differences between regions (ANOVA; $F_{3, 14} = 3.44$, $P < 0.05$; it should be noted that the Pro dataset was reduced as it was not present in all mixed standards used). A Tukey's HSD test

revealed the difference results from the Norwegian Coastal Current and the East Greenland Current data (NCC and EGC; P <0.05, 95% C.I. = 0.19, 5.74; Fig. 4.9).

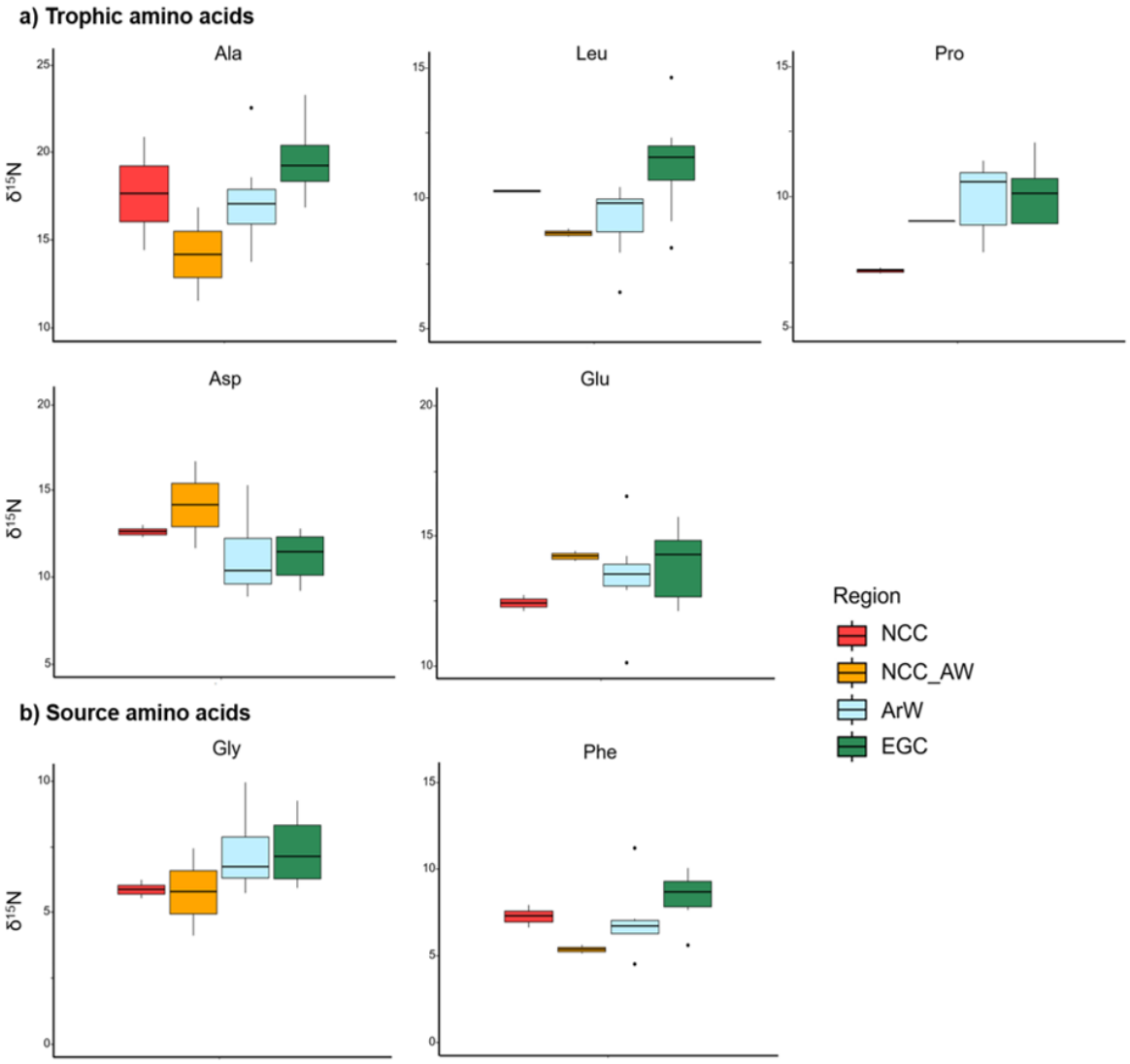

Figure 4.9. $\delta^{15}N_{AA}$ values of sediments in the Barents Sea and Fram Strait split by region (Fig. 4.1), NCC (Norwegian Coastal Current, NCC_AW (Norwegian Coastal Current with Atlantic Water), ArW (Arctic Water) and EGC (East Greenland Current). More enriched values tend to be in the trophic amino acids (a) and depleted in the source amino acids (b). Closed circles represent individual data that falls below or above the 5% and 95% quartiles. Pro was not present in all amino acid standards and the number of measurements per regions are as follows: NCC (n=2), NCC_AW (n=1), ArW (n=7) and EGC (n=8). For all other amino acids: NCC (n=2), NCC_AW (n=2), ArW (n=7) and EGC (n=8).

4.4.5 Amino acid indices

The degradation index (DI; Dauwe et al., 1999) ranged from -0.58 to 1.18 (EGC and ArW, respectively); and there was no evidence of a difference between regions (ANOVA, $F_{3,16} = 2.2$, $P > 0.05$; Fig. 4.10). The ∑V proxy for heterotrophic reworking (McCarthy et al., 2007) ranged from 1.7 to 4.2‰ (both in ArW); and again there was no evidence of a difference between regions (ANOVA, $F_{3,14} = 0.2$, $P > 0.05$; Fig. 4.10).

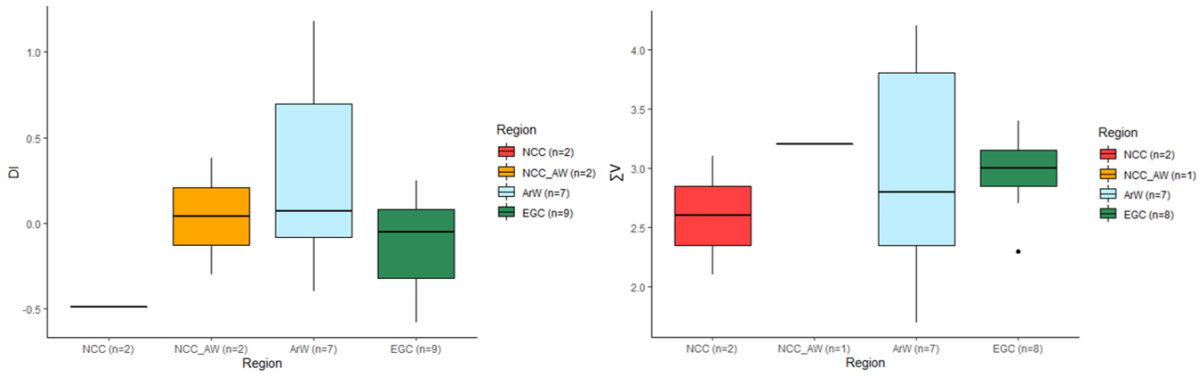

Figure 4.10 Degradation index (DI) values calculated following Dauwe et al., 1999 study and the Heterotrophic reworking proxy (∑V) values calculated following McCarthy et al., 2007 study with the exception that isoleucine is not measured in current study. Split by region, NCC (Norwegian Coastal Current, NCC_AW (Norwegian Coastal Current with Atlantic Water), ArW (Arctic Water) and EGC (East Greenland Current). Indicates no clear differences in the DI and ∑V across the Barents Sea and Fram Strait. Closed circles represent individual data that falls below or above the 5% and 95% quartiles.

4.5 Discussion

4.5.1 Impact of polar front and marginal ice zone on the organic matter preserved in sediments of the Barents Sea and Fram Strait.

C/N values have been used to distinguish between sediments influenced by marine or terrestrial inputs, where higher C/N (> 15) are ascribed to larger contributions of terrestrial organic matter and lower C/N (~6) with marine (Hedges and Oades, 1997; Stein, 2008). Previous studies have credited relatively larger values of C/N in the Barents Sea to the increased input of terrestrial organic matter (Knies and Martinez, 2009). This is in line with the highest C/N found at the fjord sampling station (ST1) likely from inmixing of terrestrial material from glacial terminus and riverine material during the summer. In addition, a relatively low C/N is found off the North East Coast of Svalbard (station B18; Fig. 4.2) which has been suggested to be more influenced by the consumption of ice algae by zooplankton leading to increased amount of marine organic matter being transported to the sediments (Stevenson and Abbott, 2019). There were no differences in C/N found between the water mass groups (Atlantic water, Arctic water, East Greenland Current and Norwegian Coastal Current; Fig. 4.1) which is likely due to the C/N not being particularly sensitive to such changes and splitting the stations in this way likely over simplifies the processes affecting marine sediments in these regions. Stevenson and Abbott (2019), found total organic carbon (TOC) concentrations to be higher along the mean position of the polar front and close to the marginal ice zone, attributing it to the higher productivity and upwelling associated with these zones leading to a greater accumulation of organisms and therefore an increase in TOC. Similarly, the gradient of increasing C/N from Norway to Svalbard (stations B1 to B11), as observed in the present study, could be due to a sampling stations proximity to the polar front

and the marginal ice zone which leads to higher rates of productivity as noted by Stevenson and Abbott (2019) or a higher rate of diagenesis preferentially removing labile nitrogen containing compounds. Across the Fram Strait there are only minor variations in C/N; a somewhat higher C/N is measured in the interior of the Strait could again be due to the position of the polar front relative to the sampling stations as seems the case the with stations between Norway and Svalbard. The higher C/N ratio associated with these samples could also be a product of the samples depth where particles have a longer residence time within the water column and therefore undergo more degradation compared to their shallower counterparts.

$\delta^{15}N_{Bulk}$ patterns display a more complex picture compared to the C/N measured in the region. Overall, $\delta^{15}N_{Bulk}$ is enriched slightly between Norway and Svalbard going northwards but fluctuations along the transect are likely localised hotspots of production caused by the in-mixing of Atlantic and Arctic waters. As primary producers fix nitrogen from nitrate during blooming conditions, the remaining nitrate pool enriches in ^{15}N and consequently the ^{15}N of particulate organic matter (POM) does too (Schubert and Calvert, 2001). During bloom conditions there is a corresponding increase in the export of POM to the sediments which also concentrates the ^{15}N signature of marine organic matter and equally leads to an increase in sedimentary ^{15}N (Sigman and Casciotti, 2001). There is also the possibility that heterotrophic reworking in the water column or post-depositional processes can lead to an increase in ^{15}N. Likewise, there was a localised enrichment in $\delta^{15}N_{Bulk}$ at the East Greenland Shelf edge and off the east coast of Svalbard. Enrichment at the East Greenland shelf edge could be due to advection of nutrients caused by the bathymetry of the shelf leading to increased amounts of primary productivity which becomes less pronounced away from the shelf, also leading to the remaining nitrate pool enriching in ^{15}N. The station

to the East of Svalbard was at the mean position of the ice edge during sample collection (Stevenson and Abbott, 2019); this might be expected to have higher ^{15}N values due to bloom conditions at the ice edges, which would also cause a relative enrichment of the remaining nitrate pool and therefore the POM also (Schubert and Calvert, 2001). Further, Tuerena et al. (2021) reported the western Fram Strait waters to be depleted in nitrate relative to the east which typically leaves an enriched ^{15}N of POM, possibly explaining the enrichment we found in sediments there.

The macromolecular analyses presented here follow closely a method used in the East Siberian Arctic Shelf (ESAS) region by Sparkes et al. (2016), however the changes in composition are more subtle in comparison to the river to offshore transects along the ESAS. Previous analyses of a North-South transect in the Barents Sea (included in the dataset presented in this study) suggested that the variations in macromolecular compounds were controlled by the ice edge position, bloom conditions and nutrient concentrations, which were all controlled by the relative position of the PF (Stevenson and Abbott, 2019) . Unlike the ESAS, increases in the relative abundance of phenols were considered to be more likely a reflection of increased export of marine organic matter in the form of polysaccharides at the marginal ice zones and the polar front rather than reflection of the terrestrial to marine inputs as observed in the ESAS. Our combined datasets further support this idea, as fluctuations in the PPRI appear to change relative to the position of the polar front and marginal ice zones which were present during sample collection (Stevenson and Abbott, 2019). There was a complex spatial picture in macromolecular data due to the assortment of organisms found around the polar front and marginal ice zones. The deviation from this trend, as with the C/N, is the fjord station which represents the highest PPRI recorded and is most likely influenced

by terrestrial inputs from the surrounding land rather than its location relative to the PF or MIZ.

The lowest PPRI is found at the East Greenland Shelf edge where we also find some of our most enriched $\delta^{15}N_{Bulk}$ values. This further supports the idea of this being a region of increased marine organic matter input to sediments either due to the advection of nutrients caused by the shelf edge bathymetry at these stations or the enriched nitrate pool due to the water column being nitrate limited, both leading to an increased ^{15}N of POM (Schubert and Calvert, 2001; Tuerena et al., 2021). However, there is still the possibility of heterotrophic reworking within the water column or post-depositional processes causing at least part of these variations.

Together, the bulk and macromolecular analysis suggest that the greatest control on the export of organic matter to the seafloor in these regions is the proximity to the marginal ice zone and the polar front, as has been previously reported, although an input of terrestrial material alongside local, bathymetric and temporal variability cannot always be excluded.

4.5.2 Amino acid compositions across the Barents Sea and Fram Strait

Amino acid compositions, although not necessarily source indicative, are a widely used tool in marine sedimentary studies to better understand diagenetic processes (Cowie and Hedges, 1992; Dauwe and Middelburg, 1998; Dauwe et al., 1999). In this dataset, the mol% amino acid compositional data revealed a grouping of Leu and Phe, both displaying the same kind of relationship to the other amino acids and molecular indices (e.g. $\delta^{15}N_{Bulk}$). A principle component analysis further confirmed this grouping, showing that Leu, Phe and the DI group on one side of PC1, meaning this component is likely a reflection of the DI and the other amino acids association to it.

The grouping of Leu and Phe, has previously been reported in the water column of the Fram Strait by Grosse et al. (2021), who suggested that Leu and Phe are concentrated in the particulate amino acid (PAA) fraction and Ala, Gly, Asp and Glu in the dissolved phase (TDAA). This was attributed to Leu and Phe being concentrated in an actively growing plankton community which are typically what is incorporated into the surface sediments alongside prokaryotes and excretion products of (zoo) plankton and higher organisms. The assimilation of amino acids by organisms differs; Leu and Phe are part of the essential amino acid group, which are synthesized by autotrophs (e.g. phytoplankton) and cannot be biosynthesised by heterotrophs (e.g. Arctic Cod) so have to be consumed through dietary routes for these organisms unlike Ala, Gly, Asp and Glu which are non-essential amino acids (Grosse et al., 2018 and 2021). It is worth noting that valine (an essential amino acid) behaved in the same way as the non-essential group, but it is a minor constituent of the amino acid pool and there were often insignificant/no correlations with other amino acids. Our dataset combined with the findings from Grosse et al. (2021) suggest that the compositions of the particulate pool in the water column maybe preserved in the surface sediments too. To verify this a direct comparison between water column particulates and sedimentary data would be needed. This is surprising as the amino acids concentrated in the PAA phase are known to be labile and to be rapidly reworked (Dauwe et al., 1999). Batista et al. (2014) found the mol% amino acid composition to be preserved in the Santa Barbara Basin from the water column to sediments accompanied by a 94% decrease in total amino acid concentration, suggesting non-selective removal of amino acids. Furthermore, Cowie and Hedges (1992) found heterotrophic bacteria can have similar amino acid compositions to those of phytoplankton. Batista et al. (2014) hypothesized this similarity in composition, between the water column and sediments, could be due to a bacterial mat forming at the sediment-water interface (SWI) and that this was

being sampled rather than the surface sediments themselves. Although bacterial mats have been previously found around the Barents Sea, e.g. Lichtschlag et al. (2010) and Grünke et al. (2012), particularly around mud volcanoes and cold methane seeps. The visual inspection of the freshly retrieved sediment cores, which retained the SWI, suggest an absence of bacterial mats which was confirmed at selected sampling stations by a shallow underwater camera system (this does not exclude bacteria from being present in the sediments). In addition, Batista et al. (2014) sampled from an oxygen minimum zone which is not directly comparable to the present study sites and Stevenson et al. (2020) analysed a sediment core from one of the studied sampling stations and no reference to bacterial mats were made at the SWI. Furthermore, a larger relative molar contribution of Gly has also been linked to microbial inputs (Dauwe and Middelburg, 1998; Dauwe et al., 1999; Yamashita and Tanoue, 2003). Gly did not dominate any of the amino acid compositions in this study suggesting microbial alteration from a bacterial mat is not why water column particulates may reflect sedimentary compositions.

The degradation index (DI) for this region did not provide evidence of any differences between water masses, although sample size for the NCC and NCC_AW groups are likely too small to draw any significant conclusions. The range of DI reported is analogous to other marine sediments (e.g. Gaye et al., 2022, ~-1 to 2) and was positively correlated with the C/N. This is the opposite of what might be expected, as higher C/N are usually associated with terrestrial inputs and higher DI with fresh planktonic material (Hedges and Oades, 1997; Dauwe et al., 1999; Stein, 2008). Although as previously noted, higher C/N values in this study are not necessarily associated with the typical concept that high C/N is indicative of increases in terrestrial input at offshore stations but could be associated with a greater amount of

degradation selectively removing the labile n-containing compounds. Again, this supports the impact the PF and MIZ has on the composition of the sedimentary organic matter.

4.5.3 The baseline sedimentary ^{15}N isoscape ($\delta^{15}N_{AA}$) in the Barents Sea and Fram Strait

CSIA-AA allows the decoupling of potential variations/contamination of $\delta^{15}N_{Bulk}$ data such as the in-mixing of inorganic nitrogen and other organic compounds that dilute or mask the isotopic signal. Here, we measured the $\delta^{15}N_{AA}$ in surface sediment samples to investigate whether the organic nitrogen fraction drives the changes in bulk elemental and isotopic compositions across the Barents Sea and Fram Strait.

The trophic amino acids were more enriched in ^{15}N relative to the source amino acids in all of the sediment samples. Gly and Phe, the source amino acids, remained relatively similar in $\delta^{15}N$ across all water mass groups but small-scale changes are likely masked by splitting the samples in this way. The results from our $\delta^{15}N_{AA}$ analysis further highlights the complexity of the region we are studying where no one grouping, e.g. water mass or distance from coast, truly encompasses all of the factors influencing samples.

There are small scale variations across our samples in $\delta^{15}N_{Bulk}$, $\delta^{15}N_{THAA}$ and $\delta^{15}N_{Phe}$ which likely reflect the locality of the stations to the PF, MIZ, terrestrial inputs alongside the differing contributions from the different water masses and post depositional processes (Fig. 4.11). Along the transect from Norway to Svalbard, the variations in $^{15}N_{Bulk}$ were relatively minor whereas fluctuations in the $^{15}N_{THAA}$ and $^{15}N_{Phe}$ displayed larger deviations. When compared to water column data from (Tuerena et al., 2021) the $\delta^{15}N\text{-}NO_3$ at depth also fluctuates very little in this transect like $\delta^{15}N_{Bulk}$ of surface sediments whereas the associated $\delta^{15}N$-PN displays greater variations. Changes in $\delta^{15}N_{Phe}$ are usually considered to be changes in the food source (inorganic nitrogen) fuelled primary productivity in the water column which

along the Barents Sea opening is more likely to be an effect of different sources of nitrate and associated levels of primary productivity (McClelland and Montoya, 2002; McCarthy et al., 2007; Chikaraishi et al., 2009). The most westerly samples from the Fram Strait, which sit on the East Greenland Shelf, display enrichments in ^{15}N across $^{15}N_{Bulk}$ as well as the $^{15}N_{THAA}$ and $^{15}N_{Phe}$ relative to the rest of the transect in the East. This further supports nitrate limitation leading to a more enriched organic nitrogen particulate pool, which is then mirrored within sediments at the compound specific level (Fig. 4.11b). Our only fjord station, which from bulk analyses appears to be more influenced by terrestrial inputs, has depleted $^{15}N_{THAA}$ and $^{15}N_{Phe}$ values relative to offshore stations. Terrestrial organic matter is known to be isotopically lighter than its marine counterpart due to fixation of nitrogen from the atmosphere which is usually lighter than nitrate ^{15}N (Schubert and Calvert, 2001; Robinson et al., 2012).

We compared the $\delta^{15}N_{Bulk}$ to the $\delta^{15}N_{THAA}$ across the regions (Fig. 4.11; Batista et al., 2014). The $^{15}N_{THAA}$ is consistently enriched relative to $^{15}N_{Bulk}$, with the offset ranging from 3.4 - 7.3 ‰ (defined as $\Delta\delta^{15}N_{THAA\text{-}Bulk}$; Fig. 4.11). Batista et al. (2014) found the offset in their study region was greatest in fresh samples and narrowed between sediment trap and sediment cores; here, on average, there was a larger offset in sediments although the previous study used preserved sediment trap samples which enriched ^{15}N by ~1‰. Batista et al. (2014) attributed the offset in their study area to changes in the biochemistry of marine organic matter through changes in the trophic structure and a differing baseline isoscape rather than the incorporation of terrestrial material. For the majority of our samples, we do not expect terrestrial inputs to be great and in fact the smallest $\Delta\delta^{15}N_{THAA\text{-}Bulk}$ is at our station most influenced by terrestrial inputs (ST1, fjord station), which contradicts the notion that terrestrial contributions have produced variations in $\Delta\delta^{15}N_{THAA\text{-}Bulk}$.

One idea is the alteration of organic matter by microbial heterotrophy, which enriches the $\delta^{15}N_{THAA}$ in sediments and POM (Calleja et al., 2013). The ∑V parameter is a proxy for total heterotrophic reworking; the range of ∑V (1.7 – 4.2‰) in the Barents Sea and Fram Strait samples suggests elevated amounts of microbial uptake and resynthesis (Batista et al., 2014). However, there is no correlation between the ∑V and $\Delta\delta^{15}N_{THAA\text{-}Bulk}$ implying that heterotrophic reworking is not responsible for the large $\Delta\delta^{15}N_{THAA\text{-}Bulk}$. Nevertheless the range of ∑V is indicative of increased amounts of microbial heterotrophy within the study region.

The most likely explanation for our observations is that the relative enrichment of $\delta^{15}N_{THAA}$ relative to $\delta^{15}N_{Bulk}$ is due to the isotopically lighter signature of inorganic nitrogen (N_{inorg}) which influences the total nitrogen bulk measurements. The presence of N_{inorg} is supported by a plot of N_{tot} versus TOC (Appendix 2), where the intercept is 0.035% N_{tot} at 0% TOC. Similar amounts of N_{inorg} have been previously reported in Arctic Ocean sediments and are said to form a significant fraction of the total nitrogen pool in sediments (Schubert and Calvert, 2001). This demonstrates that the combination of $\delta^{15}N_{Bulk}$ and $\delta^{15}N_{THAA}$ can decouple the potential issues associated with bulk measurement and provide better insights in organic nitrogen cycling.

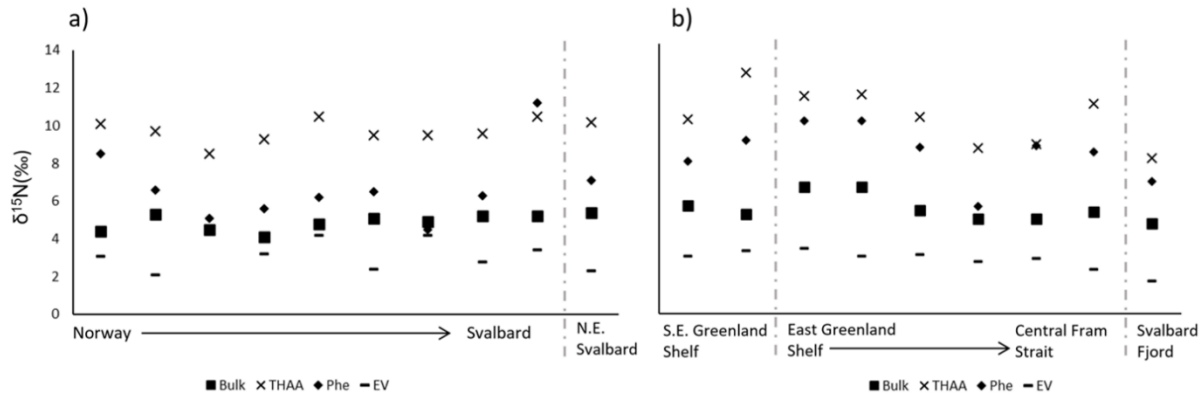

Figure 4.11 Plots comparing the $\delta^{15}N_{Bulk}$, $\delta^{15}N_{THAA}$, $\delta^{15}N_{Phe}$ and ∑V a) Barents Sea opening transect from Norway to Svalbard and b) station across the Fram Strait and fjord sample.

The bulk and macromolecular data we present appear to support previous studies in the region, in that variations in these can usually be associated with their locality to the PF and MIZ however we also find variations that could be temporal and spatial differences too. We also find that in regions where nitrate limited water masses are found, this is reflected in the $\delta^{15}N_{Bulk}$ of sediments underlying the water column. At sampling sites near to terrestrial inputs (e.g. fjord station ST1) we find a larger PPRI and depleted ^{15}N ($\delta^{15}N_{Bulk}$, $\delta^{15}N_{THAA}$ and $\delta^{15}N_{Phe}$) suggesting the major control here is the input of terrestrial organic matter. In the Barents Sea, there is little correlation between fluctuations in $\delta^{15}N_{Bulk}$ and $\delta^{15}N_{THAA}$, suggesting that the organic nitrogen pool is not the sole control on variations at the bulk level but more likely the input of inorganic nitrogen. In the Fram Strait sediments, this link seems to be stronger as is evident in the relative enrichment of $\delta^{15}N_{Bulk}$, $\delta^{15}N_{THAA}$ and $\delta^{15}N_{Phe}$ at the East Greenland Shelf and the mirroring of enrichment and depletion of ^{15}N across most of the studied sites. As this region continues to become increasingly Atlantified with less multi-year ice and a nutrient limited food web due to global climate change, it will be crucial to better constrain the processes that control the baseline isoscape across the region to assess the organic matter cycle within the region.

4.6 Conclusions and implications

This work highlights the complexity that the Barents Sea and Fram Strait region presents. Where the mixing of distinct water masses (Atlantic and Arctic flows) creating a polar front are coupled with retreating sea ice, marginal ice zones, diagenetic processes and an uncharacterised water column leading to a complicated picture presented in the surface sediments. The elemental (C/N ratios) and $\delta^{15}N_{Bulk}$ obtained from across this region reveal a pattern that matches the relative positions of the polar front and marginal ice zones coupled to an influx of terrestrial derived inputs from riverine and glacial run off. The latter is largely observed in stations close to the coast of Svalbard and within fjords. This is supported by the macromolecular compositions observed, indicating that unlike other regions of the Arctic (e.g. the ESAS) increases in the phenol abundance (pseudo terrestrial marker) far offshore are more likely a reflection of the increased contribution of polysaccharides to the sediments due to greater amounts of primary productivity, supporting previous observations. Amino acid distribution patterns across the study area do not show any distinct trends relating to the MIZ or PF although Leu and Phe generally grouped together, both in being the most abundant amino acids in the sediments and having the same correlations to other indices and amino acid abundances (e.g. C/N, PPRI and DI). In line with previous observations this was attributed to these amino acids being concentrated in the actively growing portion of particulate organic matter in the water column, suggesting that this pattern is transferred into the underlying sediments in this region. The DI across the study site did not show any distinct trends with water mass associations nor the proximity to the PF or MIZ either but values fell within the ranges reported previously for sinking particulate organic matter and marine sediments. The ^{15}N of source amino acids revealed small variations across the whole region which could

indicate that a comparable $\delta^{15}N\text{-}NO_3$ source is being utilised regardless of water mass influence, suggesting that the subsequent enrichment of $\delta^{15}N\text{-}NO_3$ as it is consumed could be masking the different $\delta^{15}N\text{-}NO_3$ signatures at the start of a bloom period. Where nitrate has been suggested to be limited in the region we found enriched $\delta^{15}N_{Phe}$, which we would expect as the residual nitrate and subsequent particulate pool also become enriched in these regions. Like the $\delta^{15}N_{Bulk}$ and PPRI, the $\delta^{15}N_{THAA}$ indicate an influx of isotopically lighter nitrogen from terrestrial sources in the fjord sample and a typically more marine value at the East Greenland Shelf edge, further supporting a nitrate limited water mass flowing through this region. Across all stations the $\delta^{15}N_{THAA}$ was enriched relative to the $\delta^{15}N_{Bulk}$, due to the inmixing of inorganic nitrogen in the sediments which dilutes the bulk signal and leads to the offset observed. This highlights the limitations of using $\delta^{15}N_{bulk}$ analyses where there is a significant amount of inorganic nitrogen present in the sediments and the valuable information $\delta^{15}N_{THAA}$ can provide in de-coupling these effects. This will be particularly important going forward as the region continues to become more Atlantified due to climate change, altering the positions of the polar front and marginal ice zones and the nitrate source to primary producers. Compound specific isotope analysis of amino acids has the potential to become an invaluable technique to correctly determine baseline isoscape across the Arctic.

References

Altabet, M. A. and Francois, R. (1994) 'Sedimentary nitrogen isotopic ratio as a recorder for surface ocean nitrate utilization', Global Biogeochemical Cycles, 8(1), pp. 103–116.

Arrigo, K. R. and van Dijken, G. L. (2015) 'Continued increases in Arctic Ocean primary production', Progress in Oceanography. Elsevier Ltd, 136, pp. 60–70. doi: 10.1016/j.pocean.2015.05.002.

Barton, B. Lenn, Yueng-Djern. Lique, C. (2018) 'Observed Atlantification of the Barents Sea Causes the Polar Front to Limit the Expansion of Winter Sea Ice', pp. 1849–1866. doi: 10.1175/JPO-D-18-0003.1.

Batista, F. C. et al. (2014) 'Compound specific amino acid δ15N in marine sediments: A new approach for studies of the marine nitrogen cycle', Geochimica et Cosmochimica Acta. Elsevier Ltd, 142, pp. 553–569. doi: 10.1016/j.gca.2014.08.002.

Burdige, D. J. and Martens, C. S. (1988) 'Biogeochemical cycling in an organic-rich coastal marine basin: 10. The role of amino acids in sedimentary carbon and nitrogen cycling', Geochimica et Cosmochimica Acta, 52(6), pp. 1 571–1584. doi: 10.1016/0016-7037(88)90226-8.

Calleja, M. L. et al. (2013) 'Changes in compound specific δ15N amino acid signatures and d/l ratios in marine dissolved organic matter induced by heterotrophic bacterial reworking', Marine Chemistry. Elsevier B.V., 149, pp. 32–44. doi: 10.1016/j.marchem.2012.12.001.

Carstens, D. et al. (2013) 'Amino acid nitrogen isotopic composition patterns in lacustrine sedimenting matter', Geochimica et Cosmochimica Acta. Elsevier Ltd, 121, pp. 328–338. doi: 10.1016/j.gca.2013.07.020.

Chikaraishi, Y. et al. (2007) 'Metabolic control of nitrogen isotope composition of amino acids in macroalgae and gastropods: Implications for aquatic food web studies', Marine Ecology Progress Series, 342(2003), pp. 85–90. doi: 10.3354/meps342085.

Chikaraishi, Y. et al. (2009) 'Determination of aquatic food-web structure based on compound-specific nitrogen isotopic composition of amino acids', Limnology and Oceanography: Methods, 7(11), pp. 740–750. doi: 10.4319/lom.2009.7.740.

Codispoti, L. A. et al. (2013) ‘Synthesis of primary production in the Arctic Ocean: III. Nitrate and phosphate based estimates of net community production’, Progress in Oceanography, 110(December 2012), pp. 126–150. doi: 10.1016/j.pocean.2012.11.006.

Cowie, G. and Hedges, J. (1992) ‘Sources and reactivities of amino acids in a coastal marine environment’, Limnology and Oceanography, 37(4), pp. 703–724.

Dai, A. et al. (2019) ‘Arctic amplification is caused by sea-ice loss under increasing CO 2’, Nature Communications. Springer US, 10(1), pp. 1–13. doi: 10.1038/s41467-018-07954-9.

Dauwe, B. et al. (1999) ‘Linking diagenetic alteration of amino acids and bulk organic matter reactivity’, Limnology and Oceanography, 44(7), pp. 1809–1814. doi: 10.4319/lo.1999.44.7.1809.

Dauwe, B. and Middelburg, J. J. (1998) ‘Amino acids and hexosamines as indicators of organic matter degradation state in North Sea sediments’, Limnology and Oceanography, 43(5), pp. 782–798. doi: 10.4319/lo.1998.43.5.0782.

Dittmar, T., Fitznar, H. P. and Kattner, G. (2001) ‘Origin and biogeochemical cycling of organic nitrogen in the eastern Arctic Ocean as evident from D-and L-amino acids’, Geochimica et Cosmochimica Acta, 65(22), pp. 4103–4114. Available at: http://linkinghub.elsevier.com/retrieve/pii/S0016703701006883.

Engelsen, O. et al. (2002) ‘Spatial variability of chlorophyll-a in the Marginal Ice Zone of the Barents Sea, with relations to sea ice and oceanographic conditions’, Journal of Marine Systems, 35(1–2), pp. 79–97. doi: 10.1016/S0924-7963(02)00077-5.

Faust, J. C. et al. (2020) ‘Does Arctic warming reduce preservation of organic matter in Barents Sea sediments?: Barents Sea surface sediment composition’, Philosophical Transactions of the Royal Society A: Mathematical, Physical and Engineering Sciences, 378(2181). doi: 10.1098/rsta.2019.0364.

Gaye, B. et al. (2022) ‘What can we learn from amino acids about oceanic organic matter cycling and degradation ?’, pp. 807–830.

Grosse, J. et al. (2021) ‘Summertime Amino Acid and Carbohydrate Patterns in Particulate and Dissolved Organic Carbon Across Fram Strait’, Frontiers in Marine Science, 8(July). doi: 10.3389/fmars.2021.684675.

Grünke, S. et al. (2012) ‘Mats of psychrophilic thiotrophic bacteria associated with cold seeps of the Barents Sea’, Biogeosciences, 9(8), pp. 2947–2960. doi: 10.5194/bg-9-2947-2012.

Guo, L. et al. (2009) ‘Chemical and isotopic composition of high-molecular-weight dissolved organic matter from the Mississippi River plume’, Marine Chemistry. Elsevier B.V., 114(3–4), pp. 63–71. doi: 10.1016/j.marchem.2009.04.002.

H.- O. Pörtner, D.C. Roberts, V. Masson-Delmotte, P. Zhai, M. Tignor, E. Poloczanska, K. Mintenbeck, A. Alegría, M. Nicolai, A. Okem, J. Petzold, B. Rama, N. M. W. (2019) IPCC Special Report on the Ocean and Cryosphere in a Changing Climate: Technical Summary.

Harris, C. L., Plueddemann, A. J. and Gawarkiewicz, G. G. (1998) ‘Norwegian / Murmansk Coastal’, 103(97), pp. 2905–2917.

Hedges, J. I. and Oades, J. M. (1997) ‘Comparative organic geochemistries of soils and marine sediments’, Organic Geochemistry, 27(7).

Hopkins, J. (2018) The Changing Arctic Ocean Cruise JR16006, RRS James Clark Ross Cruise Report No. 51 30 June–8 August 2017, (2018). Available at: https://www.bodc.ac.uk/ resources/inventories/cruise_inventory/reports/jr16006.pdf.

Knies, J. (2005) ‘Climate-induced changes in sedimentary regimes for organic matter supply on the continental shelf off northern Norway’, Geochimica et Cosmochimica Acta, 69(19), pp. 4631–4647. doi: 10.1016/j.gca.2005.05.014.

Knies, J. and Martinez, P. (2009) ‘Organic matter sedimentation in the western Barents Sea region : Terrestrial and marine contribution based on isotopic composition and organic nitrogen content’, (1), pp. 79–89.

Lewis, K. M., Dijken, G. L. Van and Arrigo, K. R. (2020) ‘Changes in phytoplankton concentration now drive increased Arctic Ocean primary production’, 202(July), pp. 198–202.

Lichtschlag, A. et al. (2010) ‘Geochemical processes and chemosynthetic primary production in different thiotrophic mats of the Håkon Mosby Mud Volcano (Barents Sea)’, Limnology and Oceanography, 55(2), pp. 931–949. doi: 10.4319/lo.2009.55.2.0931.

McCarthy, M. D. et al. (2007) ‘Amino acid nitrogen isotopic fractionation patterns as indicators of heterotrophy in plankton, particulate, and dissolved organic matter’, Geochimica et Cosmochimica Acta, 71(19), pp. 4727–4744. doi: 10.1016/j.gca.2007.06.061.

McCarthy, M. D., Lehman, J. and Kudela, R. (2013) ‘Compound-specific amino acid δ15N patterns in marine algae: Tracer potential for cyanobacterial vs. eukaryotic organic nitrogen sources in the ocean’, Geochimica et Cosmochimica Acta. Elsevier Ltd, 103, pp. 104–120. doi: 10.1016/j.gca.2012.10.037.

McClelland, J. W., Holl, C. M. and Montoya, J. P. (2003) ‘Relating low δ15N values of zooplankton to N 2-fixation in the tropical North Atlantic: Insights provided by stable isotope ratios of amino acids’, Deep-Sea Research Part I: Oceanographic Research Papers, 50(7), pp. 849–861. doi: 10.1016/S0967-0637(03)00073-6.

McClelland, J. W. and Montoya, J. P. (2002) ‘Trophic Relationships and the Nitrogen Isotopic Composition of Amino Acids in Plankton’, Ecology, 83(8), pp. 2173–2180. doi: 10.1890/0012-9658(2002)083[2173:TRATNI]2.0.CO;2.

McMahon, K. W. and McCarthy, M. D. (2016) ‘Embracing variability in amino acid δ15N fractionation: Mechanisms, implications, and applications for trophic ecology’, Ecosphere, 7(12), pp. 1–26. doi: 10.1002/ecs2.1511.

Notz, D. and Stroeve, J. (2016) ‘Observed Arctic sea-ice loss directly follows anthropogenic CO2 emission’, Science, 354(6313), pp. 747–750. doi: 10.1126/science.aag2345.

Onarheim, I. H. et al. (2015) ‘Skillful prediction of Barents Sea ice cover’, Geophysical Research Letters, 42(13), pp. 5364–5371. doi: 10.1002/2015GL064359.

Oziel, L., Sirven, J. and Gascard, J. C. (2016) ‘The Barents Sea frontal zones and water masses variability (1980-2011)’, Ocean Science, 12(1), pp. 169–184. doi: 10.5194/os-12-169-2016.

Paquette, R. et al. (1985) ‘The East Greenland Polar Front in Autumn’, 90, pp. 4866–4882.

Perner, K. et al. (2019) ‘An oceanic perspective on Greenland ’ s recent freshwater discharge since 1850’, pp. 1–10. doi: 10.1038/s41598-019-53723-z.

Pond, D. (2018) The Changing Arctic Ocean Cruise JR17005, RRS James Clark Ross Cruise Report. Available at: https://www.bodc.ac.uk/resources/inventories/cruise_inventory/reports/jr17005.pdf.

Robinson, R. S. et al. (2012) ‘A review of nitrogen isotopic alteration in marine sediments’, Paleoceanography, 27(4). doi: 10.1029/2012PA002321.

Rudels, B., Anderson, L. G. and Jones, E. P. (1996) ‘Formation and evolution of the surface mixed layer and halocline of the Arctic Ocean’, 101, pp. 8807–8821.

Schubert, C. J. and Calvert, S. E. (2001) ‘Nitrogen and carbon isotopic composition of marine and terrestrial organic matter in Arctic Ocean sediments: Implications for nutrient utilization and organic matter composition’, Deep-Sea Research Part I: Oceanographic Research Papers, 48(3), pp. 789–810. doi: 10.1016/S0967-0637(00)00069-8.

Sigman, D. M. and Casciotti, K. L. (2001) ‘Nitrogen Isotopes in the Ocean’, Encyclopedia of Ocean Sciences, (1997), pp. 40–54. doi: 10.1016/B978-012374473-9.00632-9.

Somes, C. J. et al. (2010) ‘Simulating the global distribution of nitrogen isotopes in the ocean’, 24, pp. 1–16. doi: 10.1029/2009GB003767.

Sorteberg, A. and Kvingedal, B. (2006) ‘Atmospheric forcing on the Barents Sea winter ice extent’, Journal of Climate, 19(19), pp. 4772–4784. doi: 10.1175/JCLI3885.1.

Sparkes, R. B. et al. (2016) ‘Macromolecular composition of terrestrial and marine organic matter in sediments across the East Siberian Arctic Shelf’, Cryosphere, 10(5), pp. 2485–2500. doi: 10.5194/tc-10-2485-2016.

Stein, R. (2008) Arctic Ocean Sediments: Processes, Proxies, and Paleoenvironment. Elsevier.

Stevenson, M. A. et al. (2020) ‘Transformation of organic matter in a Barents Sea sediment profile: Coupled geochemical and microbiological processes: Sediment organic matter transformation’, Philosophical Transactions of the Royal Society A: Mathematical, Physical and Engineering Sciences, 378(2181). doi: 10.1098/rsta.2020.0223.

Stevenson, M. A. and Abbott, G. D. (2019) 'Exploring the composition of macromolecular organic matter in Arctic Ocean sediments under a changing sea ice gradient', Journal of Analytical and Applied Pyrolysis. Elsevier, (February), pp. 1–10. doi: 10.1016/j.jaap.2019.02.006.

Styring, A. K. et al. (2012) 'Practical considerations in the determination of compound-specific amino acid δ15N values in animal and plant tissues by gas chromatography-combustion-isotope ratio mass spectrometry, following derivatisation to their N-acetylisopropyl esters', Rapid Communications in Mass Spectrometry, 26(19), pp. 2328–2334. doi: 10.1002/rcm.6322.

R Core Team (2022) 'R: A language and environment for statistical computing. R Foundation for Statistical Computing'. Austria, Vienna: R Core Team. Available at: https://www.r-project.org/.

Torres-Valdés, S. et al. (2013) 'Export of nutrients from the Arctic Ocean', Journal of Geophysical Research: Oceans, 118(4), pp. 1625–1644. doi: 10.1002/jgrc.20063.

Tuerena, R. E., Hopkins, Jo, et al. (2021) 'An Arctic Strait of Two Halves: The Changing Dynamics of Nutrient Uptake and Limitation Across the Fram Strait', Global Biogeochemical Cycles, 35(9), pp. 1–20. doi: 10.1029/2021GB006961.

Tuerena, R. E., Hopkins, Joanne, et al. (2021) 'Nitrate assimilation and regeneration in the Barents Sea: Insights from nitrate isotopes', Biogeosciences, 18(2), pp. 637–653. doi: 10.5194/bg-18-637-2021.

de Vega, C. et al. (2021) 'Biomarkers in Ringed Seals Reveal Recent Onset of Borealization in the High- Compared to the Mid-Latitude Canadian Arctic', 8(September), pp. 1–11. doi: 10.3389/fmars.2021.700687.

Yamashita, Y. and Tanoue, E. (2003) 'Distribution and alteration of amino acids in bulk DOM along a transect from bay to oceanic waters', Marine Chemistry, 82(3–4), pp. 145–160. doi: 10.1016/S0304-4203(03)00049-5.

Photo taken by author of Lion's mane jellyfish off the coast of Ny-Ålesund, Svalbard, September 2019

Chapter 5

Conclusions and future work

5.1 Conclusions

The main aims of this project set out at the start of this thesis were centred around a better understanding of how different organic matter sources have an impact on the organic matter compositions we find in the sediments. More specifically, looking at organic nitrogen inputs and using nitrogen isotopes at both a bulk and molecular level combined with a macromolecular technique to give a better understanding of what causes shifts at the bulk level and what this means in a rapidly changing environment like the Arctic. Prior to this project there were only a limited number of studies (Carstens *et al.*, 2013; Batista *et al.*, 2014) that had combined these bulk and molecular isotope methods and these provided useful insights into how molecular level isotope analyses can decouple the integrated signal bulk analysis exhibits and valuable information it can provide about baseline sources of nutrients to primary producers. For the first time, to the best of our knowledge, we combined the bulk and compound specific isotope approach with macromolecular analysis in marine sediments of the Arctic to provide a more complete understanding of organic matter this rapidly changing region.

The objectives set out to achieve this aim were addressed through, firstly, the collection of marine surface sediments to improve the spatial resolution of the study and capture a key region of scientific interest (Fram Strait; objective 1). The existing meta-dataset for macromolecular composition in the East Siberian Arctic Shelf (ESAS) which was first published by Sparkes *et al.* (2016) was extended to provide better spatial resolution therefore improving interpretations (objective 2). This method was applied to another key Arctic region, the Barents Sea and Fram Strait, where we extended the previously reported macromolecular data set from Stevenson and Abbott. (2019) to cover a larger proportion of the Barents Sea

and for the first time the Fram Strait. In line with the existing ESAS dataset we also analysed the Barents Sea and Fram Strait sediment samples for their elemental composition (carbon and nitrogen content) and bulk nitrogen isotopes ($\delta^{15}N_{Bulk}$). The amino acid isotope method was refined and tuned for use in marine sediments (objective 4; see methods sections in chapter 3 and 4) as this is typically used for ecological samples which require less clean up and are more abundant in amino acids. Amino acids were selected due to the significant proportion of the organic nitrogen in marine organisms that they form part of and therefore give the most complete picture of organic nitrogen transformations. Sediment samples were analysed for their amino acids composition firstly using a GC-FID technique and then for their nitrogen isotope composition using GC-IRMS (objective 4 and 5). Finally these novel datasets were combined for each region to display a more comprehensive picture of the organic nitrogen in these regions (objective 6).

Chapter 3 investigated the East Siberian Arctic Shelf, a region identified as undergoing rapid change due to climate warming. As an area dominated by continuous permafrost with large rivers cutting through the landscape, it has been particularly susceptible to increases in temperatures. Which has led to enhanced thawing of permafrost layers, leading to an increase in river discharge as permafrost melt travels across and through the land. Alongside this, the ESAS presented a unique coastal setting dominated by Ice Complex Deposits (ICDs), which are ice rich cliffs containing organic matter and are similarly being thawed and eroded by the effects of climate change. Together, the input of organic matter via fluvial and coastal erosional processes, present a complex system across the ESAS which is set to become more important as climate change progresses.

Our Initial investigations involved analysing previously published dataset of bulk isotopes and elemental data ($\delta^{13}C_{TOC}$, $\delta^{15}N_{Bulk}$ and C/N ratios), these existing publications largely focused on carbon proxies and to a much lesser extent nitrogen. Firstly, looking at the elemental composition of surface sediments (C/N ratio), this indicated a transition from terrestrial dominated inputs in the nearshore to marine in the offshore regions. It also displayed differences between the nearshore regions from the West to the East of the ESAS, suggesting a difference in the terrestrial sources close to the coast. Secondly, the analysis of $\delta^{13}C_{TOC}$, which displayed significant trends from the nearshore to the offshore regions of the ESAS, in-line with what would be expected moving from an area dominated by terrestrial inputs of organic carbon (fluvial and coastal erosion) to more marine organic matter inputs offshore. $\delta^{15}N_{Bulk}$, likewise, revealed a more terrestrial signal close to the coast and an enrichment offshore, indicating that this proxy was also tracking the terrestrial-marine transition. Despite these initial similarities in behaviour, novel statistical analysis of these two proxies showed that while in the nearshore regions the $\delta^{13}C_{TOC}$ remained similar the $\delta^{15}N_{Bulk}$ did not. Analysis showed that there was a statistical difference in the nearshore signals between the Laptev Sea and the East Siberian Sea regions, likely reflecting a difference in terrestrial contributions. To further investigate the differences in the nitrogen signal close to the coast, the ^{15}N isotopic composition of the amino acids alongside a compositional examination was completed. The amino acid composition did not differ significantly between the regions but the grouping of Leu and Phe in particulates across other regions of the Arctic has been suggested to reflect the input of actively growing phytoplankton communities as these are known to be concentrated in these organisms. In contrast, the amino acid ^{15}N values, like the $\delta^{15}N_{Bulk}$, displayed the same differences between the nearshore regions suggesting the changes are due to organic nitrogen inputs and not, for instance, caused by an

influx of inorganic nitrogen. This trend continued offshore, again similar to bulk indices, further supporting organic nitrogen (amino acids) as the driving force in differences even far offshore. Collectively these analyses provide a first insight into organic nitrogen variations in this region and provide a more comprehensive view on baseline values of organic matter in Arctic marine sediments. With implications for carbon cycling, and energy supply to the benthos, particularly as this region continues to undergo rapid changes, such as thawing permafrost/ICDs and increased river run off due to anthropogenic climate change.

Chapter 4 investigated a completely different part of the Arctic, the Barents Sea and Fram Strait regions, together forming a major gateway to the Arctic Ocean basin where warm and saline Atlantic water flows in and cold and fresher Polar water flows south. The interaction of water masses firstly creates the polar front (PF) marked with distinct transitions in temperature and salinity and secondly by a marginal ice zone (MIZ) where sea-ice exported from the north meets the warmer Atlantic waters and begins to melt. The PF and MIZ regions are known to be particularly productive, likely to increase as the Arctic Ocean becomes less light limited due to multi-year sea ice retreat.

C/N and $\delta^{15}N_{Bulk}$ offshore displayed patterns primarily related to the relative position of the station to the PF and MIZ. As with previous studies an increased contribution of organic carbon offshore was not found to reflect a substantial terrestrial input but mainly linked to the increased amount of marine organic matter transported to the sediments in these productive regions. Whilst the $\delta^{15}N_{Bulk}$ displayed a more complicated pattern, fluctuations can still be related back to the position of the PF and MIZ. Regions known to have a nitrate limited water column had elevated $\delta^{15}N_{Bulk}$ in surface sediments reflecting the enriched residual nitrate pool in the water column. A Svalbard fjord station, in contrast, displayed elevated C/N

and depleted $\delta^{15}N_{Bulk}$ which given the location can be confidently linked to terrestrial inputs from rivers or glacial terminus. Macromolecular analysis further supported these conclusions with patterns relating to the PF, MIZ and terrestrial inputs. However, the interpretations of the phenol to pyridine ratio (PPRI) offshore differed to other parts of the Arctic (e.g. the East Siberian Arctic Shelf; Chapter 3) and increases in the PPRI aren't necessarily related to increased terrestrial inputs but have previously been suggested to illustrate the enhanced transport of marine polysaccharides in these productive areas.

Amino acid compositional analysis did not reveal any distinct trends however, Leucine (Leu) and phenylalanine (Phe) were the most abundant amino acids across the entire study region and grouped together in their correlations to other amino acids and other indices measured in this study (C/N ratio, $\delta^{15}N_{Bulk}$ and PPRI). The correlations of Leu and Phe has been previously reported in this region in particulate amino acids in the water column and is attributed to the actively growing phytoplankton community being enriched in these amino acids (Grosse *et al.*, 2021). This, together with our study suggests an accumulation of these communities in surface sediments across the region.

The $\delta^{15}N$ of trophic amino acids was enriched relative to the source amino acids across all parts of the study region which is to be expected as source amino acids fractionate by only small increments compared to that of trophic amino acids. The source amino acids, particularly Phe, which reflect inputs from marine phytoplankton fluctuated more than $\delta^{15}N_{Bulk}$ indicating that organic nitrogen inputs are not necessarily the primary control on $\delta^{15}N_{Bulk}$ patterns. There could also be variations in the composition of amino acids depending on the organic matter sources and variable degradation of amino acids. $\delta^{15}N_{Phe}$ variations across the region are likely a reflection of the nitrate ($\delta^{15}N$-NO3) source utilised and whether

bloom conditions led to a nitrate limited water column and therefore a ^{15}N enriched residual pool.

The most distinct of these changes are close to the coast of Norway where Atlantic water inflows with distinct $\delta^{15}N\text{-}NO_3$, near the shelf edge of Greenland where nitrate is limited and within a fjord where terrestrial inputs are significant. The total ^{15}N of amino acids ($\delta^{15}N_{THAA}$) was consistently enriched relative to $\delta^{15}N_{Bulk}$, this coupled with a TOC/TN plot (suggesting inorganic nitrogen is present) indicates the $\delta^{15}N_{Bulk}$ is influenced by inorganic nitrogen within the sediments that is known to dilute the ^{15}N signature.

Together, these analyses suggest that in nearshore areas, such as on the ESAS but also in fjord systems (such as the one examined here near Svalbard) an influx of terrestrial derived OM has a clear regulation on the OM preserved in the surface sediments. This also highlights that with future climate warming, having an impact on the drainage basins, causing increased river run off and coastal erosion, will lead to increased amounts of terrestrial OM being incorporated into the sediments in these areas. This will need to be a consideration for the burial of organic matter into the sediments and the quality of organic matter available to the benthos.

In contrast the major controls on the organic matter export through the water column and into the sediments in offshore regions, like those in the Barents Sea and Fram strait, seem to be mainly related to the relative position of the polar front and marginal ice zone. Most likely due to the enhanced productivity in these regions leading to more organic matter being transported to the sediments. This may need to be further considered for regions like the ESAS as they see declines in sea-ice which might impact the regions productivity and the quality of food supply to the benthos. It demonstrates that Arctic regions are a complex

intermix of marine (e.g. changes in productivity, loss of sea ice) and terrestrial (e.g. increased erosion and/or river discharge) processes that affect the biogeochemical and ecological functioning of the system.

Whilst this study only represents a snapshot of the current state of affairs in these regions it does mark a significant step forward in understanding a rapidly changing part of the Arctic which is becoming increasingly nutrient limited rather than light limited as sea ice extent and thickness declines. Further, we demonstrate that for current and future assessments of sedimentary organic matter, which will have implications for preservation of organic matter and quality of nutrients for the benthos, a compound specific isotope approach will be most suitable as baseline values vary across the region and $\delta^{15}N_{Bulk}$ measurements can lead to misinterpretations.

Collectively the investigation of these two distinct Arctic regions indicates that in order to properly manage the fragile ecosystems, each region needs to be considered on its own due to the unique setting each present and variable baseline we find even within each of these regions. We present a first attempt at applying a multi-proxy approach in trying to set the isoscape for both the bulk and molecular level ^{15}N isotopes that sets a reference point for future work across all regions of the Arctic in order to manage it into the future.

5.2 Limitations and future work

The results from both data chapters presented in this thesis provide new and interesting insights into firstly the interpretation of bulk isotope, elemental data and macromolecular compositions in two distinct Arctic regions. Secondly, a first look at amino acids (compositional and isotopic) within sediments and the novel data and information they can provide on baseline sources to the food web where there is a mix of marine and terrestrial inputs and how this approach can disentangle complications of using solely bulk methods. However, we do recognise that there are many lines of inquiry that were not within the scope or timeframe of the project but would have greatly improved interpretations of results and enabled more definite conclusions to be drawn. Some of these would benefit both regions whilst some are region specific due their unique settings.

Across the two regions the datasets would have benefitted from a full water column analysis at each station. This would ideally include nitrate concentrations to understand if the nutrient is limited and therefore make assumptions about the state of the isoscape. Measurements of $\delta^{15}N\text{-}NO_3$ and $\delta^{15}N\text{-}PN$ through the full depth of the water column would have made the interpretation of firstly, the baseline (source) amino acids clearer and supported any inferences made about the transport of particulates and their preservation in surface sediments. Alongside these a $\delta^{15}N_{AA}$ analysis of phytoplankton and generally particulate nitrogen, again a full depth profile, would have made source appointment (terrestrial vs marine) much more conclusive. We also acknowledge that as part of the NERC CAO ARISE project some of these parameters were being measured by other researchers, however at time of writing only limited samples were analysed and data available. Future

work collaborating with these scientists to combine our datasets would greatly improve our interpretations and similarly theirs.

Chapter 3 presented the ESAS as an area of distinct terrestrial to marine trends from the nearshore to the offshore regions, however due to our study being limited in access to purely marine surface sediments this meant that the terrestrial end-members were not fully defined. We would recommend that future work, associated with the novel datasets we present, aim to use the same analyses but on in-situ riverine organic matter, different horizons of terrestrial permafrost in each region and on Ice Complex Deposits (ICD's). This would enable the source of the terrestrial divergence in the nitrogen pool across the shelf to be isolated and would therefore help inform future policy depending on the origins of the difference. For example, if this was found to be from ICD's we could model the predicted erosion rates into the future and better understand how this might impact the food web and isoscape. Further to this, there is the possibility for radiocarbon analysis on the isolated amino acids in these sediments, this might give more information as to origins of the compounds as ICD's are known to have formed in the Plio-Pleistocene and would therefore have a much older radiocarbon age than that of in-situ riverine production or marine productivity. To the East of the shelf there is a known influx of Pacific origin water however without samples from this region it is hard to interpret whether variations in the offshore regions of the ESAS are solely a translocation of terrestrial material or some interference from isotopically different Pacific inputs. Finally, the Changing Arctic Ocean (CAO) programme had some researches from another project (CACOON) also focussing on the ESAS, in particular the Kolyma River outflow, future collaborations with this group would likely provide further insights into our data and subsequent interpretations.

Chapter 4 focussed on the Barents Sea and Fram Strait as areas known to be undergoing rapid change currently and into the future. As our sampling campaign was part of a wider collaboration with many projects (Changing Arctic Ocean) our station locations had to fit within the wider requirements. Ideally, we would have collected more samples across more stations together with terrestrial end-members from Norway, Greenland and Svalbard (riverine and glacial), which would have improved spatial resolution and likely made interpretations of organic matter origin more straightforward. As sampling in the Arctic is a time consuming and expensive enterprise we not only collected surface sediments but full sediment cores usually a minimum of 30cm in length. It was not within the scope of this project to utilise the full length of these cores but these present a unique opportunity to look at down core trends across the region. For example, to understand when Atlantic water began to encroach on the Arctic and how quickly this happened, which would help predict future change in the region and how this might impact primary productivity. They could also be used to look at down core trends in amino acid composition and $\delta^{15}N_{AA}$ which could better indicate degradation of organic matter and heterotrophic bacterial reworking within the sediments. Like the ESAS, there were project partners from the CAO also focussing on sediments in this region, the CHAOS (the changing Arctic Ocean seafloor) project looked at the impacts of the ice-edge on benthic ecosystems and nutrient cycling. It is to be expected that their work will be intrinsically linked to the datasets we present here and future work to combine the efforts of the two will benefit both projects. Finally, as part of the ARISE project other researchers have focussed on the water column, primary producers and higher trophic level organisms such as polar bears and seals. Combining these datasets together would provide a more comprehensive overview of the state of organic matter cycling in these regions and their

subsequent burial in sediments, which would help better inform policy decisions in the region for the future.

References

Armannsson, H. (ed.) (1999) Geochemistry of the Earth's Surface. Rotterdam: A.A.Balkema.

Arrigo, K. R. and van Dijken, G. L. (2015) 'Continued increases in Arctic Ocean primary production', Progress in Oceanography. Elsevier Ltd, 136, pp. 60–70. doi: 10.1016/j.pocean.2015.05.002.

Barton, B. Lenn, Yueng-Djern. Lique, C. (2018) 'Observed Atlantification of the Barents Sea Causes the Polar Front to Limit the Expansion of Winter Sea Ice', pp. 1849–1866. doi: 10.1175/JPO-D-18-0003.1.

Batista, F. C. et al. (2014) 'Compound specific amino acid δ15N in marine sediments: A new approach for studies of the marine nitrogen cycle', Geochimica et Cosmochimica Acta. Elsevier Ltd, 142, pp. 553–569. doi: 10.1016/j.gca.2014.08.002.

Bauch, D. et al. (2011) 'Progress in Oceanography Origin of freshwater and polynya water in the Arctic Ocean halocline in summer 2007', Progress in Oceanography. Elsevier Ltd, 91(4), pp. 482–495. doi: 10.1016/j.pocean.2011.07.017.

Bauch, H. A. et al. (2001) 'Chronology of the Holocene transgression at the North Siberian margin', pp. 125–139.

Bischoff, J. et al. (2016) 'Source, transport and fate of soil organic matter inferred from microbial biomarker lipids on the East Siberian Arctic Shelf', Biogeosciences, 13(17), pp. 4899–4914. doi: 10.5194/bg-13-4899-2016.

Bowes, R. E. and Thorp, J. H. (2015) 'Consequences of employing amino acid vs. bulk-tissue, stable isotope analysis: A laboratory trophic position experiment', Ecosphere, 6(1). doi: 10.1890/ES14-00423.1.

Brahney, J. et al. (2014) 'Separating the influences of diagenesis, productivity and anthropogenic nitrogen deposition on sedimentary δ15N variations', Organic Geochemistry. Elsevier Ltd, 75, pp. 140–150. doi: 10.1016/j.orggeochem.2014.07.003.

Brock, W. and Xepapadeas, A. (2017) 'Climate change policy under polar amplification', European Economic Review. Elsevier B.V., 99, pp. 93–112. doi: 10.1016/j.euroecorev.2017.06.008.

Bröder, L. et al. (2016) 'Fate of terrigenous organic matter across the Laptev Sea from the mouth of the Lena River to the deep sea of the Arctic interior', Biogeosciences, 13(17), pp. 5003–5019. doi: 10.5194/bg-13-5003-2016.

Bromke, M. A. (2013) 'Amino acid biosynthesis pathways in diatoms', Metabolites, 3(2), pp. 294–311. doi: 10.3390/metabo3020294.

Brüchert, V. et al. (2018) 'Carbon mineralization in Laptev and East Siberian sea shelf and slope sediment', Biogeosciences, pp. 471–490.

Buchanan, P. J. et al. (2022) 'Oceanographic and biogeochemical drivers cause divergent trends in the nitrogen isoscape in a changing Arctic Ocean', Ambio. Springer Netherlands, 51(2), pp. 383–397. doi: 10.1007/s13280-021-01635-6.

Burdige, D. J. and Martens, C. S. (1988) 'Biogeochemical cycling in an organic-rich coastal marine basin: 10. The role of amino acids in sedimentary carbon and nitrogen cycling', Geochimica et Cosmochimica Acta, 52(6), pp. 1571–1584. doi: 10.1016/0016-7037(88)90226-8.

Calleja, M. L. et al. (2013) 'Changes in compound specific δ15N amino acid signatures and d/l ratios in marine dissolved organic matter induced by heterotrophic bacterial reworking', Marine Chemistry. Elsevier B.V., 149, pp. 32–44. doi: 10.1016/j.marchem.2012.12.001.

Canuel, E. A. and Martens, C. S. (1996) 'Reactivity of recently deposited organic matter : near the sediment-water Degradation interface of lipid compounds', Geochemistry, Geophysics, Geosystems, 60(10), pp. 1793–1806.

Carmack, E. and Wassmann, P. (2006) 'Progress in Oceanography Food webs and physical – biological coupling on pan-Arctic shelves : Unifying concepts and comprehensive perspectives q', Progress in Oceanography, 71, pp. 446–477. doi: 10.1016/j.pocean.2006.10.004.

Carstens, D. et al. (2013) ‘Amino acid nitrogen isotopic composition patterns in lacustrine sedimenting matter’, Geochimica et Cosmochimica Acta. Elsevier Ltd, 121, pp. 328–338. doi: 10.1016/j.gca.2013.07.020.

Charette, M. A. et al. (2020) ‘The Transpolar Drift as a Source of Riverine and Shelf - Derived Trace Elements to the Central Arctic Ocean Journal of Geophysical Research : Oceans’, pp. 1–34. doi: 10.1029/2019JC015920.

Chikaraishi, Y. et al. (2007) ‘Metabolic control of nitrogen isotope composition of amino acids in macroalgae and gastropods: Implications for aquatic food web studies’, Marine Ecology Progress Series, 342(2003), pp. 85–90. doi: 10.3354/meps342085.

Chikaraishi, Y. et al. (2009) ‘Determination of aquatic food-web structure based on compound-specific nitrogen isotopic composition of amino acids’, Limnology and Oceanography: Methods, 7(11), pp. 740–750. doi: 10.4319/lom.2009.7.740.

Cowie, G. and Hedges, J. (1992) ‘Sources and reactivities of amino acids in a coastal marine environment’, Limnology and Oceanography, 37(4), pp. 703–724.

Dauwe, B. et al. (1999) ‘Linking diagenetic alteration of amino acids and bulk organic matter reactivity’, Limnology and Oceanography, 44(7), pp. 1809–1814. doi: 10.4319/lo.1999.44.7.1809.

Dauwe, B. and Middelburg, J. J. (1998) ‘Amino acids and hexosamines as indicators of organic matter degradation state in North Sea sediments’, Limnology and Oceanography, 43(5), pp. 782–798. doi: 10.4319/lo.1998.43.5.0782.

Dittmar, T. (2004) ‘Evidence for terrigenous dissolved organic nitrogen in the Arctic deep sea’, Limnology and Oceanography, 49(1), pp. 148–156. doi: 10.4319/lo.2004.49.1.0148.

Dittmar, T., Fitznar, H. P. and Kattner, G. (2001) ‘Origin and biogeochemical cycling of organic nitrogen in the eastern Arctic Ocean as evident from D-and L-amino acids’, Geochimica et Cosmochimica Acta, 65(22), pp. 4103–4114. Available at: http://linkinghub.elsevier.com/retrieve/pii/S0016703701006883.

Dittmar, T. and Kattner, G. (2003) 'The biogeochemistry of the river and shelf ecosystem of the Arctic Ocean: a review', Marine Chemistry, 83(3–4), pp. 103–120. doi: 10.1016/S0304-4203(03)00105-1.

Doğrul Selver, A. et al. (2015) 'Distributions of bacterial and archaeal membrane lipids in surface sediments reflect differences in input and loss of terrestrial organic carbon along a cross-shelf Arctic transect', Organic Geochemistry, 83–84, pp. 16–26. doi: 10.1016/j.orggeochem.2015.01.005.

van Dongen, B. E. et al. (2008) 'Contrasting lipid biomarker composition of terrestial organic matter exported from across the Eurasian Arctic by the five great Russian Arctic rivers', Global Biogeochemical Cycles, 22(1), pp. 1–14. doi: 10.1029/2007GB002974.

Dongen, B. E. Van et al. (2000) 'Biomarkers in upper Holocene Eastern North Sea and Wadden Sea sediments', 31, pp. 1533–1543.

Dudarev, O. V. et al. (2006) 'Deposition settings on the continental shelf of the East Siberian Sea', Doklady Earth Sciences, 409(2), pp. 1000–1005. doi: 10.1134/S1028334X06060389.

European Commission (2016) 'COMMUNICATION FROM THE COMMISSION TO THE EUROPEAN PARLIAMENT AND THE COUNCIL'. Brussels. Available at: http://eur-lex.europa.eu/legal-content/EN/TXT/PDF/?uri=CELEX:52016DC0110&from=EN.

Faust, J. C. et al. (2020) 'Does Arctic warming reduce preservation of organic matter in Barents Sea sediments?: Barents Sea surface sediment composition', Philosophical Transactions of the Royal Society A: Mathematical, Physical and Engineering Sciences, 378(2181). doi: 10.1098/rsta.2019.0364.

Feng, X. et al. (2013) 'Differential mobilization of terrestrial carbon pools in Eurasian Arctic river basins', Proceedings of the National Academy of Sciences, 110(35), pp. 14168–14173. doi: 10.1073/pnas.1307031110.

Feng, X. et al. (2015) 'Multi-molecular tracers of terrestrial carbon transfer across the pan-Arctic: Comparison of hydrolyzable components with plant wax lipids and lignin phenols', Biogeosciences, 12(15), pp. 4841–4860. doi: 10.5194/bg-12-4841-2015.

Freitas, F. S. et al. (2020) 'Benthic-pelagic coupling in the Barents Sea: an integrated data-model framework', Philosophical Transactions of the Royal Society A: Mathematical, Physical and Engineering Sciences, 378(2181), p. 20190359. doi: 10.1098/rsta.2019.0359.

Gaye, B. et al. (2007) 'Particulate matter fluxes in the southern and central Kara Sea compared to sediments: Bulk fluxes, amino acids, stable carbon and nitrogen isotopes, sterols and fatty acids', Continental Shelf Research, 27(20), pp. 2570–2594. doi: 10.1016/j.csr.2007.07.003.

Granger, J. et al. (2013) 'The proportion of remineralized nitrate on the ice-covered eastern Bering Sea shelf evidenced from the oxygen isotope ratio of nitrate', Global Biogeochemical Cycles, 27(3), pp. 962–971. doi: 10.1002/gbc.20075.

Granger, J. et al. (2018) 'On the Properties of the Arctic Halocline and Deep Water Masses of the Canada Basin from Nitrate Isotope Ratios', Journal of Geophysical Research: Oceans, 123(8), pp. 5443–5458. doi: 10.1029/2018JC014110.

Grosse, J. et al. (2021) 'Summertime Amino Acid and Carbohydrate Patterns in Particulate and Dissolved Organic Carbon Across Fram Strait', Frontiers in Marine Science, 8(July). doi: 10.3389/fmars.2021.684675.

Guglielmi, G. (2018) Polar bears are wasting away in a changing climate, Nature News. Available at: http://www.nature.com/articles/d41586-018-01501-8 (Accessed: 25 April 2018).

Guo, L. et al. (2004) 'Characterization of Siberian Arctic coastal sediments: Implications for terrestrial organic carbon export', Global Biogeochemical Cycles, 18(1). doi: 10.1029/2003gb002087.

Guo, L., Ping, C. L. and Macdonald, R. W. (2007) 'Mobilization pathways of organic carbon from permafrost to arctic rivers in a changing climate', Geophysical Research Letters, 34(13), p. n/a-n/a. doi: 10.1029/2007GL030689.

Gustafsson, Ö. et al. (2000) 'Functional separation of colloids and gravitoids in surface waters based on differential settling velocity: Coupled cross-flow filtration-split flow thin-cell fractionation (CFF-SPLITT)', Limnology and Oceanography, 45(8), pp. 1731–1742. doi: 10.4319/lo.2000.45.8.1731.

H.- O. Pörtner, D.C. Roberts, V. Masson-Delmotte, P. Zhai, M. Tignor, E. Poloczanska, K. Mintenbeck, A. Alegría, M. Nicolai, A. Okem, J. Petzold, B. Rama, N. M. W. (2019) IPCC Special Report on the Ocean and Cryosphere in a Changing Climate: Technical Summary.

H. O. Pörtner, D.C. Roberts, M. Tignor, E.S. Poloczanska, K. Mintenbeck, A. Alegría, M. Craig, S. Langsdorf, S. Löschke, V. Möller, A. Okem, B. R. (eds. . (2022) Climate Change 2022: Impacts, Adaptation, and Vulnerability. Working Group II Contribution to the IPCC Sixth Assessment Report.

Harris, S. A. (2010) Global warming. Sciyo. Available at: http://cdn.intechweb.org/pdfs/12169.pdf.

Hebbeln, D., Wefer, G. and Geowissenschaften, U. B. (1991) 'Effects of ice coverage and ice-rafted material on sedimentation in the Fram Strait Jfl-', 350(April), pp. 80–81.

Hedges, J. I. and Oades, J. M. (1997) 'Comparative organic geochemistries of soils and marine sediments', Organic Geochemistry, 27(7).

Henrichs, S. M. (1992) 'Early diagenesis of organic matter in marine sediments: progress and perplexity', *Marine Chemistry*, 39(1–3), pp. 119–149. doi: 10.1016/0304-4203(92)90098-U.

Holmes, R. M. et al. (2012) 'Seasonal and Annual Fluxes of Nutrients and Organic Matter from Large Rivers to the Arctic Ocean and Surrounding Seas', Estuaries and Coasts, 35(2), pp. 369–382. doi: 10.1007/s12237-011-9386-6.

Hoque, M. A. and Pollard, W. H. (2016) 'Stability of permafrost dominated coastal cliffs in the Arctic', Polar Science. Elsevier B.V. and NIPR, 10(1), pp. 79–88. doi: 10.1016/j.polar.2015.10.004.

House of Lords (2014) Responding to a changing Arctic.

Hutchins, D. A. and Capone, D. G. (2022) 'The marine nitrogen cycle: new developments and global change', *Nature Reviews Microbiology*. Springer US, 20(7), pp. 401–414. doi: 10.1038/s41579-022-00687-z.

IPCC (2014) Climate Change 2013, the Fifth Assessment Report.

Jakobsson, M. et al. (2008) ‘An improved bathymetric portrayal of the Arctic Ocean : Implications for ocean modeling and geological , geophysical and oceanographic analyses’, 35, pp. 1–5. doi: 10.1029/2008GL033520.

Karlsson, E. S. et al. (2011) ‘Carbon isotopes and lipid biomarker investigation of sources, transport and degradation of terrestrial organic matter in the Buor-Khaya Bay, SE Laptev Sea’, Biogeosciences, 8(7), pp. 1865–1879. doi: 10.5194/bg-8-1865-2011.

Karlsson, E. S. et al. (2015) ‘Contrasting regimes for organic matter degradation in the East Siberian Sea and the Laptev Sea assessed through microbial incubations and molecular markers’, Marine Chemistry. Elsevier B.V., 170, pp. 11–22. doi: 10.1016/j.marchem.2014.12.005.

Kattsov, V. M. et al. (2007) ‘Simulation and Projection of Arctic Freshwater Budget Components by the IPCC AR4 Global Climate Models’, Journal of Hydrometeorology, 8(3), pp. 571–589. doi: 10.1175/JHM575.1.

Knies, J. (2005) ‘Climate-induced changes in sedimentary regimes for organic matter supply on the continental shelf off northern Norway’, Geochimica et Cosmochimica Acta, 69(19), pp. 4631–4647. doi: 10.1016/j.gca.2005.05.014.

Knies, J. and Martinez, P. (2009) ‘Organic matter sedimentation in the western Barents Sea region : Terrestrial and marine contribution based on isotopic composition and organic nitrogen content’, (1), pp. 79–89.

Koziorowska, K., Kuliński, K. and Pempkowiak, J. (2016) ‘Sedimentary organic matter in two Spitsbergen fjords: Terrestrial and marine contributions based on carbon and nitrogen contents and stable isotopes composition’, Continental Shelf Research, 113, pp. 38–46. doi: 10.1016/j.csr.2015.11.010.

Kumar, V. et al. (2016) ‘Evidence of Anomalously Low δ13C of Marine Organic Matter in an Arctic Fjord’, Scientific Reports. Nature Publishing Group, 6(June), pp. 1–9. doi: 10.1038/srep36192.

Lehmann, M. F. et al. (2002) ‘Preservation of organic matter and alteration of its carbon and nitrogen isotope composition during simulated and in situ early sedimentary diagenesis’,

Geochimica et Cosmochimica Acta, 66(20), pp. 3573–3584. doi: 10.1016/S0016-7037(02)00968-7.

Lemke, P. and Jacobi, H.-W. (2012) Arctic Climate Change. doi: 10.1007/978-94-007-2027-5.

Lewis, K. M., Dijken, G. L. Van and Arrigo, K. R. (2020) 'Changes in phytoplankton concentration now drive increased Arctic Ocean primary production', 202(July), pp. 198–202.

Lind, S., Ingvaldsen, R. B. and Furevik, T. (2018) 'Sea linked to declining sea-ice import', Nature Climate Change. Springer US, 8(634). doi: 10.1038/s41558-018-0205-y.

Martens, J. et al. (2021) 'CASCADE – The Circum-Arctic Sediment CArbon DatabasE', pp. 2561–2572.

Masson-Delmotte, V., P. Zhai, A. Pirani, S. L., Connors, C. Péan, S. Berger, N. Caud, Y. Chen, L. Goldfarb, M.I. Gomis, M. Huang, K. Leitzell, E. Lonnoy, J.B.R. Matthews, T. K. and Maycock, T. Waterfield, O. Yelekçi, R. Yu, and B. Z. (2021) IPCC, 2021: Summary for Policymakers. In: Climate Change 2021: The Physical Science Basis. Contribution of Working Group I to the Sixth Assessment Report of the Intergovernmental Panel on Climate Change.

McCarthy, M. D. et al. (2007) 'Amino acid nitrogen isotopic fractionation patterns as indicators of heterotrophy in plankton, particulate, and dissolved organic matter', Geochimica et Cosmochimica Acta, 71(19), pp. 4727–4744. doi: 10.1016/j.gca.2007.06.061.

McClelland, J. W. and Montoya, J. P. (2002) 'Trophic Relationships and the Nitrogen Isotopic Composition of Amino Acids in Plankton', Ecology, 83(8), pp. 2173–2180. doi: 10.1890/0012-9658(2002)083[2173:TRATNI]2.0.CO;2.

McMahon, K. W. and McCarthy, M. D. (2016) 'Embracing variability in amino acid δ15N fractionation: Mechanisms, implications, and applications for trophic ecology', Ecosphere, 7(12), pp. 1–26. doi: 10.1002/ecs2.1511.

Meredith, M., M. Sommerkorn, S. Cassotta, C. Derksen, A. Ekaykin, A. Hollowed, G. Kofinas, A. Mackintosh, J. Melbourne-Thomas, M.M.C. Muelbert, G. Ottersen, H. Pritchard, and E. A. G. S. (2019) Polar Regions. In: IPCC Special Report on the Ocean and Cryosphere in a Changing Climatee. doi: https://doi.org/10.1017/9781009157964.005.

Nagel, B. et al. (2009) ‘Stable carbon and nitrogen isotopes as indicators for organic matter sources in the Kara Sea’, Marine Geology. Elsevier B.V., 266(1–4), pp. 42–51. doi: 10.1016/j.margeo.2009.07.010.

Natalia Shakhova et al. (2010) ‘Extensive Methane Venting to the Atmosphere from Sediments of the East Siberian Arctic Shelf’, Science, 327(13), pp. 1246–1250. doi: 10.1126/science.1182221.

Oliva, M. and Fritz, M. (2018) ‘Permafrost degradation on a warmer Earth: Challenges and perspectives’, Current Opinion in Environmental Science & Health. Elsevier Ltd, 5, pp. 14–18. doi: 10.1016/j.coesh.2018.03.007.

Onarheim, I. H. et al. (2014) ‘Tellus A : Dynamic Meteorology and Oceanography Loss of sea ice during winter north of Svalbard’, 0870. doi: 10.3402/tellusa.v66.23933.

Oziel, L. et al. (2020) ‘Faster Atlantic currents drive poleward expansion of temperate phytoplankton in the Arctic Ocean’, Nature Communications. Springer US, (2020), pp. 1–8. doi: 10.1038/s41467-020-15485-5.

Pajares, S. and Ramos, R. (2019) ‘Processes and Microorganisms Involved in the Marine Nitrogen Cycle: Knowledge and Gaps’, *Frontiers in Marine Science*, 6(November). doi: 10.3389/fmars.2019.00739.

Paquette, R. et al. (1985) ‘The East Greenland Polar Front in Autumn’, 90, pp. 4866–4882.

Paytan, A. and McLaughlin, K. (2007) ‘The oceanic phosphorus cycle’, Chemical Reviews, 107(2), pp. 563–576. doi: 10.1021/cr0503613.

Perovich, D. K. and Richter-Menge, J. A. (2009) ‘Loss of Sea Ice in the Arctic’, Annual Review of Marine Science, 1(1), pp. 417–441. doi: 10.1146/annurev.marine.010908.163805.

Peterson, B. et al. (2002) ‘Increasing river dischange to the Arctic Ocean’, Science, 298(13), pp. 2171–2173. doi: 10.1126/science.1077445.

Rey, F. (2012) ‘Declining silicate concentrations in the Norwegian and Barents Seas’, ICES Journal of Marine Science, 69(2), pp. 208–212. doi: 10.1038/278097a0.

Robinson, R. S. *et al.* (2012) ‘A review of nitrogen isotopic alteration in marine sediments’, *Paleoceanography*, 27(4). doi: 10.1029/2012PA002321.

Rudy, A. C. . et al. (2017) ‘Accelerating Thermokarst Transforms Ice-Cored Terrain Triggering a Downstream Cascade to the Ocean’, pp. 80–87. doi: 10.1002/2017GL074912.

Ruppel, C. D. and Kessler, J. D. (2017) ‘The interaction of climate change and methane hydrates’, pp. 126–168. doi: 10.1002/2016RG000534.

Sánchez-García, L. et al. (2011a) ‘Inventories and behavior of particulate organic carbon in the Laptev and East Siberian seas’, Global Biogeochemical Cycles, 25(2), pp. 1–13. doi: 10.1029/2010GB003862.

Sánchez-García, L. et al. (2011b) ‘Inventories and behavior of particulate organic carbon in the Laptev and East Siberian seas’, Global Biogeochemical Cycles, 25(2), p. n/a-n/a. doi: 10.1029/2010GB003862.

Sanchez-Vidal, A. et al. (2015) ‘Particle sources and downward fluxes in the eastern Fram strait under the influence of the west Spitsbergen current’, Deep-Sea Research Part I: Oceanographic Research Papers. Elsevier, 103, pp. 49–63. doi: 10.1016/j.dsr.2015.06.002.

Savelieva, N. I. et al. (2000) ‘A climate shift in seasonal values of meteorological and hydrological parameters for Northeastern Asia’, Progress in Oceanography, 47(2–4), pp. 279–297. doi: 10.1016/S0079-6611(00)00039-2.

Schubert, C. J. and Calvert, S. E. (2001) ‘Nitrogen and carbon isotopic composition of marine and terrestrial organic matter in Arctic Ocean sediments: Implications for nutrient utilization and organic matter composition’, Deep-Sea Research Part I: Oceanographic Research Papers, 48(3), pp. 789–810. doi: 10.1016/S0967-0637(00)00069-8.

Semiletov, I. (2005) ‘The East Siberian Sea as a transition zone between Pacific-derived waters and Arctic shelf waters’, Geophysical Research Letters, 32(10), p. L10614. doi: 10.1029/2005GL022490.

Semiletov, I. et al. (2016) ‘Acidification of East Siberian Arctic Shelf waters through addition of freshwater and terrestrial carbon’, Nature Geoscience, 9(5), pp. 361–365. doi: 10.1038/ngeo2695.

Semiletov, I. and Gustafsson, Ö. (2009) ‘East Siberian shelf study alleviates scarcity of observations’, Eos, 90(17), pp. 145–146. doi: 10.1029/2009eo170001.

Semiletov, I. P. et al. (1998) 'The dispersion of siberian river flows into coastal waters: meteorological, hydrological and hydrochemical aspects.', in Lewis, E. L. et al. (eds) The freshwater budget of the Arctic Ocean. Tallinn, Estonia: Springer Science+Business Media Dordrecht, pp. 323–366. doi: 10.1007/978-94-011-4132-1.

Semiletov, I. P. et al. (2011) 'Carbon transport by the Lena River from its headwaters to the Arctic Ocean, with emphasis on fluvial input of terrestrial particulate organic carbon vs. carbon transport by coastal erosion', Biogeosciences, 8(9), pp. 2407–2426. doi: 10.5194/bg-8-2407-2011.

Sigman, D. M. and Casciotti, K. L. (2001) 'Nitrogen Isotopes in the Ocean', *Encyclopedia of Ocean Sciences*, (1997), pp. 40–54. doi: 10.1016/B978-012374473-9.00632-9.

Sigman, D. M. and States, U. (2019) Nitrogen Isotopes in the Ocean ☆. 3rd edn, Encyclopedia of Ocean Sciences, 3rd Edition. 3rd edn. Elsevier Ltd. doi: 10.1016/B978-0-12-409548-9.11605-7.

Somes, C. J. et al. (2010) 'Simulating the global distribution of nitrogen isotopes in the ocean', 24, pp. 1–16. doi: 10.1029/2009GB003767.

Sparkes, R. B. et al. (2016) 'Macromolecular composition of terrestrial and marine organic matter in sediments across the East Siberian Arctic Shelf', Cryosphere, 10(5), pp. 2485–2500. doi: 10.5194/tc-10-2485-2016.

Sparkes, R. B. et al. (2018) 'Carbonaceous material export from Siberian permafrost tracked across the Arctic Shelf using Raman spectroscopy', Cryosphere, 12(10), pp. 3293–3309. doi: 10.5194/tc-12-3293-2018.

Stein, R. and MacDonald, R. W. (2004) The Organic Carbon Cycle in the Arctic Ocean. Heidelberg: Springer-Verlag Berlin Heidelberg.

Stendel, M. and Christensen, J. H. (2002) 'Impact of global warming on permafrost conditions in a coupled GCM', Geophysical Research Letters, 29(13), pp. 5–8. doi: 10.1029/2001GL014345.

Stevenson, M. A. and Abbott, G. D. (2019) 'Exploring the composition of macromolecular organic matter in Arctic Ocean sediments under a changing sea ice gradient', Journal of

Analytical and Applied Pyrolysis. Elsevier, (February), pp. 1–10. doi: 10.1016/j.jaap.2019.02.006.

Svoboda, M. (2017) Media coverage of climate change, YALE Climate Connections. Available at: https://www.yaleclimateconnections.org/2017/03/media-coverage-of-climate-change-pt-1/ (Accessed: 25 April 2018).

Tarnocai, C. et al. (2009) 'Soil organic carbon pools in the northern circumpolar permafrost region', Global Biogeochemical Cycles, 23(2), p. n/a-n/a. doi: 10.1029/2008GB003327.

Tartu, S. et al. (2017) 'Multiple-stressor effects in an apex predator: Combined influence of pollutants and sea ice decline on lipid metabolism in polar bears', Nature Scientific Reports, 7(1), pp. 1–12. doi: 10.1038/s41598-017-16820-5.

Terhaar, J. et al. (2021) 'Around one third of current Arctic Ocean primary production sustained by rivers and coastal erosion', Nature Communications. Springer US, 12(1), pp. 1–10. doi: 10.1038/s41467-020-20470-z.

Tesdal, J. E., Galbraith, E. D. and Kienast, M. (2013) 'Nitrogen isotopes in bulk marine sediment: Linking seafloor observations with subseafloor records', Biogeosciences, 10(1), pp. 101–118. doi: 10.5194/bg-10-101-2013.

Tesi, T. et al. (2014) 'Composition and fate of terrigenous organic matter along the Arctic land-ocean continuum in East Siberia: Insights from biomarkers and carbon isotopes', Geochimica et Cosmochimica Acta, 133, pp. 235–256. doi: 10.1016/j.gca.2014.02.045.

Tesi, T. et al. (2016) 'Matrix association effects on hydrodynamic sorting and degradation of terrestrial organic matter during cross-shelf transport in the Laptev and East Siberian shelf seas', Journal of Geophysical Research: Biogeosciences, 121(3), pp. 731–752. doi: 10.1002/2015JG003067.

Tuerena, R. E. et al. (2021) 'An Arctic Strait of Two Halves: The Changing Dynamics of Nutrient Uptake and Limitation Across the Fram Strait', Global Biogeochemical Cycles, 35(9), pp. 1–20. doi: 10.1029/2021GB006961.

Våge, K. et al. (2018) 'Ocean convection linked to the recent ice edge retreat along east Greenland', Nature Communications. Springer US. doi: 10.1038/s41467-018-03468-6.

Vega, C. De et al. (2021) ‘Arctic seals as tracers of environmental and ecological change’, (2020), pp. 24–32. doi: 10.1002/lol2.10176.

Vonk, J. E. et al. (2012a) ‘Activation of old carbon by erosion of coastal and subsea permafrost in Arctic Siberia’, Nature, 489(7414), pp. 137–140. doi: 10.1038/nature11392.

Vonk, J. E. et al. (2012b) ‘Activation of old carbon by erosion of coastal and subsea permafrost in Arctic Siberia’, Nature, 489(7414), pp. 137–140. doi: 10.1038/nature11392.

Walsh, J. E. (2014) ‘Intensified warming of the Arctic: Causes and impacts on middle latitudes’, Global and Planetary Change. Elsevier B.V., 117, pp. 52–63. doi: 10.1016/j.gloplacha.2014.03.003.

Ward, J. P. J. et al. (2022) ‘Stable silicon isotopes uncover a mineralogical control on the benthic silicon cycle in the Arctic Barents Sea’, Geochimica et Cosmochimica Acta, 329, pp. 206–230. doi: 10.1016/j.gca.2022.05.005.

Webb, E. C. et al. (2016) ‘Compound-specific amino acid isotopic proxies for distinguishing between terrestrial and aquatic resource consumption’, Archaeological and Anthropological Sciences. Archaeological and Anthropological Sciences, pp. 1–18. doi: 10.1007/s12520-015-0309-5.

Weingartner, T. J. and Danielson, S. (1999) ‘The Siberian Coastal Current: A wind- and buoyancy-forced Arctic coastal current’, Journal of Geophysical Research, 104, pp. 697–713.

West, J. B. et al. (2010) ‘Isoscapes: Understanding movement, pattern, and process on earth through isotope mapping’, Isoscapes: Understanding Movement, Pattern, and Process on Earth Through Isotope Mapping, pp. 1–487. doi: 10.1007/978-90-481-3354-3.

Yang, D. et al. (2002) ‘Siberian Lena River hydrologic regime and recent change’, Journal of Geophysical Research Atmospheres, 107(23), pp. 1–10. doi: 10.1029/2002JD002542.

Zimov, S. A., Schuur, E. A. G. and Chapin, F. S. (2006) ‘Permafrost and the Global Carbon Budget’, Science, 312(June), pp. 1612–1613. doi: 10.1126/science.1128908.

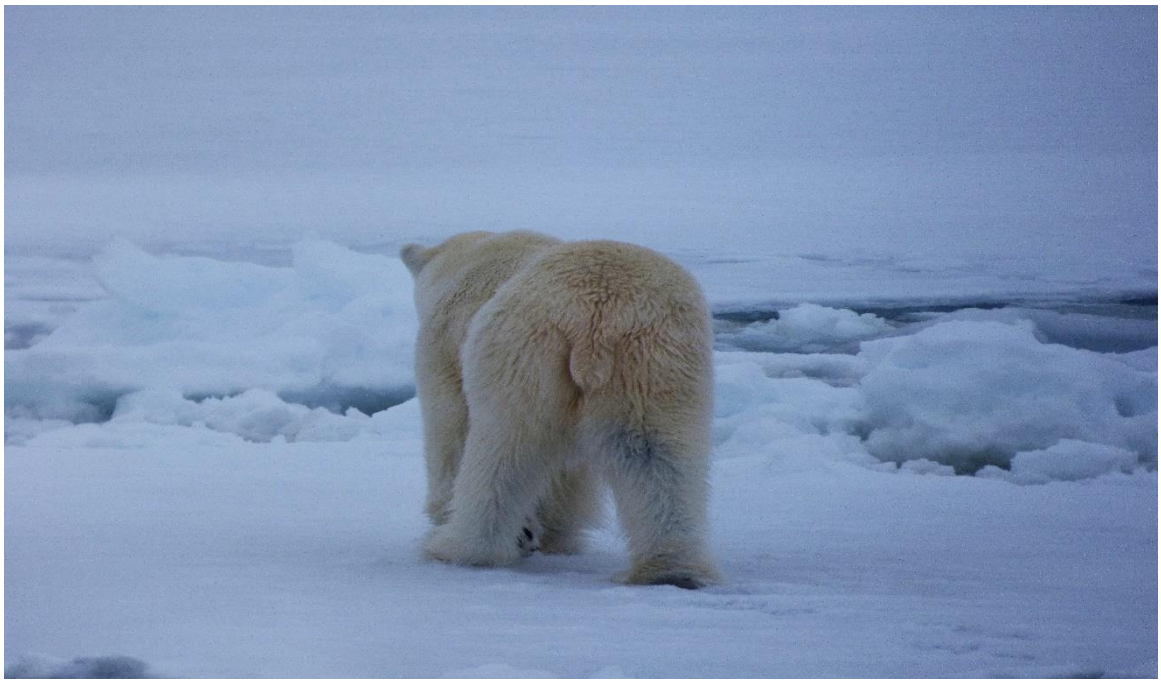

Photo taken by author of male polar bear on ice floe in the Fram Strait, May 2018

Appendix 1

Supporting information for Chapter 3: Novel amino acid compositional and $\delta^{15}N$ sedimentary analyses provide insights into contrasting biogeochemical regions across the East Siberian Arctic Shelf (ESAS)

ESAS: Sampling station map and list with latitude and longitude

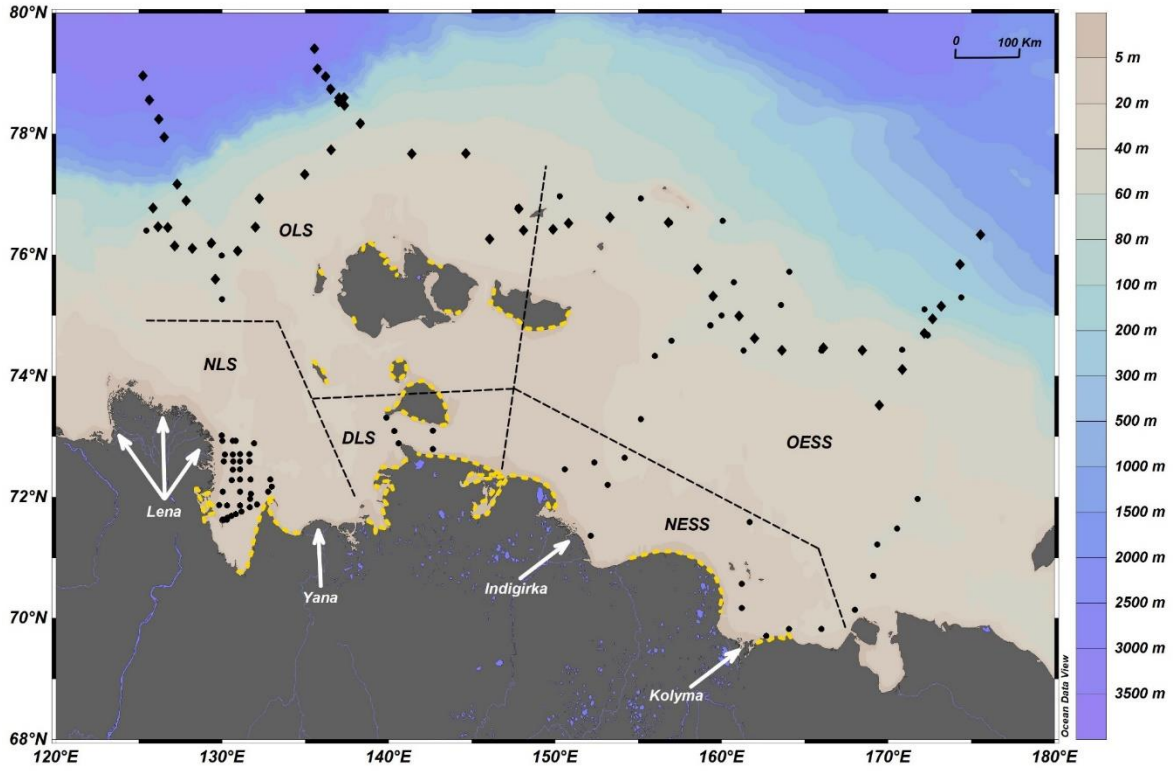

Figure A1.1 Map of the East Siberian Arctic Shelf (ESAS) showing locations of sediment samples from the ISSS-08 cruise (circles) and SWERUS-C3 cruise (diamonds) used in this study. Major river outflows are indicated by white arrows and areas of enhanced coastal erosion (>1my^{-1}, Lantuit et al., 2011) are shown in yellow. Regions of the ESAS referred to in this study are shown by the dashed black line (NLS: nearshore Laptev Sea; OLS: offshore Laptev Sea; DLS: Dmitry Laptev Strait; NESS: nearshore East Siberian Sea; OESS: offshore East Siberian Sea). Bathymetry of the shelf, slope and Arctic Ocean are shown in the colour bar (Ocean Data View, 2021)

ISSS-08 Sampling stations

Table A1.1 ESAS ISSS-08 sampling locations

Sample	Latitude	Longitude	Bottom depth (m)
Nearshore Laptev Sea (NLS)			
TB-17	72.29	132.92	21
TB-18	72.17	133.00	16
TB-19	72.09	132.78	14
TB-22	71.88	132.11	15
TB-23	71.83	131.67	20
TB-24	71.76	131.17	16
TB-25	71.72	130.83	13
TB-26	71.69	130.58	13
TB-27	71.66	130.33	11
TB-28	71.62	130.04	5
TB-30	71.87	129.83	5
TB-31	71.86	130.32	12
TB-32	71.86	131.09	12
TB-33	72.09	131.09	15
TB-34	72.29	131.09	16
TB-35	72.46	131.09	17
TB-36	72.59	131.10	17
TB-37	72.71	131.09	19
TB-38	72.93	130.84	20
TB-39	72.93	130.66	20
TB-40	72.93	130.03	6
TB-43	72.89	131.93	22
TB-44	72.71	131.66	19
TB-45	72.70	130.66	15
TB-46	72.70	130.18	6
TB-48	72.59	130.12	7
TB-49	72.59	130.68	14
TB-50	72.59	131.66	18
TB-52	72.45	130.67	18
TB-54	72.28	130.59	10
TB-55	72.29	131.72	17
TB-56	72.10	131.72	15
TB-57	72.00	131.77	10
TB-59	72.09	130.06	11

Sample	Latitude	Longitude	Bottom depth (m)
Nearshore Laptev Sea (NLS) continued			
YS-9	73.37	130.00	23
YS-10	73.18	130.00	20
YS-11	73.02	129.99	11
YS-12B	71.92	132.39	10
YS-13	71.97	131.70	19
YS-14	71.63	130.05	7
YS-15	71.63	130.05	11
YS-16	71.63	130.32	11
YS-17	71.63	130.19	10
YS-18	73.03	133.00	15
YS-19	73.04	133.46	27

ISSS-08 Sampling stations continued

Sample	Latitude	Longitude	Bottom depth (m)
Offshore Laptev Sea (OLS)			
YS-4	75.99	129.98	50
YS-5	75.27	130.02	43
YS-131	76.4	125.47	50
Dmitry Laptev Strait (DLS)			
YS-20	73.31	139.89	8
YS-21	73.09	140.35	15
YS-22	72.88	140.63	20
YS-22B	72.89	140.62	15
YS-23	72.79	142.67	10
YS-24	73.05	142.67	15
YS-25	73.14	142.67	10
Nearshore East Siberian Sea (NLS)			
YS-28	72.65	154.19	28
YS-36	69.82	166	32
YS-26	72.46	150.6	1
YS-27	72.57	152.37	18
YS-29	72.2	153.17	18
YS-30	71.36	152.15	9
YS-32	70.57	161.22	9
YS-33	70.17	161.22	8
YS-34B	69.71	162.69	10
YS-35	69.82	164.06	31

Sample	Latitude	Longitude	Bottom depth (m)
Offshore East Siberian Sea (OESS)			
YS-31	71.59	161.69	20
YS-37	70.14	168.01	42
YS-38	70.70	169.13	36
YS-39	71.22	169.37	44
YS-40	71.48	170.55	49
YS-41	71.97	171.79	43
YS-86	75.30	174.40	200
YS-88	75.10	172.19	142
YS-90	74.67	172.39	63
YS-91	74.43	170.85	56
YS-93	74.42	166.00	51
YS-95	74.42	161.34	45
YS-98	75.55	160.75	48
YS-99	75.17	163.59	50
YS-100	75.72	164.08	58
YS-102	76.56	160.07	69
YS-104	76.93	155.17	57
YS-106	76.97	150.29	43
YS-111	75.00	160.01	46
YS-112	74.83	159.33	42
YS-116	74.58	157.00	36
YS-118	74.33	156.01	28
YS-120	73.29	155.17	33

SWERUS-C3 Sampling Stations

Table A1.2 ESAS SWERUS-C3 sampling locations

Sample	Latitude	Longitude	Bottom depth (m)
SWERUS-C3			
SW-1	78.950	125.232	3120
SW-2	78.581	125.607	2900
SW-3	78.238	126.150	2601
SW-4	77.938	126.518	2186
SW-6	77.150	127.352	92
SW-13	76.777	125.830	74
SW-14	76.894	127.798	64
SW-18	76.399	125.460	52
SW-19	76.456	126.211	51
SW-20	76.454	126.742	52
SW-21	76.126	127.190	46
SW-22	76.108	128.241	48
SW-23	76.171	129.333	56
SW-24	75.599	129.558	46
SW-25	76.077	130.916	53
SW-26	76.473	132.044	52
SW-27	76.941	132.229	44
SW-28	77.342	135.007	49
SW-29	77.753	136.545	57
SW-30	78.182	138.355	69
SW-31	79.396	135.497	3056
SW-32	79.093	135.760	2540
SW-33	78.927	136.178	2264
SW-34	78.758	136.501	1880
SW-35	78.600	137.061	541
SW-36	78.581	137.338	360
SW-37	78.521	137.170	205
SW-38	78.481	137.274	118
SW-39	77.681	141.370	45
SW-40	77.681	144.690	47

Sample	Latitude	Longitude	Bottom depth (m)
SWERUS-C3 continued			
SW-43	76.78	147.79	42
SW-44	76.27	146.03	43
SW-45	76.42	148.12	40
SW-46	76.40	149.88	40
SW-47	76.52	150.81	41
SW-48	76.62	153.37	40
SW-49	76.53	156.92	47
SW-50	75.76	158.53	44
SW-51	75.30	159.48	39
SW-52	75.00	161.03	46
SW-55	74.84	159.33	-50
SW-56	74.63	161.95	48
SW-57	74.42	163.69	52
SW-58	74.44	166.05	54
SW-59	74.43	168.49	54
SW-60	73.52	169.46	43
SW-61	74.11	170.90	51
SW-63	74.68	172.37	64
SW-64	74.94	172.69	120
SW-65	75.16	173.19	170
SW-66	75.84	174.41	239
SW-67	76.33	175.58	468

ESAS Dataset links

Elemental, bulk isotope, pyrolysis and amino acids data sheets:

Title of spreadsheet	**Private link to access**	**Brief Description**
ESAS elemental and bulk isotope data	https://figshare.com/s/b3677af5e5f662db58ff	ESAS elemental data, bulk isotopic data and supplementary data from previous studies
ESAS Pyrolysis data	https://figshare.com/s/65f72e9b5dcb0d0ea049	ESAS macromolecular phenol to pyridine ratio dataset combined with previous study (Sparkes et al., 2016)
ESAS amino acid data and associated indices	https://figshare.com/s/6bb82c7be3d12d536fa4	ESAS amino acid composition data, individual amino acid nitrogen isotope data, degradation index and EV proxy for heterotrophic reworking.

ESAS Rmarkdown scripts

Link to full collection of scripts for ESAS Appendix: https://figshare.com/s/af9a2bdf5f67cd1f53c4

Individual links to Rmarkdown scripts and associated .csv files.

Title of document	Private link to access	Brief description
15N of proline	https://figshare.com/s/1192c0e63fa801196b06	Rmarkdown script and associated csv.file for the statistical analysis and plots of ^{15}N of proline in surface sediments across the ESAS.
15NAA_plots_stats	https://figshare.com/s/494800b10949ff0b06b1	Rmarkdown script and associated csv.file for the statistical analysis and plots of total hyrolysable amino acids ^{15}N in surface sediments across the ESAS.
AA_molper_analysis	https://figshare.com/s/d9ea29693fa9184aa5a0	Rmarkdown script and associated csv.file for the statistical analysis and plots of amino acids molar percentage in surface sediments across the ESAS.
AA_molper_ANOVA	https://figshare.com/s/76a20fbc5c47eb375324	Rmarkdown script and associated csv.file for the statistical ANOVA and plots of amino acids molar percentage in surface sediments across the ESAS.
Bulk13C	https://figshare.com/s/aed90a6553c8b7a81c19	Rmarkdown script and associated csv.file for the statistical analysis and plots of Bulk ^{13}C in surface sediments across the ESAS.
Bulk15N	https://figshare.com/s/f9972d7151396d13f69b	Rmarkdown script and associated csv.file for the statistical analysis

		and plots Bulk ^{15}N in surface sediments across the ESAS.
C/N Ratio	https://figshare.com/s/4e1fba880a63041b3777	Rmarkdown script and associated csv.file for the statistical analysis and plots of the C/N ratio in surface sediments across the ESAS.
Degradation Index	https://figshare.com/s/7892fb3ed078ee99747c	Rmarkdown script and associated csv.file for the statistical analysis and plots of the degradation index (DI) in surface sediments across the ESAS.
∑V Index	https://figshare.com/s/617b3cba43ad29917944	Rmarkdown script and associated csv.file for the statistical analysis and plots of the ∑V Index (heterotrophic reworking index) in surface sediments across the ESAS.
AA_molper PCA and Heatmap	https://figshare.com/s/55cfed74945af2984897	Rmarkdown script and associated csv.file for the statistical analysis and plots of amino acids molar percentage in surface sediments across the ESAS to produce a PCA and correlation heat map.
AA_molper_plots	https://figshare.com/s/710ed4c9e9eabc12e91f	Rmarkdown script and associated csv.file for the statistical analysis and plots of amino acids molar percentage in surface sediments across the ESAS.
PPRI	https://figshare.com/s/99e56322cdf8250785f9	Rmarkdown script and associated csv.file for the statistical analysis and plots of the phenol to pyridine ratio (PPRI)

		in surface sediments across the ESAS.
THAA_15N	https://figshare.com/s/787111a7e82f015623bd	Rmarkdown script and associated csv.file for the statistical analysis and plots of total hydrolysable amino acids ^{15}N in surface sediments across the ESAS.

Appendix 2

Supporting information for Chapter 4: Nitrogen cycling in Barents Sea and Fram Strait sediments

Barents Sea and Fram Strait sampling station map and list with latitude and longitude

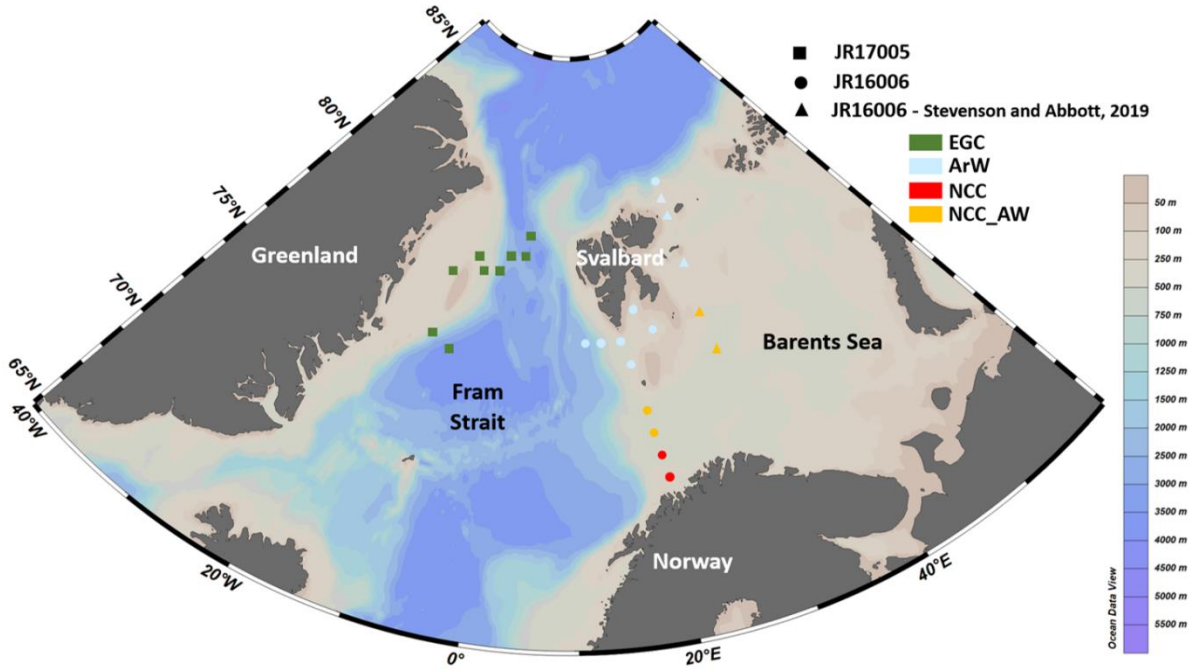

Figure A2.1 Map of the Fram Strait and Barents Sea showing locations of sediment sampling from the JR16006 (circles and triangles) and JR17005 (squares) used in this study. Station colour denotes the water mass group it has been assigned; green and the East Greenland Current (EGC); light blue and Arctic Water (ArW), red and the Norwegian Coastal Current (NCC); orange and the intermediate waters where the Atlantic and Norwegian Coastal Currents mix (NCC_AW). Bathymetry of the region are shown in the colour bar. Base map and bar created using Ocean Data View.

Barents Sea and Fram Strait sample list:

Table A2.1 ARISE and CHAOS Project sampling locations *CHAOS project supplementary samples

Sample	Latitude	Longitude	Bottom depth (m)
Barents Sea and Fram Strait (ARISE and CHAOS)			
B1	70.77	20.00	188
B2	71.70	19.67	256
B3	72.63	19.25	368
B4	73.37	18.92	476
B6	75.18	17.54	145
B7	76.00	16.83	325
B9	76.00	13.67	1005
B10	76.00	10.67	2230
B11	76.37	21.00	231
B18	81.76	30.01	3060
NT11	75.20	-5.28	3530
NT6	76.06	-8.25	1234
F21	78.60	-9.16	238
F17	79.01	-5.46	780
F15	78.59	-5.02	1244
F13	78.59	-2.60	2396
F10	79.00	0.00	2550
FS1	80.17	2.00	1890
F8	79.01	1.43	2468
ST1	77.25	19.29	147
B13*	74.30	30.00	363
B14*	76.30	30.30	294
B15*	78.15	30.01	269
B16*	80.07	30.04	287
B17*	81.17	30.20	229

C/N Plot for indication of the presence of inorganic nitrogen

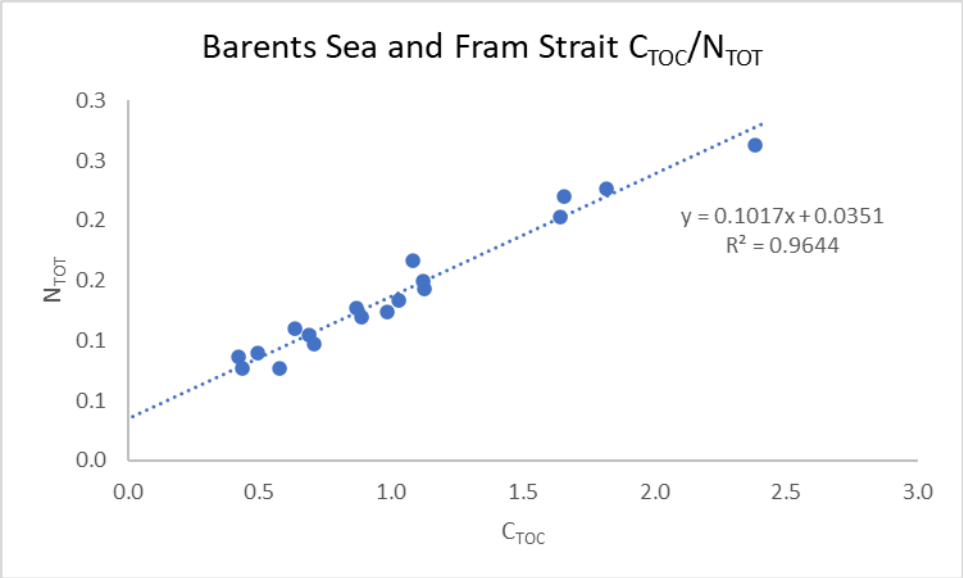

Figure A2.2 Barents Sea and Fram Strait plot of Carbon (total organic carbon) vs Nitrogen (total). Showing significant contribution of inorganic nitrogen in these sediments.

Barents Sea and Fram Strait Dataset links

Elemental, bulk isotope, pyrolysis and amino acids data sheets:

Title of spreadsheet	**Private link to access**	**Brief Description**
Barents Sea and Fram Strait elemental and bulk isotope data	https://figshare.com/s/72a29be3c2490bcc8252	Barents Sea and Fram Strait elemental data, bulk isotopic data
Barents Sea and Fram Strait Pyrolysis data	https://figshare.com/s/14d97d62ef448357ee46	Barents Sea and Fram Strait macromolecular phenol to pyridine ratio dataset
Barents Sea and Fram Strait amino acid data and associated indices	https://figshare.com/s/983f9eedf2ae1cf2aa25	Barents Sea and Fram Strait amino acid composition data, individual amino acid nitrogen isotope data, degradation index and EV proxy for heterotrophic reworking.

Barents Sea and Fram Strait Appendix links

Link to full collection for Barents Sea and Fram Strait Appendix: https://figshare.com/s/93035c6fcfa8e5c8efc1

Individual links to Rmarkdown scripts and associated .csv files.

Title of document	Private link to access	Brief description
15N_AA	https://figshare.com/s/07163802626d120d69f5	Rmarkdown script and associated csv.file for the statistical analysis and plots of ^{15}N of amino acids in surface sediments across the Barents Sea and Fram Strait
Bulk 15N	https://figshare.com/s/420033224f03a2f1bbee	Rmarkdown script and associated csv.file for the statistical analysis and plots of Bulk ^{15}N in surface sediments across the Barents Sea and Fram Strait
C/N Ratio	https://figshare.com/s/88bda0a34711b5d9bf82	Rmarkdown scripts and associated .csv files related to the analysis and lots of the C/N ratio across surface sediment in the Barents Sea and Fram Strait
Degradation Index	https://figshare.com/s/c8b75c331d66e312546e	Rmarkdown script and associated csv.file for the statistical analysis and plots of the degradation index in surface sediments across the Barents Sea and Fram Strait
∑V Proxy	https://figshare.com/s/50db0c498433757602c8	Rmarkdown scripts and associated .csv files related to the analysis and plots of EV (heterotrophic reworking) across surface sediment in the

		Barents Sea and Fram Strait
Molar percent amino acids analysis	https://figshare.com/s/c73faa89ea97e51356f7	Rmarkdown scripts and associated .csv files related to the analysis and plots of amino acid molar percent across surface sediment in the Barents Sea and Fram Strait
Molar percent amino acid ANOVA	https://figshare.com/s/515e9a2c520fbdad862e	Rmarkdown scripts and associated .csv files related to the analysis and plots of amino acid molar percent ANOVA across surface sediment in the Barents Sea and Fram Strait
Molar percent amino acid boxplots	https://figshare.com/s/ac73745af3646f746bcf	Rmarkdown scripts and associated .csv files related to the analysis and plots of amino acid molar percent across surface sediment in the Barents Sea and Fram Strait
Molar percent amino acid PCA	https://figshare.com/s/efbf4a72c58e940d0a9c	Rmarkdown scripts and associated .csv files related to the analysis and PCA plots of amino acid molar percent across surface sediment in the Barents Sea and Fram Strait
Phenol to Pyridine Ratio (PPRI)	https://figshare.com/s/02e7d4fca363d42c7e67	Rmarkdown scripts and associated .csv files related to the analysis and plots of the phenol to pyridine ratio (PPRI) across surface sediment in the Barents Sea and Fram Strait